

multic flow of non-Newtonian fluid in an  
annulus



By

Hina Sadaf

Department of Mathematics  
Quaid-i-Azam University  
Islamabad, Pakistan  
2012

Steady-state flow of non-Newtonian fluid in an  
annulus



By

Hina Sadaf

SUBMITTED IN THE PARTIAL FULFILLMENT OF THE REQUIREMENTS FOR

THE DEGREE OF

MASTER OF PHILOSOPHY

IN

MATHEMATICS

*Supervised By*

Dr. Sohail Nadeem

Department of Mathematics

Quaid-i-Azam University

Islamabad, Pakistan

2012

# Peristaltic flow of non-Newtonian fluid in an annulus


By

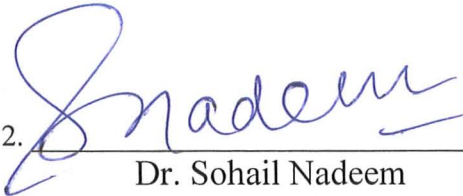
Hina Sadaf


## CERTIFICATE

*A THESIS SUBMITTED IN THE PARTIAL FULFILLMENT OF THE REQUIREMENTS FOR  
THE DEGREE OF THE MASTER OF  
PHILOSOPHY*

**We accept this thesis as conforming to the required standard**

1.   
Prof. Dr. Muhammad Ayub  
(Chairman)

2.   
Dr. Sohail Nadeem  
(Supervisor)

3.   
Dr. Khalid Hanif 31/08/2012  
(External Examiner)

**Department of Mathematics  
Quaid-i-Azam University  
Islamabad, Pakistan**

## ***Acknowledgement***

It is boundless and infinite mercy of Allah and his prophet **Muhammad (PBUH)** that I have been able to complete this project. I have no words to describe my sensation of respect about my parents, sisters and brother because without their support, kindness and encouragement it could not be possible for me to attain this target, I am highly grateful to my supervisor **Dr. Sohail Nadeem**, whose sincere and comprehensive guidance have fully added in completion of my research and gave me lot of trust and flexibility on the project. I have gained such a learning experience from my supervisor and it will help me a lot in my further studies.

I would like to express my appreciation to the **Dr. Noreen Sher Akbar** for their support and help towards my project.

Sincere thanks to all my friends for their kindness and moral support during my study. Thank you very much.

**Hina Sadaf**

## Preface

Peristalsis is a distinct pattern of smooth muscle contractions that mix the food material properly through the esophagus and intestines. Literature on peristalsis is quite extensive i.e. with the initiative work of Latham [1]. He discussed the fluid motion in peristaltic pump. After the Latham, Jaffrin and Shapiro [2] makes the developments on mathematical modeling and experimental fluid mechanics of peristaltic flows. They make the analysis under the assumption of long wave length and low Reynolds number approximation. Peristaltic motion in both mechanical and physiological situation has been discussed by the researchers of last few decades [3-8]. Recently peristaltic flow has gained many attentions of the researchers due to its wide range of applications in physiology and industry see Refs [9-13].

Nano fluid is basically the liquid suspension that contains very small particles of diameter less than 100nm. These particles can be found in the metals such as, oxides, carbides, nitrides or nonmetals (Graphite, carbon nanotubes). The pioneering work for the Nano fluids was reported by Choi [14]. He observed that the small amount of these nanoparticles significantly increases the thermal conductivity of the base fluid. Buongiorno [15] present convective transport in Nano fluids. He proposed a nonhomogeneous equilibrium model which predicts that increase in the thermal conductivity occurs due to the presence of the Brownian motion and thermophoretic parameters which are basically the diffusion of nanoparticles. Kuznetsov and Nield [16] reported the natural convective boundary layer flow of Nano fluid past a rigid flat plate. Sadik and Pramuanjaroenkij [17] discussed the review of convective heat transfer enhancement with Nano fluids. Two-dimensional boundary layer flow of Nano fluid over an impermeable stretching sheet was analyzed by Khan and Pop [18]. Heat transfer enhancement by using nanofluids in forced convection flows was visualized by Marga et al. [19]. Rana and Bhargava [20] extended the work of Khan and Pop for nonlinearly stretching sheet. The influence of endoscope on the peristaltic transport of nanofluid has

been examined by Akbar and Nadeem [21]. Peristaltic flow of a Nano fluid in a non-uniform tube has been addressed by Akbar et al. [22].

The dissertation is arranged as follows. In chapter one, we have presented the Peristaltic movement of hyperbolic tangent fluid under the effects of heat and mass transfer in an annulus. The two dimensional equations of tangent hyperbolic fluid are solved by using the assumptions of low Reynolds number and long wave length and then find their solutions analytically.

Chapter two is devoted to the study of Nano fluid model. The solutions of the simplified problem are found analytically with the help of Adomian decomposition method and Homotopy perturbation method. Finally the physically feature have been presented.

# Contents

<b>1 Peristaltic movement of hyperbolic tangent fluid under the effects of heat and mass transfer in an annulus</b>	<b>3</b>
1.1 Introduction . . . . .	3
1.2 Mathematical formulation . . . . .	3
1.3 Formulation of the Problem . . . . .	5
1.4 Solution of the problem . . . . .	9
1.5 Analytical Solution . . . . .	9
1.5.1 Zeroth-order system . . . . .	10
1.5.2 First-order system . . . . .	10
1.5.3 Zeroth-order solution . . . . .	10
1.5.4 First-order solution . . . . .	11
1.6 Volume flow rate . . . . .	12
1.7 Results and discussion . . . . .	15
1.8 Appendix1.0 . . . . .	17
<b>2 Effects of nanoparticles on the peristaltic motion of hyperbolic tangent fluid model in an annulus</b>	<b>33</b>
2.1 Introduction . . . . .	33
2.2 Flow equations . . . . .	33
2.3 Statement and formulation of the problem . . . . .	34
2.4 Analytical solution . . . . .	38
2.4.1 Zeroth-order problem . . . . .	39

2.4.2	First-order problem . . . . .	40
2.4.3	Second-order problem . . . . .	40
2.4.4	Zeroth-order solution . . . . .	40
2.4.5	First-order solution . . . . .	41
2.4.6	Second-order solution . . . . .	41
2.5	Analytical solution by Adomian decomposition method . . . . .	44
2.6	Results and discussion . . . . .	46
2.7	Conclusion . . . . .	47
2.8	Appendix 2.0 . . . . .	48



# Chapter 1

## Peristaltic movement of hyperbolic tangent fluid under the effects of heat and mass transfer in an annulus

### 1.1 Introduction

This chapter describes the peristaltic motion of a hyperbolic tangent fluid in an annulus in the presence of heat and mass transfer. Equations of tangent hyperbolic fluid are modelled and simplified by constructing the suppositions of low Reynolds number as well as long wave length. Analytical result is available for velocity profile whereas exact results are calculated for heat and concentration field. Solutions are presented through graphs. The terms for concentration field, temperature, pressure gradient and pressure rise are drawn for different fixed parameters. This is the review of paper by Akbar et al [21] and the essential details missing in the paper are incorporated.

### 1.2 Mathematical formulation

Equations of mass and momentum for an incompressible fluid, are specified as [21]

$$\operatorname{div} \tilde{\mathbf{A}} = 0, \tag{1.1}$$

$$\rho \frac{d\tilde{\mathbf{A}}}{dt} = \text{div } \tilde{\mathbf{S}} + \rho \mathbf{f}, \quad (1.2)$$

where  $\tilde{\mathbf{A}}$ ,  $\rho$ ,  $\mathbf{f}$ ,  $\tilde{\mathbf{S}}$ , gives the velocity vector, density, specific body force and Cauchy stress tensor respectively. Governing equations for hyperbolic tangent fluid is defined as

$$\tilde{\mathbf{S}} = -\tilde{\mathbf{p}}\mathbf{I} + \tilde{\boldsymbol{\tau}}, \quad (1.3)$$

$$\tilde{\boldsymbol{\tau}} = [\eta_\infty + (\eta_0 + \eta_\infty) \tanh(\Gamma \tilde{\boldsymbol{\gamma}})^m] \tilde{\boldsymbol{\gamma}}_i, \quad (1.4)$$

in which  $\tilde{\boldsymbol{\tau}}$ ,  $\eta_0$ ,  $\eta_\infty$ ,  $m$ ,  $\Gamma$ , denotes the extra stress tensor, zero shear rate viscosity, infinite rate of shear viscosity, power law index, and time constant respectively and  $\tilde{\boldsymbol{\gamma}}$  now defined as

$$\tilde{\boldsymbol{\gamma}} = \sqrt{\frac{1}{2} \sum_i \sum_j \tilde{\boldsymbol{\gamma}}_{ij} \tilde{\boldsymbol{\gamma}}_{ji}} = \sqrt{\frac{1}{2} \boldsymbol{\pi}}, \quad (1.5)$$

where

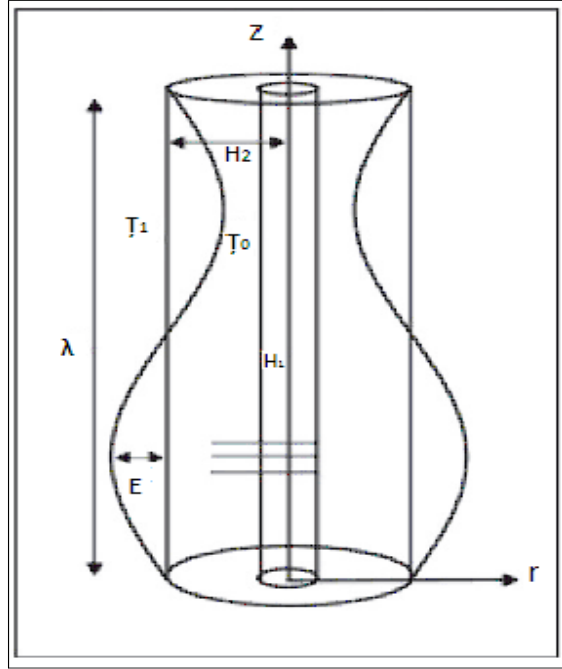
$$\boldsymbol{\pi} = \text{trace}(\text{grad } \tilde{\mathbf{A}} + (\text{grad } \tilde{\mathbf{A}})^T)^2, \quad (1.6)$$

in which  $\pi$  is the second invariant strain tensor. We study Eq. (1.4) in the case for  $\eta_\infty = 0$  and  $\Gamma \tilde{\boldsymbol{\gamma}} < 1$ . The element of extra stress tensor so inscribed as

$$\tilde{\boldsymbol{\tau}} = \eta_0 [(\Gamma \tilde{\boldsymbol{\gamma}})^m] \tilde{\boldsymbol{\gamma}}_i = \eta_0 [(1 + \Gamma \tilde{\boldsymbol{\gamma}} - 1)^m] \tilde{\boldsymbol{\gamma}}_i = \eta_0 [1 + m(\Gamma \tilde{\boldsymbol{\gamma}} - 1)] \tilde{\boldsymbol{\gamma}}_i, \quad (1.7)$$

$$\tilde{\boldsymbol{\gamma}}_i = \mathbf{L} + \mathbf{L}^T. \quad (1.8)$$

### 1.3 Formulation of the Problem



Considering the peristaltic transport in the profile of an incompressible hyperbolic tangent fluid in an annulus. Inward cylinder is rigid, and kept at temperature  $\tilde{T}_0$  however outward cylinder takes a sinusoidal wave travelling down its walls and kept at temperature  $\tilde{T}_1$ . Wall surface geometry is expressed as

$$\tilde{R}_1 = H_1, \quad (1.9)$$

$$\tilde{R}_2 = H_2 + E \sin \frac{2\pi}{\lambda} (\tilde{Z} - \tilde{s}\tilde{t}), \quad (1.10)$$

where  $H_1$ ,  $H_2$ ,  $\lambda$ ,  $E$ ,  $\tilde{s}$ , is the radius of the inward and outward cylinders, wavelength, wave amplitude, and wave speed respectively. For an annulus, velocity, temperature, and concentration fields takes the form

$$\begin{aligned}
\tilde{\mathbf{A}} &= (\tilde{\mathbf{U}}(\tilde{t}, \tilde{\mathbf{R}}, \tilde{\mathbf{Z}}), 0, \tilde{\mathbf{W}}(\tilde{t}, \tilde{\mathbf{R}}, \tilde{\mathbf{Z}})), \\
\tilde{\mathbf{T}} &= \tilde{\mathbf{T}}(\tilde{t}, \tilde{\mathbf{R}}, \tilde{\mathbf{Z}}), \quad \tilde{\mathbf{C}} = \tilde{\mathbf{C}}(\tilde{t}, \tilde{\mathbf{R}}, \tilde{\mathbf{Z}}).
\end{aligned} \tag{1.11}$$

For an incompressible hyperbolic tangent fluid model the leading equations in the fixed frame are given as

$$\frac{\partial \tilde{\mathbf{U}}}{\partial \tilde{\mathbf{R}}} + \frac{\tilde{\mathbf{U}}}{\tilde{\mathbf{R}}} + \frac{\partial \tilde{\mathbf{W}}}{\partial \tilde{\mathbf{Z}}} = 0, \tag{1.12}$$

$$\rho \left( \frac{\partial \tilde{\mathbf{U}}}{\partial \tilde{t}} + \tilde{\mathbf{U}} \frac{\partial \tilde{\mathbf{U}}}{\partial \tilde{\mathbf{R}}} + \tilde{\mathbf{W}} \frac{\partial \tilde{\mathbf{U}}}{\partial \tilde{\mathbf{Z}}} \right) = - \frac{\partial \tilde{\mathbf{P}}}{\partial \tilde{\mathbf{R}}} + \frac{1}{\tilde{\mathbf{R}}} \frac{\partial (\tilde{\mathbf{R}} \tilde{\boldsymbol{\tau}}_{\tilde{\mathbf{R}}\tilde{\mathbf{R}}})}{\partial \tilde{\mathbf{R}}} + \frac{\partial (\tilde{\boldsymbol{\tau}}_{\tilde{\mathbf{R}}\tilde{\mathbf{Z}}})}{\partial \tilde{\mathbf{Z}}} - \frac{\tilde{\boldsymbol{\tau}}_{\tilde{\theta}\tilde{\theta}}}{\tilde{\mathbf{R}}}, \tag{1.13}$$

$$\begin{aligned}
\rho \left( \frac{\partial \tilde{\mathbf{W}}}{\partial \tilde{t}} + \tilde{\mathbf{U}} \frac{\partial \tilde{\mathbf{W}}}{\partial \tilde{\mathbf{R}}} + \tilde{\mathbf{W}} \frac{\partial \tilde{\mathbf{W}}}{\partial \tilde{\mathbf{Z}}} \right) &= - \frac{\partial \tilde{\mathbf{P}}}{\partial \tilde{\mathbf{Z}}} + \frac{1}{\tilde{\mathbf{R}}} \frac{\partial (\tilde{\mathbf{R}} \tilde{\boldsymbol{\tau}}_{\tilde{\mathbf{R}}\tilde{\mathbf{Z}}})}{\partial \tilde{\mathbf{R}}} + \frac{\partial (\tilde{\boldsymbol{\tau}}_{\tilde{\mathbf{Z}}\tilde{\mathbf{Z}}})}{\partial \tilde{\mathbf{Z}}} + \rho g \alpha_{\tilde{\mathbf{T}}} (\tilde{\mathbf{T}} - \tilde{\mathbf{T}}_1) \\
&+ \rho g \alpha_{\tilde{\mathbf{C}}} (\tilde{\mathbf{C}} - \tilde{\mathbf{C}}_1),
\end{aligned} \tag{1.14}$$

Energy and mass concentration equations are defined as

$$\rho c_p \left( \frac{\partial \tilde{\mathbf{T}}}{\partial \tilde{t}} + \tilde{\mathbf{U}} \frac{\partial \tilde{\mathbf{T}}}{\partial \tilde{\mathbf{R}}} + \tilde{\mathbf{W}} \frac{\partial \tilde{\mathbf{T}}}{\partial \tilde{\mathbf{Z}}} \right) = \kappa \left( \frac{\partial^2 \tilde{\mathbf{T}}}{\partial \tilde{\mathbf{R}}^2} + \frac{1}{\tilde{\mathbf{R}}} \frac{\partial \tilde{\mathbf{T}}}{\partial \tilde{\mathbf{R}}} + \frac{\partial^2 \tilde{\mathbf{T}}}{\partial \tilde{\mathbf{Z}}^2} \right) + Q_0, \tag{1.15}$$

$$\left( \frac{\partial \tilde{\mathbf{C}}}{\partial \tilde{t}} + \tilde{\mathbf{U}} \frac{\partial \tilde{\mathbf{C}}}{\partial \tilde{\mathbf{R}}} + \tilde{\mathbf{W}} \frac{\partial \tilde{\mathbf{C}}}{\partial \tilde{\mathbf{Z}}} \right) = d \left( \frac{\partial^2 \tilde{\mathbf{C}}}{\partial \tilde{\mathbf{R}}^2} + \frac{1}{\tilde{\mathbf{R}}} \frac{\partial \tilde{\mathbf{C}}}{\partial \tilde{\mathbf{R}}} + \frac{\partial^2 \tilde{\mathbf{C}}}{\partial \tilde{\mathbf{Z}}^2} \right) + \frac{dk_{\tilde{t}}}{\tilde{t}_m} \left( \frac{\partial^2 \tilde{\mathbf{T}}}{\partial \tilde{\mathbf{R}}^2} + \frac{1}{\tilde{\mathbf{R}}} \frac{\partial \tilde{\mathbf{T}}}{\partial \tilde{\mathbf{R}}} + \frac{\partial^2 \tilde{\mathbf{T}}}{\partial \tilde{\mathbf{Z}}^2} \right). \tag{1.16}$$

In the above equations  $\tilde{\mathbf{U}}, \tilde{\mathbf{W}}$  are the corresponding velocity components in radial as well in axial directions respectively.  $\tilde{\mathbf{T}}$  is temperature,  $\rho$  denotes the density, whereas at constant pressure  $c_p$  gives the specific heat.  $\tilde{\mathbf{C}}$  is the concentration of fluid,  $\kappa$  denotes the thermal conductivity,  $\tilde{t}_m$  is medium temperature,  $d$  denotes the mass diffusivity coefficient and thermal-diffusion ratio is denoted by  $k_{\tilde{t}}$ . In the fixed coordinates  $(\tilde{\mathbf{R}}, \tilde{\mathbf{Z}})$  the flow among cylinders is unsteady. It converts steady in a wave structure  $(\tilde{t}, \tilde{z})$  moving with similar speed as the wave

movements in the  $\tilde{Z}$  direction. Both structures are connected through the following transformations.

$$\tilde{r} = \tilde{R}, \quad \tilde{z} = \tilde{Z} - \tilde{s}\tilde{t}, \quad \tilde{u} = \tilde{U}, \quad \tilde{w} = \tilde{W} - \tilde{s}, \quad (1.17)$$

where  $\tilde{u}, \tilde{w}$  are the velocity components in the wave structure. Suitable boundary limits in wave structures stand

$$\tilde{w} = -\tilde{s}, \quad \text{at } \tilde{r} = \tilde{i}_1, \quad \tilde{w} = -\tilde{s} \quad \text{at } \tilde{r} = \tilde{i}_2 = H_2 + E \sin \frac{2\pi}{\lambda}(\tilde{z}), \quad (1.18)$$

$$\tilde{T} = \tilde{T}_0 \quad \text{at } \tilde{r} = \tilde{i}_1, \quad \tilde{T} = \tilde{T}_1 \quad \text{at } \tilde{r} = \tilde{i}_2, \quad (1.19)$$

$$\tilde{C} = \tilde{C}_0 \quad \text{at } \tilde{r} = \tilde{i}_1, \quad \tilde{C} = \tilde{C}_1 \quad \text{at } \tilde{r} = \tilde{i}_2. \quad (1.20)$$

Introducing the dimensionless parameters

$$\begin{aligned} \mathbb{R} &= \frac{\tilde{R}}{H_2}, \quad r = \frac{\tilde{r}}{H_2}, \quad \mathbb{Z} = \frac{\tilde{Z}}{\lambda}, \quad z = \frac{\tilde{z}}{\lambda}, \quad \mathbb{W} = \frac{\tilde{W}}{\tilde{s}}, \quad w = \frac{\tilde{w}}{\tilde{s}}, \quad \mathbb{U} = \frac{\lambda\tilde{U}}{H_2\tilde{s}}, \quad u = \frac{\lambda\tilde{u}}{H_2\tilde{s}}, \\ \mathbb{P} &= \frac{H_2^2\tilde{P}}{\tilde{s}\lambda\eta}, \quad \theta = \frac{\tilde{T} - \tilde{T}_1}{\tilde{T}_0 - \tilde{T}_1}, \quad \mathbb{t} = \frac{\tilde{t}}{\lambda}, \quad \delta = \frac{H_2}{\lambda}, \quad R_y = \frac{\rho\tilde{s}H_2}{\eta}, \quad \sigma = \frac{\tilde{C} - \tilde{C}_1}{\tilde{C}_0 - \tilde{C}_1}, \\ i_1 &= \frac{\tilde{i}_1}{H_2} = \frac{H_1}{H_2} = \epsilon, \quad i_2 = \frac{\tilde{i}_2}{H_2} = 1 + \Phi \sin 2\pi z, \quad \mathbb{S} = \frac{H_2\tilde{S}}{\tilde{s}\eta}, \quad H_y = \frac{\Gamma\tilde{s}}{H_2}, \quad C_s = \frac{\eta}{d\rho}, \\ g_r &= \frac{\rho g \alpha_{\tilde{T}} H_2^2 (\tilde{T}_0 - \tilde{T}_1)}{\eta\tilde{s}}, \quad b_r = \frac{\rho g \alpha_{\tilde{C}} H_2^2 (\tilde{C}_0 - \tilde{C}_1)}{\eta\tilde{s}}, \quad \dot{\gamma} = \frac{H_2\tilde{\gamma}}{\tilde{s}}, \quad \Phi = \frac{E}{H_2}, \\ B &= \frac{Q_0 H_2^2}{k(\tilde{T}_0 - \tilde{T}_1)}, \quad R_s = \frac{\rho d k_{\tilde{t}} (\tilde{T}_0 - \tilde{T}_1)}{\eta \tilde{t}_m (\tilde{C}_0 - \tilde{C}_1)}, \quad P_r = \frac{\eta c_p}{k}, \quad \tau = \frac{\tilde{\tau} H_2}{\eta\tilde{s}}. \end{aligned} \quad (1.21)$$

In above equations  $b_r, C_s, R_s, g_r, H_y, \Phi < 1$  is the local concentration Grashof number, Schmidt number, Soret number, local temperature Grashof number, Weissenberg number and amplitude ratio respectively. Using Eqs. (1.17) and (1.21) in Eqs. (1.12) to (1.16), we obtain

$$\frac{\partial \mathfrak{u}}{\partial r} + \frac{\mathfrak{u}}{r} + \frac{\partial w}{\partial z} = 0, \quad (1.22)$$

$$\hat{\delta}^3 R_y \left( \mathfrak{u} \frac{\partial \mathfrak{u}}{\partial r} + w \frac{\partial \mathfrak{u}}{\partial z} \right) = -\frac{\partial \mathbb{P}}{\partial r} + \hat{\delta}^2 \frac{\partial}{\partial z} (\tau_{rz}) + \frac{\hat{\delta}}{r} \frac{\partial}{\partial r} (r \tau_{rr}) - \frac{\hat{\delta}}{r} \tau_{\theta\theta}, \quad (1.23)$$

$$\hat{\delta} R_y \left( \mathfrak{u} \frac{\partial w}{\partial r} + w \frac{\partial w}{\partial z} \right) = -\frac{\partial \mathbb{P}}{\partial z} + \frac{1}{r} \frac{\partial}{\partial r} (r \tau_{rz}) + \hat{\delta} \frac{\partial}{\partial z} (\tau_{zz}) + g_r \theta + b_r \sigma, \quad (1.24)$$

$$\hat{\delta} p_r R_y \left( \mathfrak{u} \frac{\partial \theta}{\partial r} + w \frac{\partial \theta}{\partial z} \right) = \frac{\partial^2 \theta}{\partial r^2} + \frac{1}{r} \frac{\partial \theta}{\partial r} + \hat{\delta}^2 \frac{\partial^2 \theta}{\partial z^2} + B, \quad (1.25)$$

$$R_y \hat{\delta} \left( \mathfrak{u} \frac{\partial \sigma}{\partial r} + w \frac{\partial \sigma}{\partial z} \right) = \frac{1}{C_s} \left( \frac{1}{r} \frac{\partial}{\partial r} (r \frac{\partial \sigma}{\partial r}) + \hat{\delta}^2 \frac{\partial^2 \sigma}{\partial z^2} \right) + R_s \left( \frac{1}{r} \frac{\partial}{\partial r} (r \frac{\partial \theta}{\partial r}) + \hat{\delta}^2 \frac{\partial^2 \theta}{\partial z^2} \right), \quad (1.26)$$

where

$$\begin{aligned} \tau_{rr} &= 2\hat{\delta}[1 + m(H_y \dot{\gamma} - 1)] \frac{\partial \mathfrak{u}}{\partial r}, \\ \tau_{rz} &= [1 + m(H_y \dot{\gamma} - 1)] \left( \frac{\partial \mathfrak{u}}{\partial z} \hat{\delta}^2 + \frac{\partial w}{\partial r} \right), \\ \tau_{zz} &= 2\hat{\delta}[1 + m(H_y \dot{\gamma} - 1)] \frac{\partial w}{\partial z}, \\ \tau_{\theta\theta} &= 2\hat{\delta}[1 + m(H_y \dot{\gamma} - 1)] \frac{\mathfrak{u}}{r}, \end{aligned} \quad (1.27)$$

$$\dot{\gamma} = [2\hat{\delta}^2 \left( \frac{\partial \mathfrak{u}}{\partial r} \right)^2 + \left( \frac{\partial \mathfrak{u}}{\partial z} \hat{\delta}^2 + \frac{\partial w}{\partial r} \right)^2 + 2\hat{\delta}^2 \left( \frac{\partial w}{\partial z} \right)^2 + 2\hat{\delta}^2 \frac{\mathfrak{u}^2}{r^2}]^{\frac{1}{2}}. \quad (1.28)$$

in which  $\hat{\delta}$ ,  $P_r$ ,  $R_y$ ,  $H_y$  be the wave, Prandtl number, Weissenberg, and Reynolds number respectively. By suppositions of low Reynolds number and long wave length, avoiding the relations of order  $\hat{\delta}$  and greater, Eqs. (1.23) to (1.26) take the form

$$\frac{\partial \mathbb{P}}{\partial r} = 0, \quad (1.29)$$

$$\frac{\partial \mathbb{P}}{\partial z} = \frac{1}{r} \frac{\partial}{\partial r} \left[ r \left( 1 + m(H_y \frac{\partial w}{\partial r} - 1) \right) \frac{\partial w}{\partial r} \right] + g_r \theta + b_r \sigma, \quad (1.30)$$

$$\frac{\partial^2 \theta}{\partial r^2} + \frac{1}{r} \frac{\partial \theta}{\partial r} + B = 0, \quad (1.31)$$

$$\frac{1}{C_s} \left( \frac{1}{r} \frac{\partial}{\partial r} \left( r \frac{\partial \sigma}{\partial r} \right) \right) + R_s \left( \frac{1}{r} \frac{\partial}{\partial r} \left( r \frac{\partial \theta}{\partial r} \right) \right) = 0. \quad (1.32)$$

Eq. (1.29) displays that  $\mathbb{P}$  is not a function of  $r$ . The consistent dimensionless boundary conditions for the problem in consideration are defined as

$$\begin{aligned} w &= -1 \text{ at } r = i_1 = \epsilon, \quad w = -1 \text{ at } r = i_2 = 1 + \Phi \sin(2\pi z), \\ \sigma &= \theta = 1 \text{ at } r = i_1, \quad \sigma = \theta = 0 \text{ at } r = i_2, \end{aligned} \quad (1.33)$$

## 1.4 Solution of the problem

Eq. (1.31) is the second order linear nonhomogeneous partial differential equation. Its solution sustaining the boundary limits can be straightforward inscribed as

$$\theta = \frac{1}{\beta_{11}} (\beta_{12} \ln r + \beta_{13} r^2 + \beta_{14}). \quad (1.34)$$

Invoking Eq. (1.34) into Eq. (1.32) the solution of resultant equation supporting the boundary conditions (1.33) take the form

$$\sigma = -\frac{R_s S_c}{\beta_{11}} (\beta_{12} \ln r + \beta_{13} r^2 + \beta_{14}) + \beta_{17} \ln r + \beta_{18}. \quad (1.35)$$

where all  $\beta_{ij}$  are defined in appendix.

## 1.5 Analytical Solution

Substitution of Eqs. (1.34) and (1.35) into the Eq. (1.30), yields

$$\begin{aligned} \frac{\partial \mathbb{P}}{\partial z} &= \frac{1}{r} \frac{\partial}{\partial r} \left[ r \left( 1 + m \left( H_y \frac{\partial w}{\partial r} - 1 \right) \right) \frac{\partial w}{\partial r} \right] + g_r \left( \frac{1}{\mathfrak{B}_{11}} (\mathfrak{B}_{12} \ln r + \mathfrak{B}_{13} r^2 + \mathfrak{B}_{14}) \right) \\ &\quad + b_r \left( -\frac{R_s C_s}{\mathfrak{B}_{11}} (\mathfrak{B}_{12} \ln r + \mathfrak{B}_{13} r^2 + \mathfrak{B}_{14}) + \mathfrak{B}_{17} \ln r + \mathfrak{B}_{18} \right). \end{aligned} \quad (1.36)$$

To find the results of Eq. (1.36), we have used regular perturbation method. For regular perturbation procedure, we expand  $w$ ,  $F_i$  and  $\mathbb{P}$  as

$$\begin{aligned} w &= w_0 + H_y w_1 + \dots, \\ F_i &= F_{0i} + H_y F_{1i} + \dots, \\ \mathbb{P} &= \mathbb{P}_0 + H_y \mathbb{P}_1 + \dots, \end{aligned} \quad (1.37)$$

where  $F_i$  is flow rate.

Substituting Eq. (1.37) into Eqs. (1.36) and (1.33), equating the like powers of  $H_y$  we obtain the following systems

### 1.5.1 Zeroth-order system

$$\frac{\partial \mathbb{P}_0}{\partial z} = \frac{1}{r} \frac{\partial}{\partial r} \left( r(1-m) \frac{\partial w_0}{\partial r} \right) + r^2 \mathfrak{B}_{19} + \mathfrak{B}_{20} \ln r + \mathfrak{B}_{21}, \quad (1.38)$$

$$w_0 = -1, \text{ at } r = i_1 = \varepsilon, \quad w_0 = -1, \quad r = i_2 = 1 + \Phi \sin 2\pi z. \quad (1.39)$$

### 1.5.2 First-order system

$$\frac{\partial \mathbb{P}_1}{\partial z} = \frac{1}{r} \frac{\partial}{\partial r} \left( r(1-m) \frac{\partial w_1}{\partial r} + r m \left( \frac{\partial w_0}{\partial r} \right)^2 \right), \quad (1.40)$$

$$w_1 = 0, \text{ at } r = i_1 = \varepsilon, \quad w_1 = 0, \quad r = i_2 = 1 + \Phi \sin 2\pi z. \quad (1.41)$$

### 1.5.3 Zeroth-order solution

The solution of Eq. (1.38) filling the boundary conditions (1.39) takes the form



$$\begin{aligned}
w_0 = & \frac{d\mathbb{P}_0}{dz} \left( \frac{r^2}{4(1-m)} + \beta_{29} \ln r + \beta_{28} \right) + \beta_{22}r^4 + \beta_{24}r^2 + \beta_{23}r^2 \ln r \\
& + \beta_{30} \ln r + \beta_{27}.
\end{aligned} \tag{1.42}$$

#### 1.5.4 First-order solution

Invoking Eq. (1.42) into Eq. (1.40), the solution of resultant equation sustaining the boundary conditions (1.41) take the form

$$\begin{aligned}
w_1 = & \frac{d\mathbb{P}_1}{dz} \left( \frac{r^2}{4(1-m)} + \beta_{29} \ln r + \beta_{28} \right) + r^7\beta_{43} + r^6\beta_{44} + r^5\beta_{45} \\
& + r^4\beta_{46} + r^3\beta_{47} + r^2\beta_{48} + r\beta_{41} - \frac{1}{r}\beta_{42} + \beta_{49}r^6 \ln r \\
& + \beta_{50}r^5 \ln(r) + \beta_{51}r^4 \ln r + \beta_{52}r^5(\ln r)^2 + \beta_{53}r^2 \ln r \\
& + \frac{\beta_{54}(\ln r)}{(1-m)} + \beta_{55}.
\end{aligned} \tag{1.43}$$

The resulting expression for velocity field is defined

$$\begin{aligned}
w = & \frac{d\mathbb{P}}{dz} \left( \frac{r^2}{4(1-m)} + \beta_{29} \ln r + \beta_{28} \right) + \beta_{22}r^4 + \beta_{24}r^2 + \beta_{23}r^2 \ln r \\
& + \beta_{30} \ln(r) + \beta_{27} + H_y(r^7\beta_{43} + r^6\beta_{44} + r^5\beta_{45} + r^4\beta_{46} + r^3\beta_{47} \\
& + r^2\beta_{48} + r\beta_{41} - \frac{1}{r}\beta_{42} + \beta_{49}r^6 \ln(r) + \beta_{50}r^5 \ln(r) + \beta_{51}r^4 \ln r \\
& + \beta_{52}r^5(\ln r)^2 + \beta_{53}r^2 \ln r + \frac{\beta_{54}(\ln r)}{(1-m)} + \beta_{55}).
\end{aligned} \tag{1.44}$$

The dimensionless time mean flow rate  $F_{0i}$  and  $F_{1i}$  are defined as

$$F_{0i} = \int_{i_1}^{i_2} r w_0 dr, \tag{1.45}$$

$$F_{1i} = \int_{i_1}^{i_2} r w_1 dr. \tag{1.46}$$

Switching Eqs. (1.42) and (1.43) into Eqs (1.45) and (1.46), we obtain

$$F_{0i} = \beta_{56} + \beta_{57}\left(\frac{d\mathbb{P}_0}{dz}\right), \quad (1.47)$$

$$F_{1i} = \beta_{72} + \beta_{57}\left(\frac{d\mathbb{P}_1}{dz}\right), \quad (1.48)$$

with the aid of Eqs. (1.47) and (1.48) we acquire as

$$\frac{d\mathbb{P}}{dz} = \frac{F_i}{\beta_{57}} + \beta_{73}. \quad (1.49)$$

## 1.6 Volume flow rate

In the fixed coordinates volume flow rate in the instantaneous position is specified by

$$\bar{Q}_1 = 2\pi \int_{\tilde{\mathbb{R}}_1}^{\tilde{\mathbb{R}}_2} \tilde{\mathbb{R}}\tilde{\mathbb{W}}d\tilde{\mathbb{R}}, \quad (1.50)$$

where  $\tilde{\mathbb{R}}_2$  is a function of  $\tilde{\mathbb{Z}}$  and  $\tilde{\mathbb{t}}$ . Invoking Eq. (1.17) into Eq. (1.50) and then integrating produces

$$\bar{Q}_1 = \bar{q}_a + \pi\tilde{s}(\tilde{i}_2^2 - \tilde{i}_1^2), \quad (1.51)$$

where

$$\bar{q}_a = 2\pi \int_{\tilde{i}_1}^{\tilde{i}_2} \tilde{r}\tilde{w}d\tilde{r}, \quad (1.52)$$

In the moving coordinates system the volume flow rate is independent of time as mention in Eq. (1.52). Here  $\tilde{i}_2$  is the function of  $\tilde{\mathbb{Z}}$  alone. Using dimensionless variables we find

$$F_i = \frac{\bar{q}_a}{2\pi H_2^2 \tilde{s}} = \int_{\tilde{i}_1}^{\tilde{i}_2} rwdr. \quad (1.53)$$

Over a period  $T = \frac{\lambda}{\tilde{s}}$  the time-mean flow at a fixed  $\tilde{Z}$  position is defined as

$$\tilde{Q} = \frac{1}{T} \int_0^T \bar{Q}_1 d\tilde{t}. \quad (1.54)$$

Invoking Eq. (1.51) into Eq. (1.54) and integrating, we attain

$$\tilde{Q} = \bar{q}_a + \pi \tilde{s} \left( \tilde{i}_2^2 - \tilde{i}_1^2 \right), \quad (1.55)$$

which can be inscribed as

$$\frac{\tilde{Q}}{2\pi H_2^2 \tilde{s}} = \frac{\tilde{q}_a}{2\pi H_2^2 \tilde{s}} + \frac{1}{2} \left( 1 + \frac{\Phi^2}{2} - \epsilon^2 \right), \quad (1.56)$$

Dimensionless time-mean flow can be defined as

$$Q = \frac{\tilde{Q}}{2\pi H_2^2 \tilde{s}}, \quad F_i = \frac{\tilde{q}_a}{2\pi H_2^2 \tilde{s}}. \quad (1.57)$$

With the aid of Eq. (1.57), Eq. (1.56) take the formula

$$Q = F_i + \frac{1}{2} \left( 1 + \frac{\Phi^2}{2} - \epsilon^2 \right). \quad (1.58)$$

The Pressure rise distribution  $\Delta \mathbb{P}$  and frictional forces on the outward and inward cylinders are  $F^a$  and  $F^b$  in non dimensional systems are define as

$$\Delta \mathbb{P} = \int_0^1 \left( \frac{d\mathbb{P}}{dz} \right) dz, \quad (1.59)$$

$$F^a = \int_0^1 \tilde{i}_1^2 \left( -\frac{d\mathbb{P}}{dz} \right) dz, \quad (1.60)$$

$$F^b = \int_0^1 \tilde{i}_2^2 \left( -\frac{d\mathbb{P}}{dz} \right) dz. \quad (1.61)$$

By substituting Eq. (1.49) into Eq. (1.59) to (1.61) with  $\tilde{i}_1 = \epsilon$ ,  $\tilde{i}_2 = 1 + \Phi \sin(2\pi z)$ , we acquire the  $\Delta \mathbb{P}$  ( $\mathbb{P}$ ressure rise) and the  $F^b$ ,  $F^a$  (frictional forces) on the outward and inward

cylinders as

$$\Delta \mathbb{P} = \int_0^1 \left( \frac{F_i}{\beta_{57}} + \beta_{73} \right) dz, \quad (1.62)$$

$$F^a = \int_0^1 -i_1^2 \left( \frac{F_i}{\beta_{57}} + \beta_{73} \right) dz, \quad (1.63)$$

$$F^b = \int_0^1 -i_2^2 \left( \frac{F_i}{\beta_{57}} + \beta_{73} \right) dz. \quad (1.64)$$

The velocities in terms of stream functions are defined as

$$u = \frac{-1}{r} \left( \frac{\partial \Psi}{\partial z} \right) \text{ and } w = \frac{1}{r} \left( \frac{\partial \Psi}{\partial r} \right). \quad (1.65)$$

Making use of Eq. (1.44) into Eq. (1.65), we get stream function as

$$\begin{aligned} \Psi = & \frac{d\mathbb{P}}{dz} \left( \frac{r^4}{16(1-m)} + \beta_{29} \left( \frac{r^2 \ln(r)}{2} - \frac{r^2}{4} \right) + \beta_{28} \frac{r^2}{2} \right) + \beta_{22} \frac{r^6}{6} + \beta_{24} \frac{r^4}{4} + \beta_{27} \frac{r^2}{2} \\ & + \beta_{23} \left( \frac{r^4 \ln(r)}{4} - \frac{r^4}{16} \right) + \beta_{30} \left( \frac{r^2 \ln(r)}{2} - \frac{r^2}{4} \right) + H_y (r^9 \beta_{58} + r^8 \beta_{59} + r^7 \beta_{60} \\ & + r^6 \beta_{61} + r^5 \beta_{62} + r^4 \beta_{63} + r^3 \beta_{64} + r^2 \beta_{65} - r \beta_{42} + \beta_{66} r^8 \ln(r) + \beta_{67} r^7 \ln r \\ & + \beta_{68} r^6 \ln r + \beta_{69} r^4 \ln r + \beta_{70} r^7 (\ln r)^2 + \beta_{71} r^2 \ln r). \end{aligned} \quad (1.66)$$

For study, we have experimental five wave forms specifically, sinusoidal wave, square wave, triangular wave, trapezoidal wave, and multisinusoidal wave. Expressions of above mention waves in dimensionless form can be written as

1. Multisinusoidal wave:

$$i_2(z) = 1 + \Phi \sin(2f\pi z), \quad (1.67)$$

2. Square wave:

$$i_2(z) = 1 + \Phi \left\{ \frac{4}{\pi} \sum_{v=1}^{\infty} \frac{(-1)^{v+1}}{(2v-1)} \cos(2\pi(2v-1)z) \right\}, \quad (1.68)$$

3. Triangular wave:

$$i_2(z) = 1 + \Phi \left\{ \frac{8}{\pi^3} \sum_{v=1}^{\infty} \frac{(-1)^{v+1}}{(2v-1)} \sin(2\pi(2v-1)z) \right\}, \quad (1.69)$$

4. Trapezoidal wave:

$$i_2(z) = 1 + \Phi \left\{ \frac{32}{\pi^2} \sum_{v=1}^{\infty} \frac{\sin \frac{\pi}{8}(2v-1)}{(2v-1)^2} \sin(2\pi(2v-1)z) \right\}, \quad (1.70)$$

5. Sinusoidal wave:

$$i_2(z) = 1 + \Phi \sin(2\pi z), \quad (1.71)$$

The expression for Pressure rise  $\Delta P$  and the friction forces are considered numerically by mathematica, where as constants are defined in appendix.

## 1.7 Results and discussion

Graphical analysis of Pressure rise, inward and outward friction forces, stream lines and Pressure gradient are represented in this unit. Figs. (1.1) and (1.2) shows the velocity profile for different values of  $g_r$  and  $b_r$ . From these figures, it is detected that the velocity profile increases when the values of  $g_r$  and  $b_r$  increases in the range  $r \in [0.2, 0.65]$  otherwise decreases. Figs (1.3) to (1.5) represent the variation of concentration field for different values of  $R_s$  (Soret number),  $C_s$  (Schmidth number), and  $B$  (absorbtion parameter). It is also shown by these figures that concentration field decreases when the values of  $R_s$ ,  $C_s$  and  $B$  increases. The variation of temperature profile for various values of  $B$  is depicted in the Fig. (1.6) it is revealed that concentration field increases when values of  $B$  (absorbtion parameter) increases. The effects of various parameters such as Weissenberg number  $H_y$ , amplitude ratio  $\Phi$ , power law index  $m$ , and different wave forms, on  $\Delta P$  (Pressure rise) are represented in the Figs. (1.7) to (1.10). Figs. (1.7) to (1.9) shows that when the values of parameters  $H_y$ ,  $\Phi$ ,  $m$ , increases, Pressure rise decreases as well as increases for the different values of time mean flow rate. Peristaltic pumping regions are  $Q \in [-2, -0.1]$ ,  $Q \in [-2, 0.1]$ ,  $Q \in [-2, -0.11]$ , other wise it is co pumping or augmented pumping regions. In Fig. (1.10) Peristaltic pumping region is  $Q \in [-2, 0]$ , other

wise it is augmented pumping region. Moreover Trapezoidal wave shows good agreement in the peristaltic pumping region. Behavior of the inward and outward frictional forces are displayed in the Figs. (1.11) to (1.18). It is detected from these figures that the inward and outward frictional forces shows the opposite behavior comparatively Pressure rise. Inward and the outward frictional forces behave in a similar manner for the same values of emerging parameters. Moreover it is also detected that the outward friction force is larger than inward friction force for the similar values of emerging parameters. Figs. (1.19) to (1.23) represented the effects of Pressure gradient for different values of  $\Phi$ . Figs. (1.19) to (1.21) shows that Pressure gradient is small for the regions  $z \in [1, 1.5]$  and  $[2.1, 2.5]$ , and is large for the regions  $z \in [1.6, 1.9]$ . Fig. (1.22), shows a small Pressure gradient for the regions  $z \in [1.1, 1.3]$ ,  $z \in [1.6, 1.8]$ , and  $z \in [2.2, 2.4]$  and also shows that a large Pressure gradient occurs for the regions  $z \in [1.31, 1.59]$ , and  $z \in [1.81, 2.19]$ . Fig. (1.23) represents a small Pressure gradient for the region  $z \in [1.76, 2.25]$  and a large Pressure gradient for the region  $z \in [1.25, 1.75]$ . Effects on the streamlines due to the different values of  $\Phi$  for the trapping phenomenon in the case of five different wave forms is depicted in the Figs. (1.24) to (1.28) It is experimental that in the case of Triangular wave, trapped bolus has small magnitude when it is related to other waves.

## 1.8 Appendix1.0

$$\begin{aligned}
\beta_{11} &= 4(\ln i_1 - \ln i_2), \quad \beta_{12} = 4 + B(i_1^2 - i_2^2), \quad \beta_{13} = B(\ln i_2 - \ln i_1), \\
\beta_{14} &= B(i_2^2 \ln i_1 - i_1^2 \ln i_2) - 4 \ln i_2, \quad \beta_{15} = \frac{-R_s C_s}{\beta_{11}} (\beta_{12} \ln i_1 + \beta_{13} i_1^2 + \beta_{14}), \\
\beta_{16} &= \frac{-R_s C_s}{\beta_{11}} (\beta_{12} \ln i_2 + \beta_{13} i_2^2 + \beta_{14}), \quad \beta_{17} = \frac{1 - \beta_{15} + \beta_{16}}{\ln i_1 - \ln i_2}, \\
\beta_{18} &= \frac{\ln i_2 - \beta_{15} \ln i_2 + \beta_{16} \ln i_1}{\ln i_2 - \ln i_1}, \quad \beta_{19} = \frac{g_r \beta_{13}}{\beta_{11}} - \frac{R_s C_s b_r \beta_{13}}{\beta_{11}}, \\
\beta_{20} &= \frac{g_r \beta_{12}}{\beta_{11}} - \frac{R_s C_s b_r \beta_{12}}{\beta_{11}} + b_r \beta_{17}, \quad \beta_{21} = \frac{g_r \beta_{14}}{\beta_{11}} - \frac{R_s C_s b_r \beta_{14}}{\beta_{11}} + b_r \beta_{18}, \\
\beta_{22} &= \frac{-\beta_{19}}{16(1-m)}, \quad \beta_{23} = \frac{-\beta_{20}}{4(1-m)}, \quad \beta_{24} = \frac{\beta_{20}}{4(1-m)} - \frac{\beta_{21}}{4(1-m)}, \\
\beta_{25} &= \frac{-(1-m)}{\ln i_1 - \ln i_2} (\beta_{22}(i_1^4 - i_2^4) + \beta_{23}(i_1^2 \ln i_1 - i_2^2 \ln i_2) + \beta_{24}(i_1^2 - i_2^2)), \\
\beta_{26} &= -\frac{i_1^2 - i_2^2}{4(\ln i_1 - \ln i_2)}, \quad \beta_{27} = -1 + \frac{1}{(\ln i_1 - \ln i_2)} (\beta_{22}(i_1^4 \ln i_2 - i_2^4 \ln i_1) \\
&\quad + \beta_{23}(i_1^2 \ln i_2 \ln i_1 - i_2^2 \ln i_2 \ln i_1) + \beta_{24}(i_1^2 \ln i_2 - i_2^2 \ln i_1)), \\
\beta_{28} &= \frac{i_1^2 \ln i_2 - i_2^2 \ln i_1}{4(1-m)(\ln i_1 - \ln i_2)}, \quad \beta_{29} = \frac{\beta_{26}}{(1-m)}, \quad \beta_{30} = \frac{\beta_{25}}{(1-m)}, \quad \beta_{31} = 4\beta_{22}, \\
\beta_{32} &= \beta_{23} + 2\beta_{24} + \frac{1}{2(1-m)} \frac{d\mathcal{P}_0}{dz}, \quad \beta_{33} = \beta_{29} \frac{d\mathcal{P}_0}{dz} + \beta_{30}, \quad \beta_{34} = 2\beta_{23}, \\
\beta_{35} &= \frac{-m\beta_{31}^2}{(1-m)}, \quad \beta_{36} = \frac{-2m\beta_{31}\beta_{32}}{(1-m)}, \quad \beta_{37} = \frac{-m}{(1-m)} (2\beta_{31}\beta_{33} + \beta_{32}^2), \\
\beta_{38} &= \frac{-m}{(1-m)} (2\beta_{33}\beta_{34}^2), \quad \beta_{39} = \frac{-m}{(1-m)} (2\beta_{32}\beta_{34}^2), \quad \beta_{40} = \frac{-m}{(1-m)} (2\beta_{31}\beta_{34}^2), \\
\beta_{41} &= \frac{-m}{(1-m)} (2\beta_{32}\beta_{33}), \quad \beta_{42} = \frac{-m\beta_{33}^2}{(1-m)}, \quad \beta_{43} = \frac{\beta_{35}}{7}, \quad \beta_{44} = \frac{-\beta_{40}}{36}, \\
\beta_{45} &= \frac{\beta_{36}}{5} - \frac{2m\beta_{34}^4}{125(1-m)}, \quad \beta_{46} = \frac{-\beta_{39}}{16}, \quad \beta_{47} = \frac{\beta_{37}}{3}, \quad \beta_{48} = \frac{-\beta_{38}}{4}, \\
\beta_{49} &= \frac{\beta_{46}}{6}, \quad \beta_{50} = \frac{2m\beta_{34}^4}{25(1-m)}, \quad \beta_{51} = \frac{\beta_{39}}{4}, \quad \beta_{52} = \frac{-m\beta_{34}^4}{5(1-m)}, \\
\beta_{53} &= \frac{\beta_{38}}{2}, \quad \beta_{54} = (1-m)(-\beta_{53}i_1^2 - \beta_{51}i_1^4 - \beta_{50}i_1^5 - \beta_{49}i_1^6 + \frac{\beta_{42}}{i_1 \ln i_1} \\
&\quad - \frac{\beta_{41}i_1}{\ln i_1} - \frac{\beta_{48}i_1^2}{\ln i_1} - \frac{\beta_{47}i_1^3}{\ln i_1} - \frac{\beta_{46}i_1^4}{\ln i_1} - \frac{\beta_{45}i_1^5}{\ln i_1} - \frac{\beta_{44}i_1^6}{\ln i_1} - \frac{\beta_{43}i_1^7}{\ln i_1} \\
&\quad - \beta_{52}i_1^5 \ln i_1) + \left( \frac{\ln i_1}{(1-m)} - \frac{\ln i_2}{(1-m)} \right) \left( -\frac{\beta_{42}}{i_2} + i_2 \beta_{41} + i_2^2 \beta_{48} \right)
\end{aligned}$$

$$\begin{aligned}
& +i_2^3\beta_{47} + i_2^4\beta_{46} + i_2^5\beta_{45} + i_2^6\beta_{44} + i_2^7\beta_{43} - i_1^2 \ln i_2 \beta_{53} - i_1^4 \ln i_2 \beta_{51} \\
& -i_1^5 \ln i_2 \beta_{50} - i_1^6 \ln i_2 \beta_{49} + i_2^2 \ln i_2 \beta_{53} + i_2^4 \ln i_2 \beta_{51} + i_2^5 \ln i_2 \beta_{50} \\
& +i_2^6 \ln i_2 \beta_{49} + \frac{\ln i_2 \beta_{42}}{i_1 \ln i_1} - \frac{i_1 \ln i_2 \beta_{41}}{\ln i_1} - \frac{i_1^2 \ln i_2 \beta_{48}}{\ln i_1} - \frac{i_1^3 \ln(i_2) \beta_{47}}{\ln i_1} \\
& - \frac{i_1^4 \ln(i_2) \beta_{46}}{\ln i_1} - \frac{i_1^5 \ln i_2 \beta_{45}}{\ln i_1} - \frac{i_1^6 \ln i_2 \beta_{44}}{\ln i_1} - \frac{i_1^7 \ln i_2 \beta_{43}}{\ln i_1} \\
& -i_1^5 \ln i_1 \ln i_2 \beta_{52} + i_2^5 (\ln i_2)^2 \beta_{52}, \\
\beta_{55} = & -\frac{1}{(\ln i_1 - \ln i_2)} \left( -\frac{\ln i_1 \beta_{42}}{i_2} + i_2 \ln i_1 \beta_{41} + i_2^2 \ln i_1 \beta_{48} + i_2^3 \ln i_1 \beta_{47} \right. \\
& +i_2^4 \ln i_1 \beta_{46} + i_2^5 \ln i_1 \beta_{45} + i_2^6 \ln i_1 \beta_{44} + i_2^7 \ln i_1 \beta_{43} + \frac{\ln i_2 \beta_{42}}{i_1} - i_1 \ln i_2 \beta_{41} \\
& -i_1^2 \ln i_2 \beta_{48} - i_1^3 \ln i_2 \beta_{47} - i_1^4 \ln i_2 \beta_{46} - i_1^5 \ln i_2 \beta_{45} - i_1^6 \ln i_2 \beta_{44} - i_1^7 \ln i_2 \beta_{43} \\
& -i_1^2 \ln i_1 \ln i_2 \beta_{53} - i_1^4 \ln i_1 \ln i_2 \beta_{51} - i_1^5 \ln i_1 \ln i_2 \beta_{50} - i_1^6 \ln i_1 \ln i_2 \beta_{49} \\
& +i_2^2 \ln i_1 \ln i_2 \beta_{53} + i_2^4 \ln i_1 \ln i_2 \beta_{51} + i_2^5 \ln i_1 \ln i_2 \beta_{50} + i_2^6 \ln i_1 \ln i_2 \beta_{49} \\
& \left. -i_1^5 (\ln i_1)^2 \ln(i_2) \beta_{52} + i_2^5 \ln i_1 (\ln i_2)^2 \beta_{52} \right), \\
\beta_{56} = & \frac{\beta_{22}(i_2^6 - i_1^6)}{6} + \beta_{23} \left( \left( \frac{i_2^4 \ln i_2}{4} - \frac{i_2^4}{16} \right) - \left( \frac{i_1^4 \ln i_2}{4} - \frac{i_1^4}{16} \right) \right) + \frac{\beta_{24}(i_2^4 - i_1^4)}{4} \\
& + \beta_{30} \left( \left( \frac{i_2^2 \ln i_2}{2} - \frac{i_1^2 \ln i_2}{2} \right) - \frac{(i_2^2 - i_1^2)}{4} \right) + \frac{\beta_{27}(i_2^2 - i_1^2)}{2}, \\
\beta_{57} = & \frac{(i_2^4 - i_1^4)}{16(1-m)} + \beta_{29} \left( \left( \frac{i_2^2 \ln i_2}{2} - \frac{i_1^2 \ln i_1}{2} \right) - \frac{(i_2^2 - i_1^2)}{4} \right) + \frac{\beta_{28}(i_2^2 - i_1^2)}{2}, \\
\beta_{58} = & \frac{\beta_{43}}{9}, \beta_{59} = \frac{\beta_{44}}{8} - \frac{\beta_{49}}{64}, \beta_{60} = \frac{\beta_{45}}{7} - \frac{\beta_{50}}{49} + \frac{2\beta_{52}}{7(49)}, \beta_{61} = \frac{\beta_{46}}{6} - \frac{\beta_{51}}{36}, \\
\beta_{62} = & \frac{\beta_{47}}{5}, \beta_{63} = \frac{\beta_{48}}{4} - \frac{\beta_{53}}{16}, \beta_{64} = \frac{\beta_{41}}{3}, \beta_{65} = \frac{\beta_{55}}{2} - \frac{\beta_{54}}{4(1-m)}, \beta_{66} = \frac{\beta_{49}}{8}, \\
\beta_{67} = & \frac{\beta_{50}}{7} - \frac{2\beta_{52}}{49}, \beta_{68} = \frac{\beta_{51}}{6}, \beta_{69} = \frac{\beta_{53}}{4}, \beta_{70} = \frac{\beta_{52}}{7}, \beta_{71} = \frac{\beta_{54}}{2(1-m)}, \\
\beta_{72} = & (i_2^9 - i_1^9)\beta_{58} + (i_2^8 - i_1^8)\beta_{59} + (i_2^7 - i_1^7)\beta_{60} + (i_2^6 - i_1^6)\beta_{61} + (i_2^5 - i_1^5)\beta_{62} \\
& + (i_2^4 - i_1^4)\beta_{63} + (i_2^3 - i_1^3)\beta_{64} + (i_2^2 - i_1^2)\beta_{65} - \beta_{42}(i_2 - i_1) + \beta_{66}(i_2^8 \ln(i_2) \\
& - i_1^8 \ln(i_1)) + \beta_{67}(i_2^7 \ln(i_2) - i_1^7 \ln(i_1)) + \beta_{68}(i_2^6 \ln(i_2) - i_1^6 \ln(i_1)) \\
& + \beta_{69}(i_2^4 \ln(i_2) - i_1^4 \ln(i_1)) + \beta_{70}((i_2^7 (\ln(i_2))^2 - i_1^8 (\ln(i_2))^2) + \beta_{71}((i_2^2 \ln(i_2) \\
& - i_1^2 \ln(i_1)), \\
\beta_{73} = & \frac{-\beta_{56} - H_y \beta_{72}}{\beta_{57}}.
\end{aligned}$$



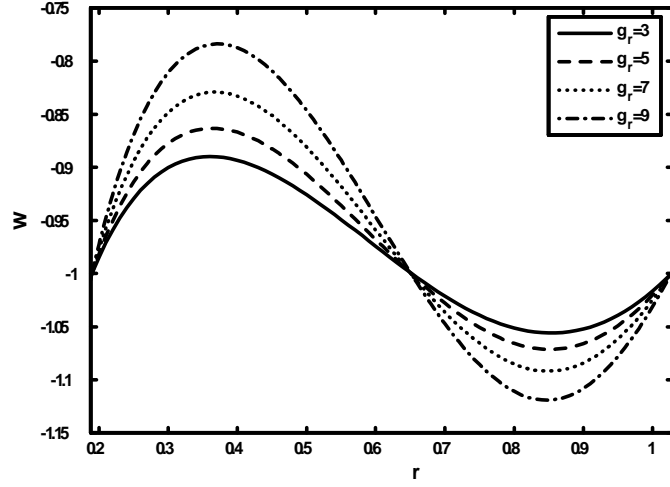


**Fig. (1.1)**, Velocity field for  $z = 0.01$ ,  $m = 0.23$ ,  $Q = 0.02$ ,  $\Phi = 0.43$ ,  $H_y = 0.07$ ,  $B = 0.06$ ,  
 $\epsilon = 0.19$ ,  $C_s = 4.53$ ,  $b_r = 5.61$ ,  $R_s = 3.82$ .

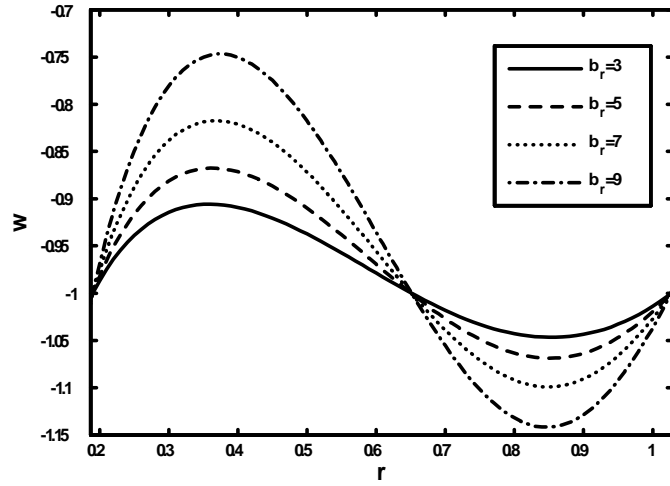


**Fig. (1.2)**, Velocity field for  $z = 0.01$ ,  $R_s = 3.82$ ,  $m = 0.23$ ,  $Q = 0.02$ ,  $B = 0.06$ ,  $\Phi = 0.43$ ,  
 $b_r = 5.61$ ,  $\epsilon = 0.19$ ,  $C_s = 4.53$ ,  $H_y = 0.07$ .

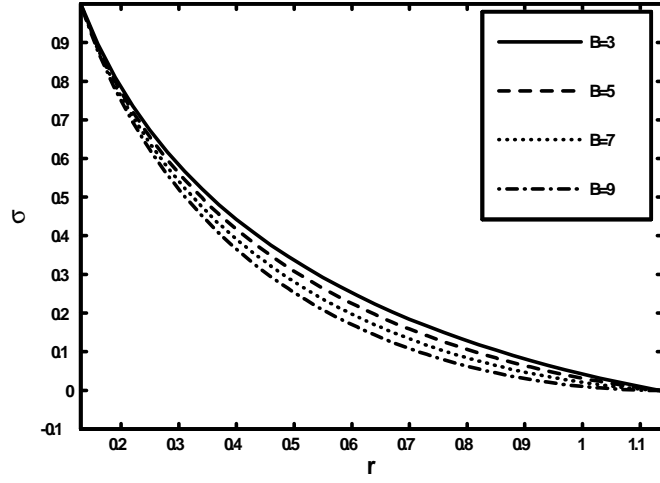


**Fig. (1.3)**, Concentration field for  $\Phi = 0.14$ ,  $H_y = 0.33$ ,  $\epsilon = 0.13$ ,  $z = 0.3$ ,  $b_r = 0.13$ ,  
 $R_s = 0.32$ ,  $C_s = 0.31$ ,  $g_r = 0.21$ .

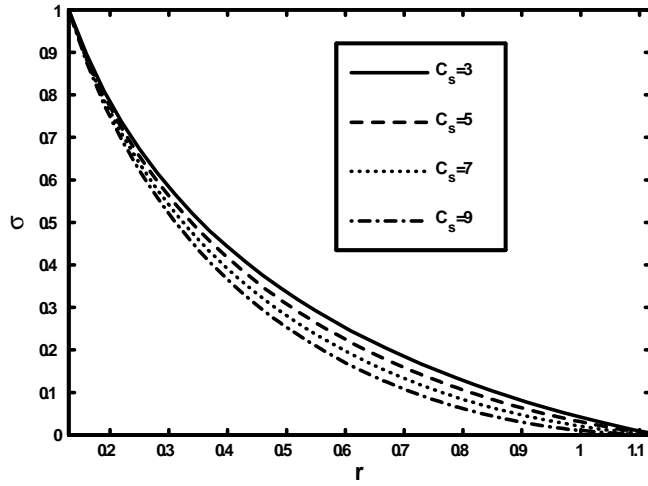


**Fig. (1.4)**, Concentration field for  $z = 0.3$ ,  $\Phi = 0.14$ ,  $\epsilon = 0.13$ ,  $b_r = 0.21$ ,  $H_y = 0.33$ ,  
 $R_s = 0.31$ ,  $B = 0.32$ ,  $g_r = 0.13$ .

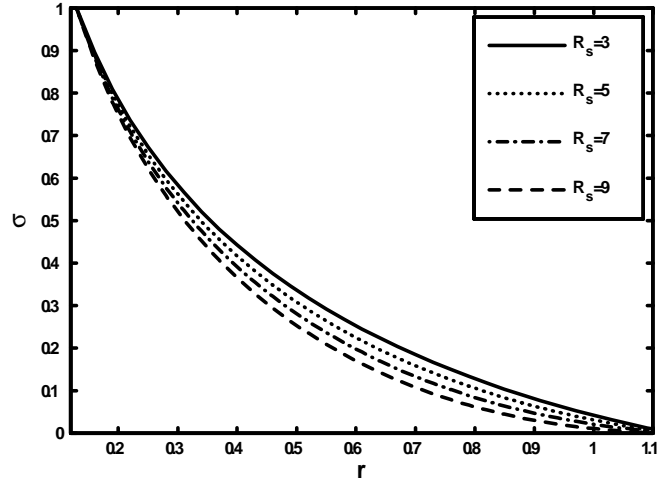


**Fig. (1.5)**, Concentration field for  $H_y = 0.33$ ,  $\Phi = 0.14$ ,  $z = 0.3$ ,  $g_r = 0.13$ ,  $b_r = 0.21$ ,  
 $C_s = 0.31$ ,  $\epsilon = 0.13$ ,  $B = 0.32$ .

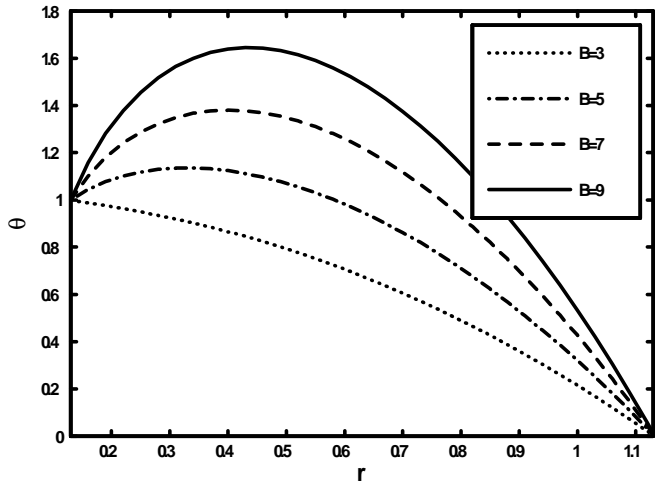


**Fig. (1.6)**, Temperature field for  $\Phi = 0.14$ ,  $H_y = 0.33$ ,  $z = 0.3$ ,  $b_r = 0.21$ ,  $g_r = 0.13$ ,  
 $R_s = 0.31$ ,  $C_s = 0.32$ ,  $\epsilon = 0.13$ .

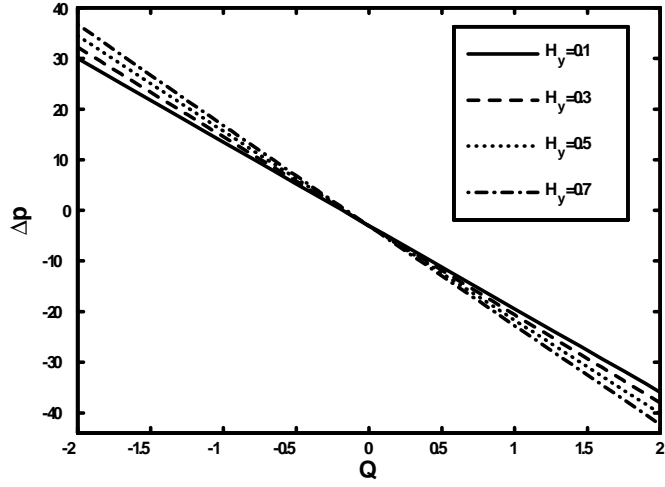


**Fig. (1.7)**, Pressure rise versus flow rate for  $\Phi = 0.07$ ,  $B = 0.23$ ,  $\epsilon = 0.01$ ,  $C_s = 3.91$ ,  
 $g_r = 2.64$ ,  $b_r = 4.92$ ,  $R_s = 3.33$ ,  $m = 0.24$ .

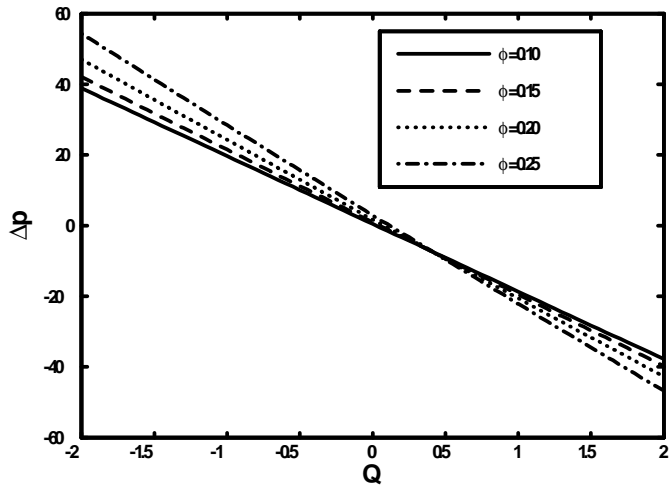


**Fig. (1.8)**, Pressure rise distribution for  $m = 0.11$ ,  $H_y = 0.12$ ,  $B = 0.3$ ,  $\epsilon = 0.01$ ,  $C_s = 0.31$ ,  
 $g_r = 0.33$ ,  $b_r = 0.26$ ,  $R_s = 0.42$ .

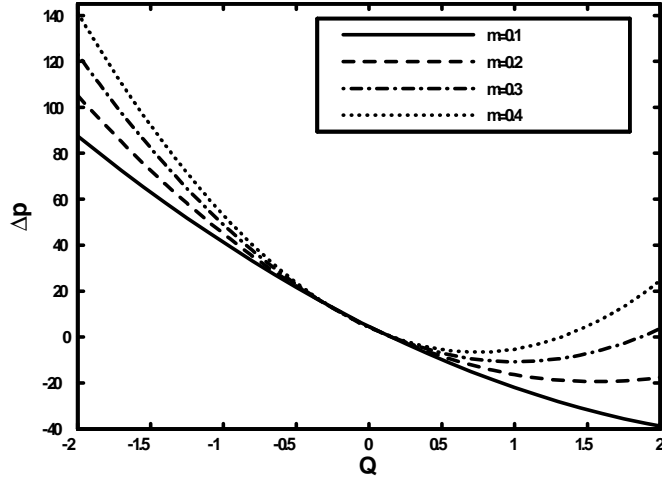


**Fig. (1.9)**, Pressure rise versus flow rate for  $\Phi = 0.28$ ,  $H_y = 0.63$ ,  $B = 0.11$ ,  $\epsilon = 0.02$ ,  
 $C_s = 0.51$ ,  $g_r = 0.63$ ,  $b_r = 0.71$ ,  $R_s = 0.32$ .

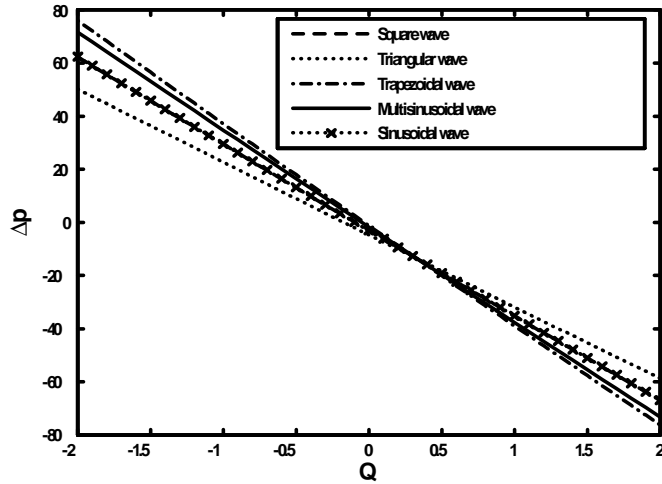


**Fig. (1.10)**, Pressure rise versus flow rate distribution for  $\Phi = 0.18$ ,  $H_y = 0.21$ ,  $B = 1.09$ ,  
 $f = 2$ ,  $\epsilon = 0.09$ ,  $C_s = 2.4$ ,  $g_r = 3.3$ ,  $b_r = 4.2$ ,  $R_s = 2.5$ ,  $m = 0.01$ .

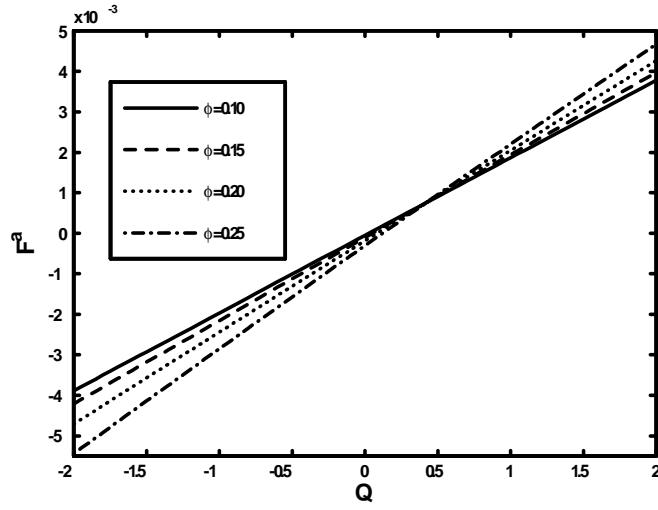


**Fig. (1.11)**, Friction force (on inward cylinder ) versus flow rate for  $H_y = 0.12$ ,  $B = 0.3$ ,  $R_s = 0.42$ ,  $\epsilon = 0.01$ ,  $b_r = 0.26$ ,  $C_s = 0.31$ ,  $m = 0.11$ ,  $g_r = 0.33$ .

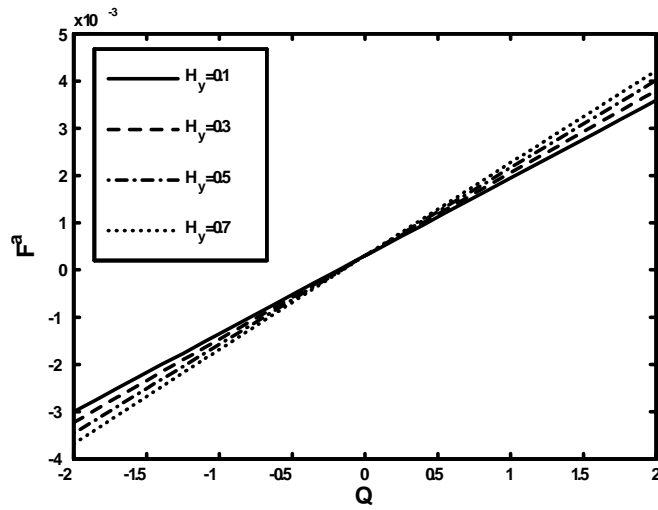


**Fig. (1.12)**, Friction force (on inward cylinder ) versus flow rate for  $\Phi = 0.07$ ,  $B = 0.23$ ,  $\epsilon = 0.01$ ,  $g_r = 2.64$ ,  $C_s = 3.91$ ,  $b_r = 4.92$ ,  $m = 0.24$ ,  $R_s = 3.33$ .

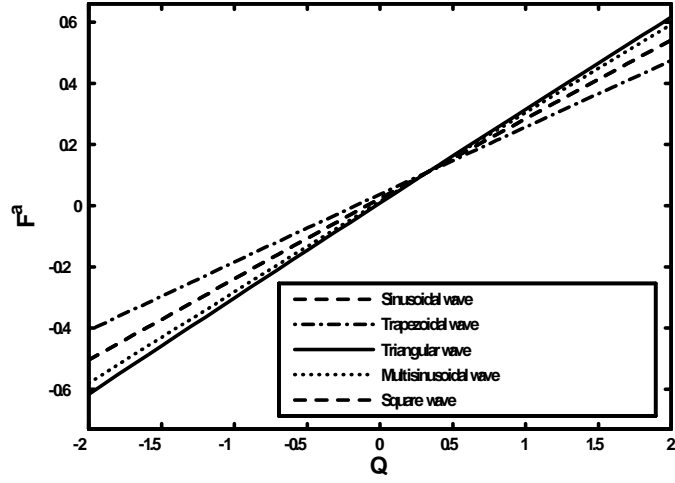


**Fig. (1.13)**, Friction force (outward cylinder ) versus flow rate for  $\Phi = 0.18$ ,  $H_y = 0.21$ ,  $C_s = 2.4$ ,  $g_r = 3.3$ ,  $B = 1.09$ ,  $f = 2$ ,  $\epsilon = 0.09$ ,  $m = 0.01$ ,  $b_r = 4.2$ ,  $R_s = 2.5$ .

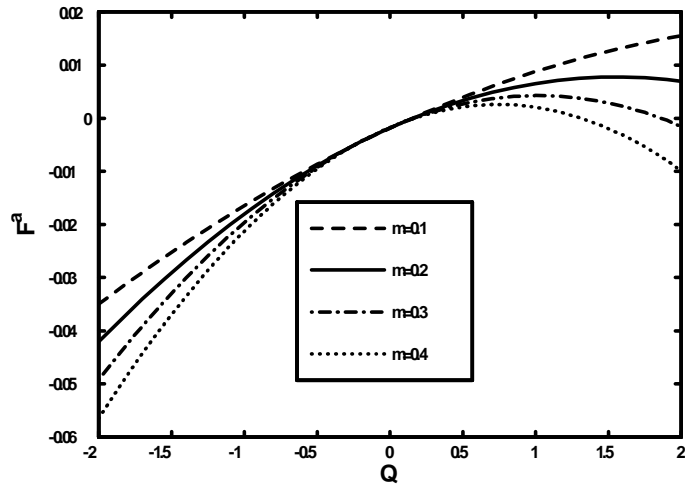


**Fig. (1.14)**, Friction force (inward cylinder ) versus flow rate for  $g_r = 0.63$ ,  $H_y = 0.63$ ,  $R_s = 0.32$ ,  $B = 0.11$ ,  $\epsilon = 0.02$ ,  $C_s = 0.51$ ,  $b_r = 0.71$ ,  $\Phi = 0.28$ .

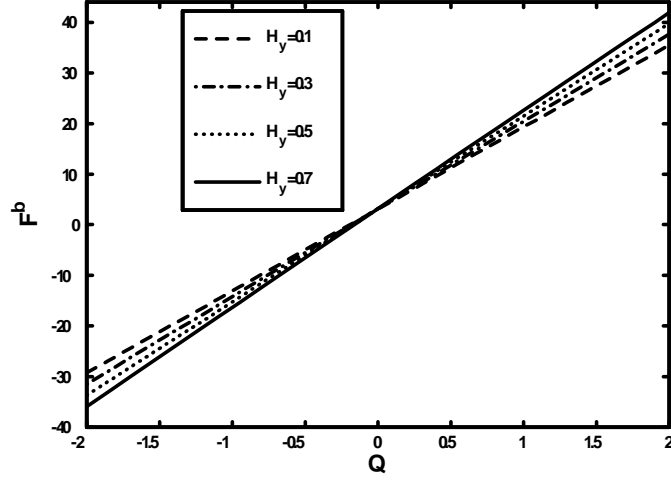


**Fig. (1.15)**, Friction force (outward cylinder ) versus flow rate for  $\Phi = 0.07$ ,  $B = 0.23$ ,  $\epsilon = 0.01$ ,  $C_s = 3.91$ ,  $g_r = 2.64$ ,  $b_r = 4.92$ ,  $R_s = 3.33$ ,  $m = 0.24$ .

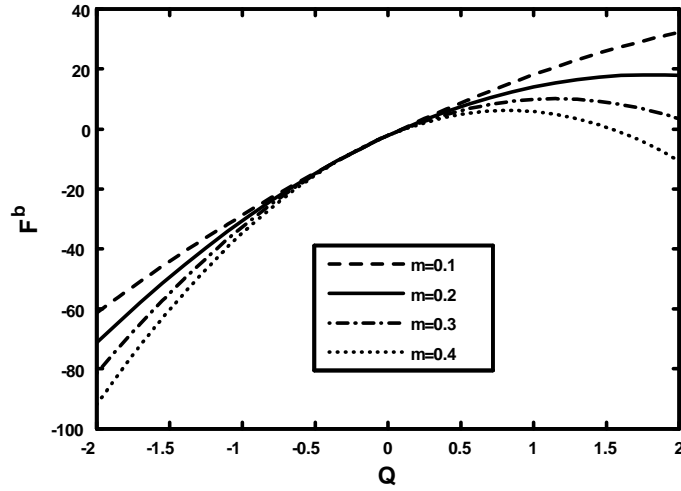


**Fig. (1.16)**, Friction force (outward cylinder ) versus flow rate for  $\Phi = 0.28$ ,  $B = 0.11$ ,  $R_s = 0.32$ ,  $\epsilon = 0.02$ ,  $C_s = 0.51$ ,  $g_r = 0.63$ ,  $b_r = 0.71$ ,  $H_y = 0.63$ .



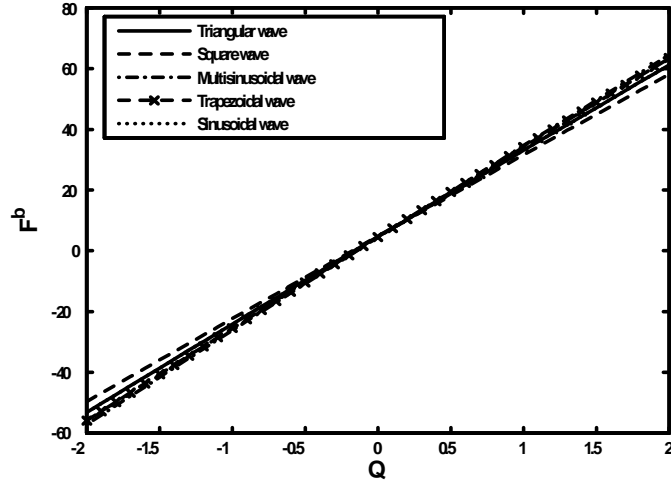


**Fig. (1.17)**, Friction force (inward cylinder ) versus flow rate for  $\Phi = 0.18$ ,  $H_y = 0.21$ ,  $B = 1.09$ ,  $m = 0.01$ ,  $\epsilon = 0.09$ ,  $g_r = 3.3$ ,  $C_s = 2.4$ ,  $b_r = 4.2$ ,  $f = 2$ ,  $R_s = 2.5$ .

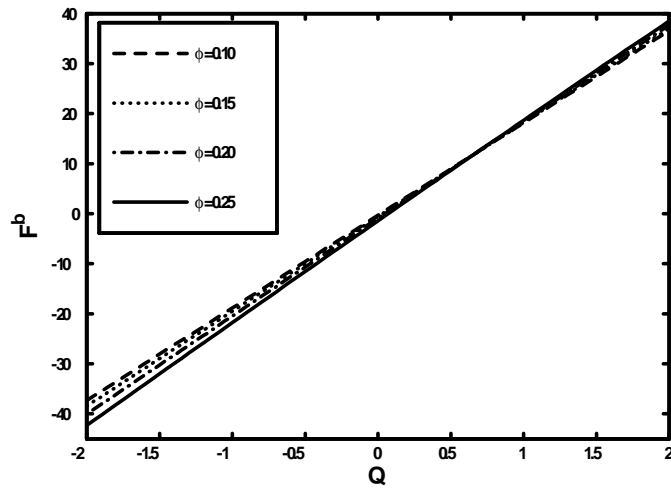


**Fig. (1.18)**, Friction force (outward cylinder ) versus flow rate for  $g_r = 0.33$ ,  $m = 0.11$ ,  $B = 0.3$ ,  $\epsilon = 0.01$ ,  $H_y = 0.12$ ,  $b_r = 0.26$ ,  $C_s = 0.31$ ,  $R_s = 0.42$ .

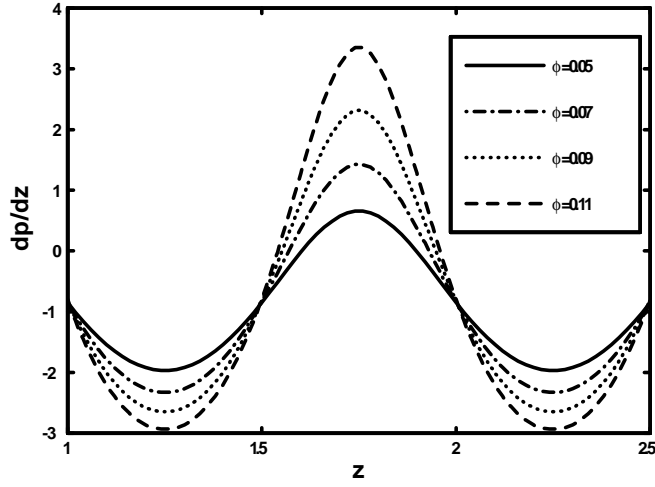


**Fig. (1.19)**, Pressure gradient (Sinusoidal wave) for  $m = 0.23$ ,  $H_y = 0.16$ ,  $B = 0.23$ ,  $Q = 0.02$ ,  $\epsilon = 0.11$ ,  $g_r = 3.44$ ,  $b_r = 3.77$ ,  $R_s = 2.62$ ,  $C_s = 3.88$ .

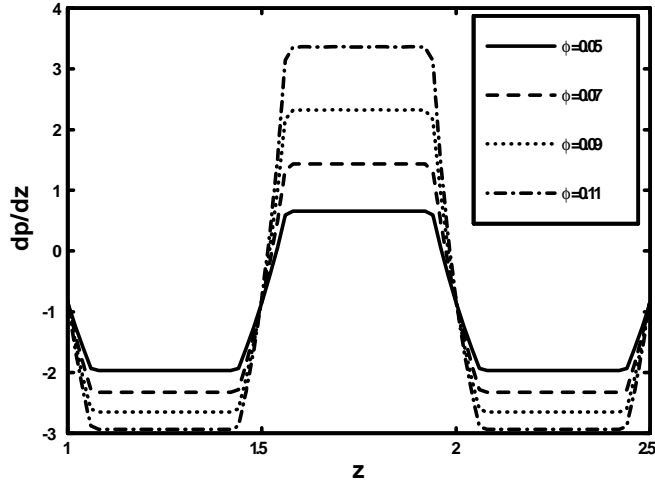


**Fig. (1.20)**, Pressure gradient (trapezoidal wave) for  $b_r = 3.77$ ,  $m = 0.23$ ,  $B = 0.23$ ,  $\epsilon = 0.11$ ,  $H_y = 0.16$ ,  $g_r = 3.44$ ,  $Q = 0.02$ ,  $C_s = 3.88$ ,  $R_s = 2.62$ .

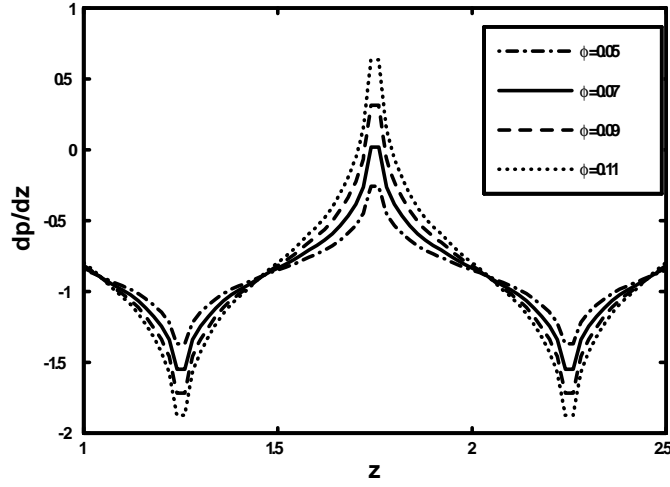


**Fig. (1.21)**, Pressure gradient (Triangular wave) for  $m = 0.23$ ,  $H_y = 0.16$ ,  $B = 0.23$ ,  $\epsilon = 0.11$ ,  $R_s = 2.62$ ,  $Q = 0.02$ ,  $g_r = 3.44$ ,  $b_r = 3.77$ ,  $C_s = 3.88$ .

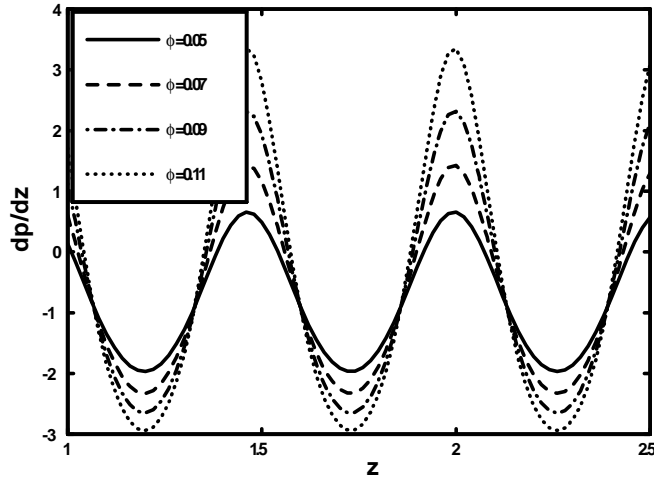


**Fig. (1.22)**, Pressure gradient (Multisinusoidal wave) for  $R_s = 2.62$ ,  $H_y = 0.16$ ,  $m = 0.23$ ,  $B = 0.23$ ,  $\epsilon = 0.11$ ,  $Q = 0.02$ ,  $g_r = 3.44$ ,  $b_r = 3.77$ ,  $C_s = 3.88$ .

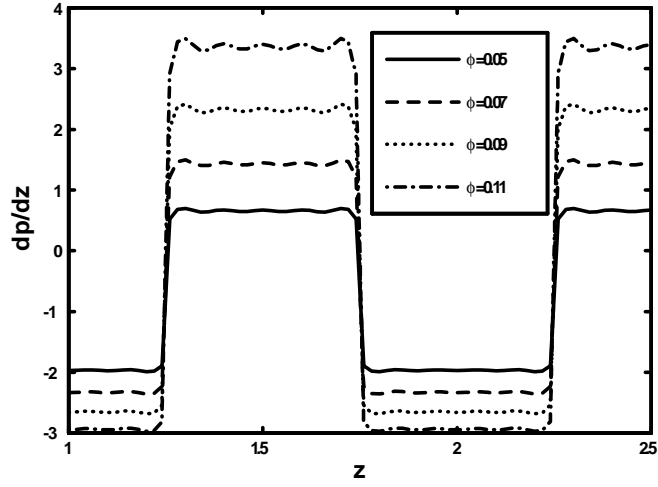


**Fig. (1.23)**, Pressure gradient (Square wave)  $H_y = 0.16$ ,  $m = 0.23$ ,  $b_r = 3.77$ ,  $C_s = 3.88$ ,  
 $B = 0.23$ ,  $Q = 0.02$ ,  $\epsilon = 0.11$ ,  $g_r = 3.44$ ,  $R_s = 2.62$ .

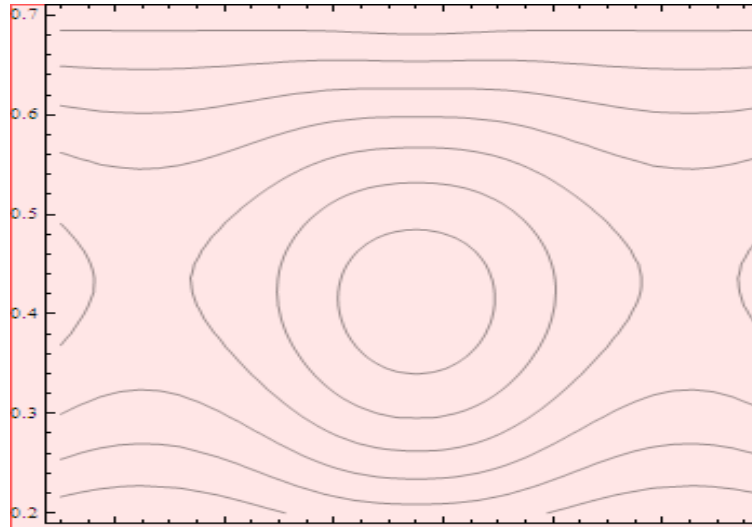


**Fig. (1.24)**, Stream lines (Sinusoidal wave) for  $m = 0.02$ ,  $H_y = 0.14$ ,  $B = 0.12$ ,  $Q = 0.94$ ,  
 $\epsilon = 0.38$ ,  $C_s = 3.99$ ,  $g_r = 4.44$ ,  $b_r = 5.22$ ,  $R_s = 5.13$ ,  $\Phi = 0.11$ .

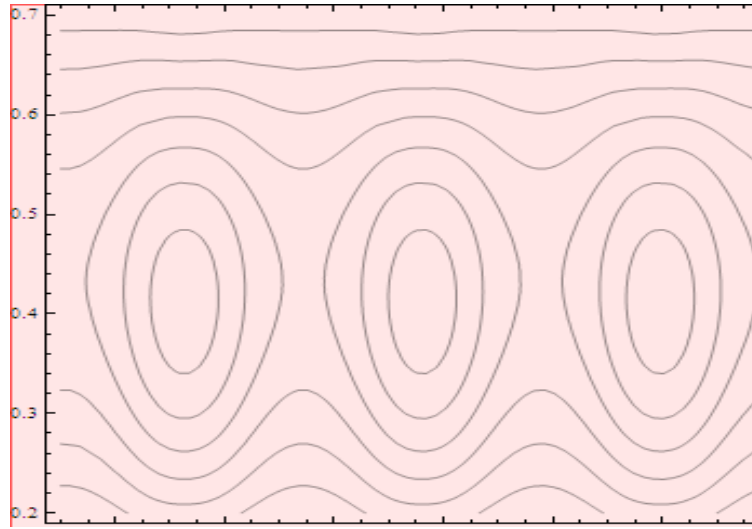


**Fig. (1.25)**, Stream lines (Multisinusoidal wave) for  $m = 0.02$ ,  $b_r = 5.22$ ,  $B = 0.12$ ,  $\Phi = 0.11$ ,  
 $Q = 0.94$ ,  $H_y = 0.14$ ,  $\epsilon = 0.38$ ,  $C_s = 3.99$ ,  $g_r = 4.44$ ,  $R_s = 5.13$ .

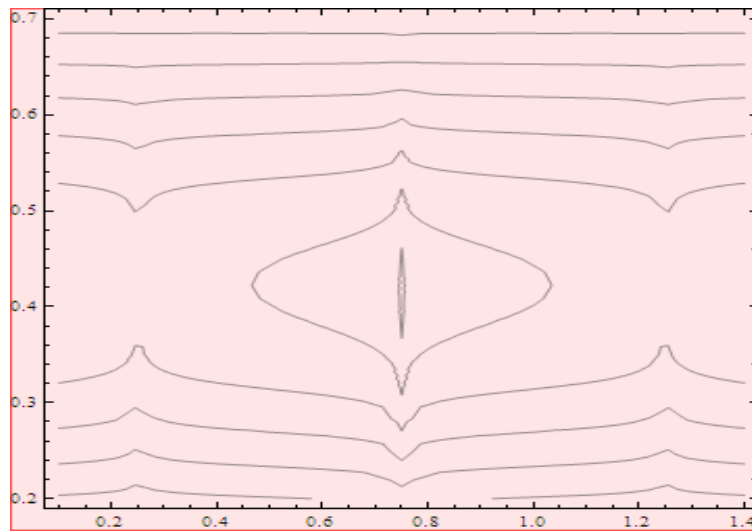


**Fig. (1.26)**, Stream lines (Triangular wave) for  $\Phi = 0.11$ ,  $m = 0.02$ ,  $b_r = 5.22$ ,  $H_y = 0.14$ ,  
 $B = 0.12$ ,  $Q = 0.94$ ,  $C_s = 3.99$ ,  $\epsilon = 0.38$ ,  $g_r = 4.44$ ,  $R_s = 5.13$ .

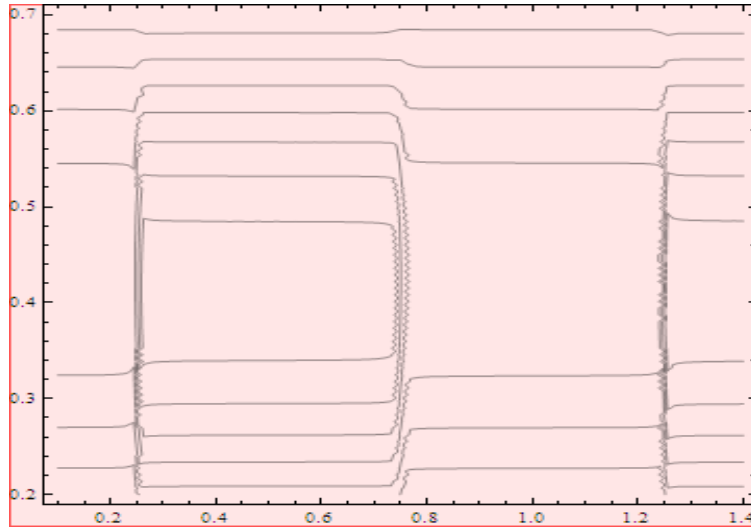


**Fig. (1.27)**, Stream lines (Square wave) for  $m = 0.02$ ,  $R_s = 5.13$ ,  $Q = 0.94$ ,  $b_r = 5.22$ ,  $\epsilon = 0.38$ ,  $B = 0.12$ ,  $C_s = 3.99$ ,  $g_r = 4.44$ ,  $H_y = 0.14$ ,  $\Phi = 0.11$ .

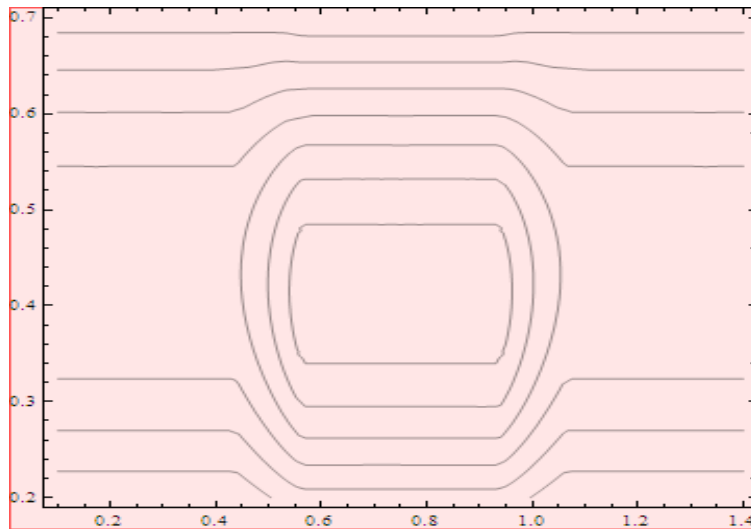


**Fig. (1.28)**, Stream lines for (Trapezoidal wave)  $m = 0.02$ ,  $g_r = 4.44$ ,  $H_y = 0.14$ ,  $b_r = 5.22$ ,  $\epsilon = 0.38$ ,  $B = 0.12$ ,  $\Phi = 0.11$ ,  $Q = 0.94$ ,  $C_s = 3.99$ ,  $R_s = 5.13$ .

## Chapter 2

# Effects of nanoparticles on the peristaltic motion of hyperbolic tangent fluid model in an annulus

### 2.1 Introduction

In this chapter, we have presented the effects of nanoparticles on the peristaltic flow of hyperbolic tangent fluid in an annulus. Tangent hyperbolic fluid equations are simplified by suppositions of low Reynolds number and long wave length. Analytical solution have been computed with the help of homotopy perturbation and Adomian decomposition method for velocity, temperature and nanoparticle concentration. Solutions are presented through graphs. The results of  $\Delta P$  (Pressure rise), temperature, nanoparticle concentration and Pressure gradient are drawn for numerous inserted parameters. The relationship of both the analytical solutions are also offered.

### 2.2 Flow equations

Governing equations for an incompressible hyperbolic tangent fluid for mass, momentum, energy and nanoparticle concentration are defined as [22 – 23]

$$\operatorname{div} \tilde{\mathbf{A}} = 0, \tag{2.1}$$

$$\rho \frac{d\tilde{\mathbf{A}}}{dt} = \text{div} \tilde{\mathbf{S}} + \rho \mathbf{f}, \quad (2.2)$$

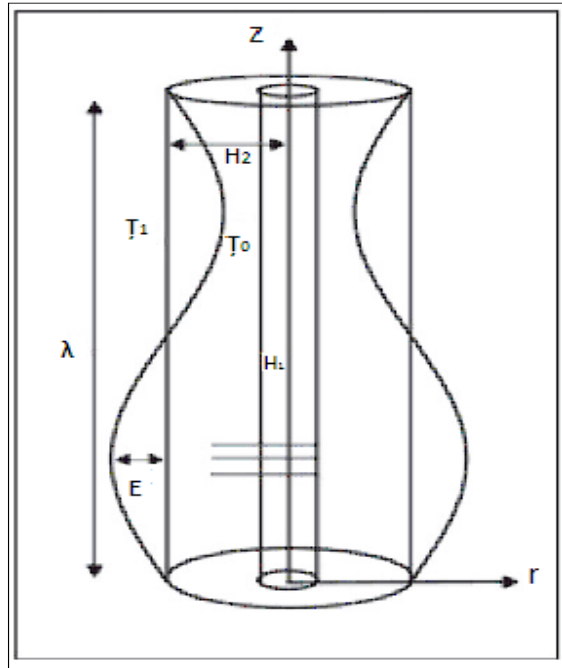
$$(\rho c)_f \frac{d\tilde{T}}{dt} = k \nabla^2 \tilde{T} + (\rho c)_p [d_b \nabla \tilde{C} \cdot \nabla \tilde{T} + \left(\frac{d_{\tilde{T}}}{\tilde{T}_1}\right) \nabla \tilde{T} \cdot \nabla \tilde{T}], \quad (2.3)$$

$$\frac{d\tilde{C}}{dt} = d_b \nabla^2 \tilde{C} + \left(\frac{d_{\tilde{T}}}{\tilde{T}_1}\right) \nabla^2 \tilde{T}, \quad (2.4)$$

where  $\tilde{\mathbf{A}}$ , is the velocity component,  $\tilde{C}$  the nanoparticle phenomenon,  $d_b$  the Brownian diffusion coefficient and  $d_{\tilde{T}}$  the thermophoretic diffusion coefficient.

### 2.3 Statement and formulation of the problem

Considering the Peristaltic transport of an incompressible hyperbolic tangent fluid in an annulus. Inward cylinder is rigid and sustained at temperature  $\tilde{T}_0$  and the nanoparticle velocity  $\tilde{C}_0$  while the outward cylinder takes a sinusoidal wave moving down its walls having temperature  $\tilde{T}_1$  and nanoparticle velocity  $\tilde{C}_1$ . The wall surface geometry is defined as





$$\tilde{R}_1 = H_1, \quad (2.5)$$

$$\tilde{R}_2 = H_2 + E \sin \frac{2\pi}{\lambda} (\tilde{z} - \tilde{s}\tilde{t}). \quad (2.6)$$

where  $H_1, H_2$  denotes the inward and outward radius of cylinders,  $E$  amplitude of wave,  $\lambda$  wavelength,  $\tilde{s}$  wave speed and  $\tilde{t}$  is time. With the help of Eq. (1.11), Eqs. (2.1) to (2.4) take the following form

$$\frac{\partial \tilde{U}}{\partial \tilde{R}} + \frac{\tilde{U}}{\tilde{R}} + \frac{\partial \tilde{W}}{\partial \tilde{Z}} = 0, \quad (2.7)$$

$$\rho \left[ \frac{\partial \tilde{U}}{\partial \tilde{t}} + \tilde{U} \frac{\partial \tilde{U}}{\partial \tilde{R}} + \tilde{W} \frac{\partial \tilde{U}}{\partial \tilde{Z}} \right] = -\frac{\partial \tilde{P}}{\partial \tilde{R}} + \frac{1}{\tilde{R}} \frac{\partial (\tilde{R} \tilde{\tau}_{\tilde{R}\tilde{R}})}{\partial \tilde{R}} + \frac{\partial (\tilde{\tau}_{\tilde{R}\tilde{Z}})}{\partial \tilde{Z}} - \frac{\tilde{\tau}_{\tilde{\theta}\tilde{\theta}}}{\tilde{R}}, \quad (2.8)$$

$$\begin{aligned} \rho \left( \frac{\partial \tilde{W}}{\partial \tilde{t}} + \tilde{U} \frac{\partial \tilde{W}}{\partial \tilde{R}} + \tilde{W} \frac{\partial \tilde{W}}{\partial \tilde{Z}} \right) &= -\frac{\partial \tilde{P}}{\partial \tilde{Z}} + \frac{1}{\tilde{R}} \frac{\partial (\tilde{R} \tilde{\tau}_{\tilde{R}\tilde{Z}})}{\partial \tilde{R}} + \frac{\partial (\tilde{\tau}_{\tilde{Z}\tilde{Z}})}{\partial \tilde{Z}} + \rho g \alpha_{\tilde{T}} (\tilde{T} - \tilde{T}_1) \\ &+ \rho g \alpha_{\tilde{C}} (\tilde{C} - \tilde{C}_1), \end{aligned} \quad (2.9)$$

$$\begin{aligned} \left( \frac{\partial \tilde{T}}{\partial \tilde{t}} + \tilde{U} \frac{\partial \tilde{T}}{\partial \tilde{R}} + \tilde{W} \frac{\partial \tilde{T}}{\partial \tilde{Z}} \right) &= \alpha \left( \frac{\partial^2 \tilde{T}}{\partial \tilde{R}^2} + \frac{1}{\tilde{R}} \frac{\partial \tilde{T}}{\partial \tilde{R}} + \frac{\partial^2 \tilde{T}}{\partial \tilde{Z}^2} \right) + \tau_1 \left\{ d_b \left( \frac{\partial \tilde{C}}{\partial \tilde{R}} \frac{\partial \tilde{T}}{\partial \tilde{R}} + \frac{\partial \tilde{C}}{\partial \tilde{Z}} \frac{\partial \tilde{T}}{\partial \tilde{Z}} \right) \right. \\ &\left. + \frac{d_{\tilde{T}}}{\tilde{T}_1} \left[ \left( \frac{\partial \tilde{T}}{\partial \tilde{R}} \right)^2 + \left( \frac{\partial \tilde{T}}{\partial \tilde{Z}} \right)^2 \right] \right\}, \end{aligned} \quad (2.10)$$

$$\left( \frac{\partial \tilde{C}}{\partial \tilde{t}} + \tilde{U} \frac{\partial \tilde{C}}{\partial \tilde{R}} + \tilde{W} \frac{\partial \tilde{C}}{\partial \tilde{Z}} \right) = d_b \left( \frac{\partial^2 \tilde{C}}{\partial \tilde{R}^2} + \frac{1}{\tilde{R}} \frac{\partial \tilde{C}}{\partial \tilde{R}} + \frac{\partial^2 \tilde{C}}{\partial \tilde{Z}^2} \right) + \frac{d_{\tilde{T}}}{\tilde{T}_1} \left( \frac{\partial^2 \tilde{T}}{\partial \tilde{R}^2} + \frac{1}{\tilde{R}} \frac{\partial \tilde{T}}{\partial \tilde{R}} + \frac{\partial^2 \tilde{T}}{\partial \tilde{Z}^2} \right), \quad (2.11)$$

in the above equations,  $\tilde{C}$  is the nanoparticle volume fraction,  $d_{\tilde{T}}$  the thermophoretic diffusion coefficient,  $d_b$  the Brownian diffusion coefficients of mass diffusivity  $\tau_1 = \frac{(\rho c)_p}{(\rho c)_f}$  depicts the ratio of the effective heat capacity in the case of nano particle material and heat capacity

of the fluid. In the fixed coordinates  $(\tilde{\mathbf{R}}, \tilde{\mathbf{Z}})$  the flow in the cylinders is unsteady, it converts steady in a wave frame  $(\tilde{\mathbf{r}}, \tilde{\mathbf{z}})$  moving with same speed as the wave moves in the  $\tilde{\mathbf{Z}}$  directions. The conversions between the wave references are

$$\tilde{\mathbf{r}} = \tilde{\mathbf{R}}, \quad \tilde{\mathbf{z}} = \tilde{\mathbf{Z}} - \tilde{s}\tilde{\mathbf{t}}, \quad \tilde{\mathbf{u}} = \tilde{\mathbf{U}}, \quad \tilde{\mathbf{w}} = \tilde{\mathbf{W}} - \tilde{s}, \quad (2.12)$$

In the wave reference  $\tilde{\mathbf{u}}$  and  $\tilde{\mathbf{w}}$  are the velocity components. The boundary limits are expressed as

$$\begin{aligned} \tilde{\mathbf{w}} &= -\tilde{s}, \text{ at } \tilde{\mathbf{r}} = \tilde{\mathbf{i}}_1, \quad \tilde{\mathbf{w}} = -\tilde{s} \text{ at } \tilde{\mathbf{r}} = \tilde{\mathbf{i}}_2 = H_2 + E \sin \frac{2\pi}{\lambda}(\tilde{\mathbf{z}}), \\ \tilde{\mathbf{T}} &= \tilde{\mathbf{T}}_0 \text{ at } \tilde{\mathbf{r}} = \tilde{\mathbf{i}}_1, \quad \tilde{\mathbf{T}} = \tilde{\mathbf{T}}_1 \text{ at } \tilde{\mathbf{r}} = \tilde{\mathbf{i}}_2, \\ \tilde{\mathbf{C}} &= \tilde{\mathbf{C}}_0 \text{ at } \tilde{\mathbf{r}} = \tilde{\mathbf{i}}_1, \quad \tilde{\mathbf{C}} = \tilde{\mathbf{C}}_1 \text{ at } \tilde{\mathbf{r}} = \tilde{\mathbf{i}}_2. \end{aligned} \quad (2.13)$$

Introducing the dimensionless variables

$$\begin{aligned} \mathbf{R} &= \frac{\tilde{\mathbf{R}}}{H_2}, \quad \mathbf{r} = \frac{\tilde{\mathbf{r}}}{H_2}, \quad \mathbf{W} = \frac{\tilde{\mathbf{W}}}{\tilde{s}}, \quad \mathbf{w} = \frac{\tilde{\mathbf{w}}}{\tilde{s}}, \quad \mathbf{Z} = \frac{\tilde{\mathbf{Z}}}{\lambda}, \quad z = \frac{\tilde{\mathbf{z}}}{\lambda}, \quad \mathbf{U} = \frac{\lambda\tilde{\mathbf{U}}}{H_2\tilde{s}}, \\ \mathbf{u} &= \frac{\lambda\tilde{\mathbf{u}}}{H_2\tilde{s}}, \quad \mathbf{t} = \frac{\tilde{\mathbf{t}}}{\lambda}, \quad \mathbf{P} = \frac{H_2^2\tilde{\mathbf{P}}}{\tilde{s}\lambda\eta}, \quad \theta = \frac{\tilde{\mathbf{T}} - \tilde{\mathbf{T}}_1}{\tilde{\mathbf{T}}_0 - \tilde{\mathbf{T}}_1}, \quad \hat{\delta} = \frac{H_2}{\lambda}, \quad R_y = \frac{\rho\tilde{s}H_2}{\eta}, \\ \tilde{\mathbf{S}} &= \frac{H_2\tilde{\mathbf{S}}}{\tilde{s}\eta}, \quad \mathbf{i}_1 = \frac{\tilde{\mathbf{i}}_1}{H_2} = \frac{H_1}{H_2} = \epsilon, \quad \mathbf{i}_2 = \frac{\tilde{\mathbf{i}}_2}{H_2} = 1 + \Phi \sin 2\pi z, \quad H_y = \frac{\Gamma\tilde{s}}{H_2}, \\ \alpha &= \frac{k}{(\rho c)_f}, \quad B_m = \frac{(\rho c)_p d_b(\tilde{\mathbf{C}}_0 - \tilde{\mathbf{C}}_1)}{(\rho c)_f \alpha}, \quad T_m = \frac{(\rho c)_p d_{\tilde{\mathbf{T}}}(\tilde{\mathbf{T}}_0 - \tilde{\mathbf{T}}_1)}{(\rho c)_f \tilde{\mathbf{T}}_1 \alpha}, \\ g_r &= \frac{\rho g \alpha_{\tilde{\mathbf{T}}} H_2^2 (\tilde{\mathbf{T}}_0 - \tilde{\mathbf{T}}_1)}{\eta \tilde{s}}, \quad b_r = \frac{\rho g \alpha_{\tilde{\mathbf{C}}} H_2^2 (\tilde{\mathbf{C}}_0 - \tilde{\mathbf{C}}_1)}{\eta \tilde{s}}, \quad \Phi = \frac{E}{H_2}, \quad \tau = \frac{\tilde{\tau} H_2}{\eta \tilde{s}} \\ \dot{\gamma} &= \frac{H_2 \tilde{\gamma}}{\tilde{s}}, \quad \sigma = \frac{\tilde{\mathbf{C}} - \tilde{\mathbf{C}}_1}{\tilde{\mathbf{C}}_0 - \tilde{\mathbf{C}}_1}. \end{aligned} \quad (2.14)$$

We define  $T_m, b_r, R_y, g_r, H_y, B_m, \hat{\delta}, \Phi < 1$  are the thermophoresis parameter, local nanoparticle Grashof number, Reynolds number, local temperature Grashof number, Weissenberg number, Brownian motion parameter, wave number and  $\Phi$  is the amplitude ratio respectively. Using

Eqs. (2.12) and (2.14) into Eqs. (2.7) to (2.11), we obtain

$$\frac{\partial \mathfrak{U}}{\partial r} + \frac{\mathfrak{U}}{r} + \frac{\partial w}{\partial z} = 0, \quad (2.15)$$

$$\hat{\delta}^3 R_y \left( \mathfrak{U} \frac{\partial \mathfrak{U}}{\partial r} + w \frac{\partial \mathfrak{U}}{\partial z} \right) = -\frac{\partial \mathbb{P}}{\partial r} + \hat{\delta}^2 \frac{\partial}{\partial z} (\tau_{rz}) + \frac{\hat{\delta}}{r} \frac{\partial}{\partial r} (r \tau_{rr}) - \frac{\hat{\delta}}{r} \tau_{\theta\theta}, \quad (2.16)$$

$$\hat{\delta} R_y \left( \mathfrak{U} \frac{\partial \mathfrak{U}}{\partial r} + w \frac{\partial w}{\partial z} \right) = -\frac{\partial \mathbb{P}}{\partial z} + \frac{1}{r} \frac{\partial}{\partial r} (r \tau_{rz}) + \hat{\delta} \frac{\partial}{\partial r} (\tau_{zz}) + g_r \theta + b_r \sigma, \quad (2.17)$$

$$\frac{1}{r} \frac{\partial}{\partial r} \left( r \frac{\partial \theta}{\partial r} \right) + B_m \frac{\partial \sigma}{\partial r} \frac{\partial \theta}{\partial r} + T_m \left( \frac{\partial \theta}{\partial r} \right)^2 = 0, \quad (2.18)$$

$$\left( \frac{1}{r} \frac{\partial}{\partial r} \left( r \frac{\partial \sigma}{\partial r} \right) \right) + \frac{T_m}{B_m} \left( \frac{1}{r} \frac{\partial}{\partial r} \left( r \frac{\partial \theta}{\partial r} \right) \right) = 0, \quad (2.19)$$

where

$$\tau_{rr} = 2\hat{\delta} [1 + m(H_y \dot{\gamma} - 1)] \frac{\partial \mathfrak{U}}{\partial r}, \quad (2.20)$$

$$\tau_{rz} = [1 + m(H_y \dot{\gamma} - 1)] \left( \frac{\partial \mathfrak{U}}{\partial z} \hat{\delta}^2 + \frac{\partial w}{\partial r} \right), \quad (2.21)$$

$$\tau_{zz} = 2\hat{\delta} (1 + m(H_y \dot{\gamma} - 1)) \frac{\partial w}{\partial z}, \quad (2.22)$$

$$\tau_{\theta\theta} = 2\hat{\delta} (1 + m(H_y \dot{\gamma} - 1)) \frac{\mathfrak{U}}{r}, \quad (2.23)$$

$$\dot{\gamma} = \left[ 2\hat{\delta}^2 \left( \frac{\partial \mathfrak{U}}{\partial r} \right)^2 + \left( \frac{\partial \mathfrak{U}}{\partial z} \hat{\delta}^2 + \frac{\partial w}{\partial r} \right)^2 + 2\hat{\delta}^2 \left( \frac{\partial w}{\partial z} \right)^2 + 2\hat{\delta}^2 \frac{\mathfrak{U}^2}{r^2} \right]^{\frac{1}{2}}. \quad (2.24)$$

We note that Eqs. (2.16) and (2.17) are non-linear, therefore, we are interested to solve our problem incorporating the suppositions of low Reynolds number and long wavelength, avoiding the terms of order  $\hat{\delta}$  and greater, Eqs. (2.16) to (2.19) take the following form

$$\frac{\partial \mathbb{P}}{\partial r} = 0, \quad (2.25)$$

$$\frac{\partial \mathbb{P}}{\partial z} = \frac{1}{r} \frac{\partial}{\partial r} \left[ r \left( 1 + m \left( H_y \frac{\partial w}{\partial r} - 1 \right) \right) \frac{\partial w}{\partial r} \right] + g_r \theta + b_r \sigma, \quad (2.26)$$

$$\frac{1}{r} \frac{\partial}{\partial r} \left( r \frac{\partial \theta}{\partial r} \right) + B_m \frac{\partial \sigma}{\partial r} \frac{\partial \theta}{\partial r} + T_m \left( \frac{\partial \theta}{\partial r} \right)^2 = 0, \quad (2.27)$$

$$\left( \frac{1}{r} \frac{\partial}{\partial r} \left( r \frac{\partial \sigma}{\partial r} \right) \right) + \frac{T_m}{B_m} \left( \frac{1}{r} \frac{\partial}{\partial r} \left( r \frac{\partial \theta}{\partial r} \right) \right) = 0. \quad (2.28)$$

Eq. (2.25) illustrates that  $\mathbb{P}$  is not a function of  $r$ . The resultant dimensionless boundary limits for the problem under concern are given as

$$\begin{aligned} w &= -1 \text{ at } r = i_1, \quad w = -1 \text{ at } r = i_2 = 1 + \Phi \sin(2\pi z), \\ \sigma &= \theta = 1 \text{ at } r = i_1, \quad \sigma = \theta = 0 \text{ at } r = i_2. \end{aligned} \quad (2.29)$$

## 2.4 Analytical solution

To achieve the solution of above equations, we used homotopy perturbation method. The homotopy perturbation method advises that we write Eqs. (2.26) to (2.28), as [24]

$$H(\sigma, j) = (1 - j) [\mathcal{L}(\sigma) - \mathcal{L}(\sigma_{20})] + j \left[ \mathcal{L}(\sigma) + \frac{T_m}{B_m} \left( \frac{1}{r} \frac{\partial}{\partial r} \left( r \frac{\partial \theta}{\partial r} \right) \right) \right], \quad (2.30)$$

$$H(\theta, j) = (1 - j) [\mathcal{L}(\theta) - \mathcal{L}(\theta_{20})] + j \left[ \mathcal{L}(\theta) + B_m \frac{\partial \theta}{\partial r} \frac{\partial \sigma}{\partial r} + T_m \left( \frac{\partial \theta}{\partial r} \right)^2 \right], \quad (2.31)$$

$$H(w, j) = (1 - j) [\mathcal{L}(w) - \mathcal{L}(w_{20})] + j \left[ \mathcal{L}(w) - \frac{\partial \mathbb{P}}{\partial z} + \frac{1}{r} \frac{\partial}{\partial r} \left( r m H_y \left( \frac{\partial w}{\partial r} \right)^2 \right) + g_r \theta + b_r \sigma \right]. \quad (2.32)$$

The linear operator and the initial guesses are chosen as

$$\begin{aligned}
\mathcal{L}_{\theta r} &= \frac{1}{r} \frac{\partial}{\partial r} \left( r \frac{\partial}{\partial r} \right), \quad \mathcal{L}_{\sigma r} = \frac{1}{r} \frac{\partial}{\partial r} \left( r \frac{\partial}{\partial r} \right), \quad \mathcal{L}_{w r} = \frac{1}{r} \frac{\partial}{\partial r} \left( r(1-m) \frac{\partial}{\partial r} \right), \\
\sigma_{20}(r, z) &= \left( \frac{r - i_2}{i_1 - i_2} \right), \quad \theta_{20}(r, z) = \left( \frac{r - i_2}{i_1 - i_2} \right), \\
w_{20}(r) &= -1 + \frac{d\mathbb{P}_0}{dz} \left( \frac{r^2}{4(1-m)} + \ell_{49} \ln(r) + \ell_{50} \right).
\end{aligned} \tag{2.33}$$

According to HPM, we define

$$\begin{aligned}
\theta &= \theta_0 + j\theta_1 + j^2\theta_2 + \dots, \\
\sigma &= \sigma_0 + j\sigma_1 + j^2\sigma_2 + \dots, \\
w &= w_0 + jw_1 + j^2w_2 + \dots, \\
F_i &= F_{0i} + jF_{1i} + j^2F_{2i} + \dots
\end{aligned} \tag{2.34}$$

with the help of above equations, Eqs. (2.30) to (2.32) after equating the like powers of  $j$  give the following systems.

#### 2.4.1 Zeroth-order problem

$$\begin{aligned}
\mathcal{L}(\sigma_0) - \mathcal{L}(\sigma_{10}) &= 0, \\
\mathcal{L}(\theta_0) - \mathcal{L}(\theta_{10}) &= 0, \\
\mathcal{L}(w_0) - \mathcal{L}(w_{10}) &= 0,
\end{aligned} \tag{2.35}$$

$$\begin{aligned}
\theta_0 = \sigma_0 &= 1 \text{ at } r = i_1, \\
\theta_0 = \sigma_0 &= 0 \text{ at } r = i_2 = 1 + \Phi \sin 2\pi z, \\
w_0 &= -1 \text{ at } r = i_1, \\
w_0 &= -1 \text{ at } r = i_2 = 1 + \Phi \sin 2\pi z.
\end{aligned} \tag{2.36}$$

### 2.4.2 First-order problem

$$\begin{aligned}
\mathcal{L}(\sigma_1) &= -\mathcal{L}(\sigma_{10}) - \frac{T_m}{B_m} \left( \frac{1}{r} \frac{\partial}{\partial r} \left( r \frac{\partial \theta_0}{\partial r} \right) \right), \\
\mathcal{L}(\theta_1) &= -\mathcal{L}(\theta_{10}) - B_m \frac{\partial \sigma_0}{\partial r} \frac{\partial \theta_0}{\partial r} - T_m \left( \frac{\partial \theta_0}{\partial r} \right)^2, \\
\mathcal{L}(w_1) &= -\mathcal{L}(w_{10}) - \frac{1}{r} \frac{\partial}{\partial r} (r m H_y \left( \frac{\partial w_0}{\partial r} \right)^2) - g_r \theta_0 - b_r \sigma_0 + \frac{\partial \mathbb{P}_1}{\partial z}.
\end{aligned} \tag{2.37}$$

$$\theta_1 = \sigma_1 = 0 \text{ at } r = i_1,$$

$$\theta_1 = \sigma_1 = 0 \text{ at } r = i_2 = 1 + \Phi \sin 2\pi z,$$

$$w_1 = 0 \text{ at } r = i_1,$$

$$w_1 = 0 \text{ at } r = i_2 = 1 + \Phi \sin 2\pi z. \tag{2.38}$$

### 2.4.3 Second-order problem

$$\mathcal{L}(\sigma_2) = -\frac{T_m}{B_m} \left( \frac{1}{r} \frac{\partial}{\partial r} \left( r \frac{\partial \theta_1}{\partial r} \right) \right), \tag{2.39}$$

$$\mathcal{L}(\theta_2) = -B_m \frac{\partial \theta_1}{\partial r} \frac{\partial \sigma_0}{\partial r} - B_m \frac{\partial \theta_0}{\partial r} \frac{\partial \sigma_1}{\partial r} - 2T_m \frac{\partial \theta_0}{\partial r} \frac{\partial \theta_1}{\partial r},$$

$$\mathcal{L}(w_2) = \frac{\partial \mathbb{P}_2}{\partial z} - \frac{1}{r} \frac{\partial}{\partial r} (2r m H_y \left( \left( \frac{\partial w_0}{\partial r} \right) \left( \frac{\partial w_1}{\partial r} \right) \right)) - g_r \theta_1 - b_r \sigma_1.$$

$$\theta_2 = \sigma_2 = 0 \text{ at } r = i_1,$$

$$\theta_2 = \sigma_2 = 0 \text{ at } r = i_2 = 1 + \Phi \sin 2\pi z,$$

$$w_2 = 0 \text{ at } r = i_1,$$

$$w_2 = 0 \text{ at } r = i_2 = 1 + \Phi \sin 2\pi z. \tag{2.40}$$

We can write the solutions of these problems as

### 2.4.4 Zeroth-order solution

The zeroth order solution are defined as

$$\theta_0(r) = \frac{r}{\ell_{11}} - \ell_{12}, \quad (2.41)$$

$$\sigma_0(r) = \frac{r}{\ell_{11}} - \ell_{12}, \quad (2.41a)$$

$$w_0(r) = -1 + \frac{d\mathcal{P}_0}{dz} \left( \frac{r^2}{4(1-m)} + \ell_{49} \ln(r) + \ell_{50} \right). \quad (2.41b)$$

### 2.4.5 First-order solution

With the help of expressions (2.41) to (2.41b), solution of first order system (2.37) subject to boundary condition (2.38) are directly defined as

$$\theta_1(r) = r^2 \ell_{16} - \frac{r}{\ell_{11}} + \ell_{17} \ln(r) + \ell_{20}, \quad (2.42)$$

$$\sigma_1(r) = \ell_{21} r + \ell_{23} \ln(r) + \ell_{26}, \quad (2.42a)$$

$$w_1(r) = r^3 \ell_{51} + r^2 \ell_{52} + r \ell_{53} + \ell_{59} \ln(r) + \frac{1}{r} \ell_{54} + \ell_{60} \\ + \frac{d\mathcal{P}_1}{dz} \left( \frac{r^2}{4(1-m)} + \ell_{49} \ln(r) + \ell_{50} \right). \quad (2.42b)$$

### 2.4.6 Second-order solution

Making use of zeroth and first order solution, the solution of second order problem is defined as

$$\theta_2(r) = r^3 \ell_{39} - r^2 \ell_{40} + r \ell_{41} + \ell_{43} \ln(r) + \ell_{45}, \quad (2.43)$$

$$\sigma_2(r) = r^2 \ell_{28} - r \ell_{29} + \ell_{34} \ln(r) + \ell_{35}, \quad (2.43a)$$

$$w_2(r) = r^4 \ell_{68} + r^3 \ell_{69} + r^2 \ell_{70} + r \ell_{71} - \frac{1}{r} \ell_{74} - \frac{\ell_{75}}{r^2} + \ell_{73} r^2 \ln(r) \\ + \ell_{78} \ln(r) + \ell_{77} + \frac{d\mathcal{P}_2}{dz} \left( \frac{r^2}{4(1-m)} + \ell_{49} \ln(r) + \ell_{50} \right). \quad (2.43b)$$

Using all these solutions into Eq. (2.34), and setting  $j \rightarrow 1$ , we finally arrive at

$$\sigma = \ell_{28} r^2 + r \ell_{36} + \ell_{37} \ln r + \ell_{38}. \quad (2.44)$$

$$\theta = \ell_{39}r^3 + r^2\ell_{46} + \ell_{41}r + \ell_{47}\ln r + \ell_{48}. \quad (2.45)$$

$$\begin{aligned} w = & -1 + \left(\frac{r^2}{4(1-m)} + \ell_{49}\ln r + \ell_{50}\right)\frac{d\mathbb{P}}{dz} + r^4\ell_{68} + r^3\ell_{79} + r^2\ell_{80} \\ & + r\ell_{81} + \frac{1}{r}\ell_{82} - \frac{\ell_{75}}{r^2} + \ell_{83}\ln r + \ell_{73}r^2\ln r + \ell_{84}. \end{aligned} \quad (2.46)$$

in which all  $\ell_{ij}$  are defined in appendix.

The expression for Pressure gradient can be obtain as

$$\frac{d\mathbb{P}}{dz} = \frac{F_i}{\ell_{86}} + \ell_{89}. \quad (2.47)$$

Flow rate in dimensionless form is already defined in Eq. (1.58), however for the sake of simplicity we define it again as

$$Q = F_i + \frac{1}{2} \left(1 + \frac{\Phi^2}{2} - \epsilon^2\right). \quad (2.48)$$

The expressions for dimensionless time mean flow rate  $F_i$ , Pressure rise  $\Delta\mathbb{P}$  and friction forces on the outward and inward cylinders are  $F^a$  and  $F^b$  respectively, which are already defined in Chapter one (see Eqs. (1.59) to (1.61)). With the help of Eqs. (2.47) , Eqs. (1.59) to (1.61) take the following form

$$\Delta\mathbb{P} = \int_0^1 \left(\frac{F_i}{\ell_{86}} + \ell_{89}\right)dz, \quad (2.49)$$

$$F^a = \int_0^1 -r_1^2 \left(\frac{F_i}{\ell_{86}} + \ell_{89}\right)dz, \quad (2.50)$$

$$F^b = \int_0^1 -r_2^2 \left(\frac{F_i}{\ell_{86}} + \ell_{89}\right)dz. \quad (2.51)$$

The velocities and stream function relation are defined as

$$u = \frac{-1}{r} \left(\frac{\partial\Psi}{\partial z}\right) \text{ and } w = \frac{1}{r} \left(\frac{\partial\Psi}{\partial r}\right). \quad (2.52)$$



Making use of Eq. (2.46) into Eq. (2.52), we get stream function

$$\begin{aligned}
\Psi = & \frac{-r^2}{2} + \frac{d\mathbb{P}}{dz} \left( \frac{r^4}{16(1-m)} + \ell_{49} \left( \frac{r^2 \ln(r)}{2} - \frac{r^2}{4} \right) + \ell_{50} \frac{r^2}{2} \right) \\
& + \ell_{68} \frac{r^6}{6} + \frac{\ell_{79}}{5} r^5 + \ell_{80} \frac{r^4}{4} + \frac{\ell_{81}}{3} r^3 + \ell_{84} \frac{r^2}{2} + \ell_{82} r \\
& - \ell_{75} \ln(r) + \ell_{83} \left( \frac{r^2 \ln(r)}{2} - \frac{r^2}{4} \right) + \ell_{73} \left( \frac{r^4 \ln(r)}{4} - \frac{r^4}{16} \right). \tag{2.53}
\end{aligned}$$

For study, we have measured five wave forms explicitly, multisinusoidal, triangular, trapezoidal, square, and sinusoidal. For different waves dimensionless expression can be stated as

1. Multisinusoidal wave:

$$i_2(z) = 1 + \Phi \sin(2d\pi z). \tag{2.54}$$

2. Triangular wave:

$$i_2(z) = 1 + \Phi \left\{ \frac{8}{\pi^3} \sum_{y=1}^{\infty} \frac{(-1)^{y+1}}{(2y-1)} \sin(2\pi(2y-1)z) \right\}. \tag{2.55}$$

3. Trapezoidal wave:

$$i_2(z) = 1 + \Phi \left\{ \frac{32}{\pi^2} \sum_{y=1}^{\infty} \frac{\sin \frac{\pi}{8}(2y-1)}{(2y-1)^2} \sin(2\pi(2y-1)z) \right\}. \tag{2.56}$$

4. Square wave:

$$i_2(z) = 1 + \Phi \left\{ \frac{4}{\pi} \sum_{n=1}^{\infty} \frac{(-1)^{y+1}}{(2y-1)} \cos(2\pi(2y-1)z) \right\}. \tag{2.57}$$

5. Sinusoidal wave:

$$i_2(z) = 1 + \Phi \sin(2\pi z). \tag{2.58}$$

## 2.5 Analytical solution by Adomian decomposition method

To develop the solution of Eqs. (2.26) to (2.28), we employ the Adomian decomposition method.

We inscribe Eqs. (2.26) to (2.28) in the operator form as [25 – 27]

$$\mathcal{L}_r \sigma + \frac{T_m}{B_m} \mathcal{L}_r \theta = 0, \quad (2.59)$$

$$\mathcal{L}_r \theta + B_m \frac{\partial \theta}{\partial r} \frac{\partial \sigma}{\partial r} + T_m \left( \frac{\partial \theta}{\partial r} \right)^2 = 0, \quad (2.60)$$

$$\mathcal{L}_w \theta - \frac{\partial \mathbb{P}}{\partial z} + \frac{1}{r} \frac{\partial}{\partial r} (rm H_y \left( \frac{\partial w}{\partial r} \right)^2) + g_r \theta + b_r \sigma = 0. \quad (2.61)$$

The linear and the inverse operator are taken as

$$\begin{aligned} \mathcal{L}_{\theta r} &= \mathcal{L}_{\sigma r} = \frac{1}{r} \frac{\partial}{\partial r} \left( r \frac{\partial}{\partial r} \right), \quad \mathcal{L}_{w r} = \frac{1}{r} \frac{\partial}{\partial r} \left( r(1-m) \frac{\partial}{\partial r} \right), \\ \mathcal{L}_{\theta r}^{-1}[\cdot] &= \int_{r_2}^r \left[ \frac{1}{r} \int_{r_2}^r r[\cdot] dr \right] dr, \quad \mathcal{L}_{\sigma r}^{-1}[\cdot] = \int_{r_2}^r \left[ \frac{1}{r} \int_{r_2}^r r[\cdot] dr \right] dr, \\ \mathcal{L}_{w r}^{-1}[\cdot] &= \int_{r_2}^r \left[ \frac{1}{r(1-m)} \int_{r_2}^r r[\cdot] dr \right] dr \end{aligned} \quad (2.62)$$

Applying  $\mathcal{L}_r^{-1}$  to the Eqs. (2.59) to (2.61) and it takes the form

$$\sigma(r, z) = \sigma_{20}(r, z) - \frac{T_m}{B_m} [\theta(r, z) - \theta_{20}(r, z)], \quad (2.63)$$

$$\theta(r, z) = \theta_{20}(r, z) - \int_{r_2}^r \left[ \frac{1}{r} \int_{r_2}^r r [B_m \frac{\partial \theta}{\partial r} \frac{\partial \sigma}{\partial r}] dr \right] dr - \int_{r_2}^r \left[ \frac{1}{r} \int_{r_2}^r r [T_m \left( \frac{\partial \theta}{\partial r} \right)^2] dr \right] dr, \quad (2.64)$$

$$\begin{aligned} w(r, z) &= w_{20}(r, z) + \int_{r_2}^r \left[ \frac{1}{r(1-m)} \int_{r_2}^r r \left[ \frac{\partial \mathbb{P}}{\partial z} \right] dr \right] dr - \int_{r_2}^r \left[ \frac{1}{r(1-m)} \int_{r_2}^r r \left[ \frac{1}{r} \frac{\partial}{\partial r} (rm H_y \left( \frac{\partial w}{\partial r} \right)^2) \right] dr \right] dr \\ &\quad - \int_{r_2}^r \left[ \frac{1}{r(1-m)} \int_{r_2}^r r (g_r \theta + b_r \sigma) dr \right] dr. \end{aligned} \quad (2.65)$$

Now we decompose  $\sigma$ ,  $\theta$ ,  $w$  as

$$\sigma = \sum_{z=0}^{\infty} \sigma_z, \quad \theta = \sum_{z=0}^{\infty} \theta_z, \quad w = \sum_{z=0}^{\infty} w_z \quad (2.66)$$

Substituting Eq. (2.66) into the Eqs. (2.63) to (2.65) and comparing. Finally we arrive in the combine form as

$$\sigma = -\frac{T_m}{B_m} \left( \frac{r - i_2}{i_1 - i_2} \right) + C_1 \ln r + C_2 + \dots, \quad (2.67)$$

$$\begin{aligned} \theta = & -\frac{T_m}{B_m} \left( \frac{r - i_2}{i_1 - i_2} \right) + C_3 \ln r + C_4 + r^2 b_{18} + r b_9 + b_{10} \ln r \\ & + b_{11} (\ln r)^2 + b_{12} + \dots, \end{aligned} \quad (2.68)$$

$$\begin{aligned} w = & a_1 \ln r + a_2 + \frac{1}{2(1-m)} \frac{d\mathbb{P}}{dz} \left( \frac{r^2}{2} - i_2^2 \ln r + b_{18} \right) - r^3 b_{21} - r^2 b_{22} \\ & - b_{23} r^2 \ln r + b_{24} \ln r + b_{25} + \dots, \end{aligned} \quad (2.69)$$

where  $C_1$  to  $C_4$  and  $a_1$ ,  $a_2$  are evaluated by using the following conditions

$$\begin{aligned} \theta &= \sigma = 1 \text{ at } r = i_1, \\ \theta &= \sigma = 0 \text{ at } r = i_2 = 1 + \Phi \sin 2\pi z, \\ w &= -1 \text{ at } r = i_1, \\ w &= -1 \text{ at } r = i_2 = 1 + \Phi \sin 2\pi z. \end{aligned} \quad (2.70)$$

Where as all the constants are defined in appendix

## 2.6 Results and discussion

In this unit Pressure rise, inward and outward friction forces, Pressure gradient, and stream lines are analyzed. Figs 2.2. to 2.37 are showed for this purpose. Numerical integration is performed by using mathematics software to calculate pressure rise  $\Delta P$  and inward and outward friction forces. Fig. (2.1) shows the comparison of velocity profile for Homotopy perturbation Method (HPM) and Adomian Decomposition Method (ADM). The velocity field  $w$  for different values of  $g_r, B_m, b_r, T_m$  are presented in the Figs. (2.2) to (2.5) It is observed that the velocity increased by increasing values of  $g_r, b_r, B_m, T_m$ .  $r \in [0.2, 0.8]$ ,  $r \in [0.2, 0.75]$ ,  $r \in [0.2, 0.75]$ ,  $r \in [0.65, 1]$ . other wise decreases. Pressure rise for various physical parameters such as  $\Phi, H_y, m, T_m, B_m$  and for different wave forms are observed in the Fig. 6 to 11. Peristaltic pumping regions for  $\Phi = 0.10, 0.15, 0.20, 0.25$ , are  $(Q \in [-2, 0.03], Q \in [-2, 0.05], Q \in [-2, 0.07], Q \in [-2, 0.09])$  respectively as shown in Fig 6, other wise augmented pumping region occur. For Figs 7, 8 and 11. peristaltic pumping interval is  $(Q \in [-2, 0.2])$ . For the different values of  $T_m$  such as  $T_m = 3, 5, 7$ , and  $9$ , peristaltic pumping regions are given by the intervals  $(Q \in [-2, 0.45], Q \in [-2, 0.5], Q \in [-2, 0.55], Q \in [-2, 0.6])$ , respectively (see Fig, 9). Peristaltic pumping regions for the different values of  $B_m$  such as  $B_m = 0.1, 0.3, 0.5, 0.7$ , are given by the intervals  $(Q \in [-2, -0.35], Q \in [-2, 0.1], Q \in [-2, 0.15], Q \in [-2, 0.2])$ , respectively as displayed in the Fig, 10. other wise it is augmented pumping region appear for all the intervals. Figs. (2.12) to (2.23) are plotted to show the friction forces for inward and outward cylinder . It can be observed that inward and outward friction forces have reverse behavior related to the Pressure rise. Variation of concentration field for different values of  $T_m, B_m$  are displayed in the Figs. (2.24) and (2.25). It is noticed that concentration field decreases when the values of  $T_m$ , are increasing and it increases when the values of  $B_m$  increases Figs. (2.26) and (2.27) are presented to see the variation of temperature profile for different values of  $T_m$ , and  $B_m$  temperature profile increases by increasing values of  $T_m, B_m$ . The deviation of Pressure gradient for numerous values of  $\Phi$  are describes in the Figs. (2.28) to (2.32) From Figs. (2.28) to (2.30) it is shown that in the regions  $z \in [0.5, 1]$ ,  $z \in [1.5, 2]$ , and  $z \in [1.1, 1.49]$  small and large Pressure gradient occur respectively. Figs. (2.31) the Pressure gradient is small for  $z \in [1.26, 1.75]$ , and huge Pressure gradient obtained by the interval  $z \in [0.75, 1.25]$ , for Figs. (2.32) the Pressure gradient is small for  $z \in [0.91, 1.24]$ ,  $z \in [1.61, 1.8]$  and huge Pressure gradient follows for  $z \in [0.6, 0.9]$ ,  $z \in [1.25, 1.6]$ . The trapping

occurrence for five different wave forms can be understood in the Fig. (2.33) to (2.37). It is depicted that the size of the trapped bolus in Triangular wave is minor as associated to the other waves.

## 2.7 Conclusion

This study inspects the Effects of nanoparticles on the peristaltic flow of hyperbolic tangent fluid in an annulus. Leading points of the phenomenon are given as:

1. The solution of non-linear coupled partial differential equations are attained by Homotopy perturbation Method (HPM) and compared with solutions attained by Adomian Decomposition (ADM). Both techniques avoid linearization and other assumptions. The solutions arrived by HPM is much easier when we compared to (ADM). To understand the viability of this method more terms of series are calculated obviously accuracy increases if more components are included in the series, but at the expense of large increase in the difficulty of calculations.
2. Same behavior observed in the figures of inward and outward frictional forces but outward friction forces are large as compared to inward forces.
3. Temperature profile grows with an increase in  $T_m$  and  $B_m$ .
4. Concentration field declines with increase in  $T_m$  and increases with increase in  $B_m$ .
5. It is detected that friction forces have reverse behavior when we related to the Pressure rise
6. The magnitude of trapping bolus in triangular wave is minor when we related to the other waves.

## 2.8 Appendix 2.0

$$\begin{aligned}
\ell_{11} &= i_1 - i_2, \ell_{12} = \frac{i_2}{\ell_{11}}, \ell_{13} = T_m + B_m, \ell_{13'} = 2T_m + B_m, \ell_{14} = \ln i_1 - \ln i_2, \\
\ell_{15} &= i_2^2 - i_1^2, \ell_{16} = \frac{-\ell_{13}}{4\ell_{11}^2}, \ell_{17} = \frac{1}{\ell_{14}} + \frac{\ell_{15}\ell_{16}}{\ell_{14}}, \ell_{18} = i_2^2 \ln i_1 - i_1^2 \ln i_2, \\
\ell_{19} &= \frac{-\ln i_2}{\ell_{14}} - \frac{\ell_{16}\ell_{18}}{\ell_{14}}, \ell_{20} = \ell_{12} + \ell_{19}, \ell_{21} = \frac{-\ell_{13}}{B_m\ell_{11}}, \ell_{22} = \frac{\ell_{12}\ell_{13}}{B_m}, \\
\ell_{23} &= \frac{-\ell_{21}\ell_{11}}{\ell_{14}}, \ell_{24} = i_1 \ln i_2 - i_2 \ln i_1, \ell_{25} = \frac{\ell_{21}\ell_{24}}{\ell_{14}} - \ell_{22}, \ell_{26} = \ell_{22} + \ell_{25}, \\
\ell_{27} &= \frac{-T_m}{B_m}, \ell_{28} = \ell_{16}\ell_{27}, \ell_{29} = \frac{\ell_{27}}{\ell_{11}}, \ell_{30} = \ell_{17}\ell_{27}, \ell_{31} = \ell_{20}\ell_{27}, \\
\ell_{32} &= \frac{\ell_{15}\ell_{28} + \ell_{11}\ell_{29} - \ell_{14}\ell_{30}}{\ell_{14}}, \ell_{33} = -\frac{\ell_{18}\ell_{28} + \ell_{24}\ell_{29} + \ell_{14}\ell_{31}}{\ell_{14}}, \ell_{34} = \ell_{30} + \ell_{32}, \\
\ell_{35} &= \ell_{31} + \ell_{33}, \ell_{36} = \frac{1}{\ell_{11}} + \ell_{21} - \ell_{29}, \ell_{37} = \ell_{23} + \ell_{34}, \ell_{38} = \ell_{26} - \ell_{12} + \ell_{35}, \\
\ell_{39} &= \frac{-2\ell_{13'}\ell_{16}}{9\ell_{11}}, \ell_{40} = \frac{-\ell_{13'}}{4\ell_{11}^2} + \frac{B_m\ell_{21}}{4\ell_{11}}, \ell_{41} = \frac{-\ell_{13'}\ell_{17}}{\ell_{11}} - \frac{B_m\ell_{23}}{\ell_{11}}, \ell_{42} = i_1^3 - i_2^3, \\
\ell_{43} &= \frac{-\ell_{39}\ell_{42} - \ell_{15}\ell_{40} - \ell_{11}\ell_{41}}{\ell_{14}}, \ell_{44} = i_1^3 \ln i_2 - i_2^3 \ln i_1, \ell_{45} = \frac{\ell_{39}\ell_{44} + \ell_{18}\ell_{40} + \ell_{24}\ell_{41}}{\ell_{14}}, \\
\ell_{46} &= \ell_{16} - \ell_{40}, \ell_{47} = \ell_{17} + \ell_{43}, \ell_{48} = -\ell_{12} + \ell_{20} + \ell_{45}, \ell_{49} = \frac{-(i_1^2 - i_2^2)}{4(1-m)\ell_{14}}, \\
\ell_{50} &= \frac{(i_1^2 \ln i_2 - i_2^2 \ln i_1)}{4(1-m)\ell_{14}}, \ell_{51} = \frac{-nH_y}{12(1-m)^3} \left(\frac{dp_0}{dz}\right)^2 - \frac{g_r + b_r}{9\ell_{11}(1-m)}, \\
\ell_{52} &= \frac{(g_r + b_r)\ell_{12}}{4(1-m)} - \frac{1}{4(1-m)} \frac{dp_0}{dz}, \ell_{53} = \frac{-nH_y\ell_{49}}{(1-m)^2} \left(\frac{dp_0}{dz}\right)^2, \ell_{54} = \frac{nH_y\ell_{49}^2}{(1-m)} \left(\frac{dp_0}{dz}\right)^2, \\
\ell_{55} &= -\ell_{49} \frac{dp_0}{dz}, \ell_{56} = 1 - \ell_{50} \frac{dp_0}{dz}, \ell_{57} = \frac{-(1-m)}{\ell_{14}} (\ell_{51}(i_1^3 - i_2^3) + \ell_{52}(i_1^2 - i_2^2) + \ell_{53}(i_1 - i_2) \\
&\quad + \ell_{54}(\frac{1}{i_1} - \frac{1}{i_2}) + \ell_{55}(\ln i_1 - \ln i_2)), \\
\ell_{58} &= \frac{1}{\ell_{14}} (\ell_{51}(i_1^3 \ln i_2 - i_2^3 \ln i_1) + \ell_{52}(i_1^2 \ln i_2 - i_2^2 \ln i_1) + \ell_{53}(i_1 \ln i_2 - i_2 \ln i_1) + \ell_{54}(\frac{\ln i_2}{i_1} \\
&\quad - \frac{\ln i_1}{i_2}) + \ell_{56}(\ln i_2 - \ln i_1)), \\
\ell_{59} &= \ell_{55} + \frac{\ell_{57}}{(1-m)}, \ell_{60} = \ell_{56} + \ell_{58}, \ell_{61} = \frac{3\ell_{51}}{2(1-m)} \frac{d\mathbb{P}_0}{dz}, \\
\ell_{62} &= \frac{\ell_{52}}{(1-m)} \frac{d\mathbb{P}_0}{dz} + \frac{d\mathbb{P}_0}{dz} \frac{d\mathbb{P}_1}{dz} \frac{1}{4(1-m)^2}, \ell_{63} = \frac{\ell_{53}}{2(1-m)} \frac{d\mathbb{P}_0}{dz} + 3\ell_{49}\ell_{51} \frac{d\mathbb{P}_0}{dz}, \\
\ell_{64} &= \frac{\ell_{59}}{2(1-m)} \frac{d\mathbb{P}_0}{dz} + \frac{d\mathbb{P}_0}{dz} \frac{d\mathbb{P}_1}{dz} \frac{\ell_{49}}{(1-m)} + 2\ell_{49}\ell_{52} \frac{d\mathbb{P}_0}{dz}, \ell_{65} = -\frac{\ell_{54}}{2(1-m)} \frac{d\mathbb{P}_0}{dz} \\
&\quad + \ell_{49}\ell_{53} \frac{d\mathbb{P}_0}{dz},
\end{aligned}$$

$$\begin{aligned}
\ell_{66} &= \ell_{49}^2 \frac{d\mathbb{P}_0}{dz} \frac{d\mathbb{P}_1}{dz} + \ell_{49}\ell_{59} \frac{d\mathbb{P}_0}{dz}, \ell_{67} = -\ell_{49}\ell_{54} \frac{d\mathbb{P}_0}{dz}, \ell_{68} = \frac{-2mH_y\ell_{61}}{4(1-m)} - \frac{\ell_{16}g_r}{16(1-m)} \\
\ell_{69} &= \frac{-2mH_y\ell_{62}}{3(1-m)} + \frac{g_r}{9\ell_{11}(1-m)} - \frac{b_r\ell_{21}}{9(1-m)}, \ell_{70} = \frac{-mH_y\ell_{63}}{(1-m)} + \frac{g_r\ell_{17}}{4(1-m)} - \frac{b_r\ell_{26}}{4(1-m)} \\
&\quad - \frac{g_r\ell_{20}}{4(1-m)} + \frac{b_r\ell_{23}}{4(1-m)}, \\
\ell_{71} &= \frac{-2mH_y\ell_{64}}{(1-m)}, \ell_{72} = \frac{-2mH_y\ell_{65}}{(1-m)}, \ell_{73} = \frac{-g_r\ell_{17}}{4(1-m)} - \frac{b_r\ell_{23}}{4(1-m)}, \ell_{74} = \frac{-2mH_y\ell_{66}}{(1-m)}, \\
\ell_{75} &= \frac{-mH_y\ell_{67}}{(1-m)}, \ell_{76} = \frac{-(1-m)}{\ell_{14}} (\ell_{68}(i_1^4 - i_2^4) + \ell_{69}(i_1^3 - i_2^3) + \ell_{70}(i_1^2 - i_2^2) + \ell_{71}(i_1 - i_2) \\
&\quad + \ell_{72}(\ln i_1 - \ln i_2) + \ell_{73}(i_1^2 \ln i_1 - i_2^2 \ln i_2) + \ell_{74}(\frac{1}{i_2} - \frac{1}{i_1}) + \ell_{75}(\frac{1}{i_2^2} - \frac{1}{i_1^2})), \\
\ell_{77} &= \frac{1}{\ell_{14}} (\ell_{68}(i_1^4 \ln i_2 - i_2^4 \ln i_1) + \ell_{69}(i_1^3 \ln i_2 - i_2^3 \ln i_1) + \ell_{70}(i_1^2 \ln i_2 - i_2^2 \ln i_1) \\
&\quad + \ell_{71}(i_1 \ln i_2 - i_2 \ln i_1) + \ell_{73}(i_1^2 \ln i_1 \ln i_2 - i_2^2 \ln i_1 \ln i_2) - \ell_{74}(\frac{\ln i_2}{i_1} - \frac{\ln i_1}{i_2}) \\
&\quad + \ell_{75}(\frac{\ln i_1}{i_2^2} - \frac{\ln i_2}{i_1^2})) \\
\ell_{78} &= \ell_{72} + \frac{\ell_{76}}{(1-m)}, \ell_{79} = \ell_{69} + \ell_{51}, \ell_{80} = \ell_{52} + \ell_{70}, \ell_{81} = \ell_{53} + \ell_{71}, \ell_{82} = \ell_{54} - \ell_{74}, \\
\ell_{83} &= \ell_{59} + \ell_{78}, \ell_{84} = \ell_{60} + \ell_{77}, \ell_{85} = \frac{i_2^2 - i_1^2}{2}, \ell_{86} = \frac{i_2^4 - i_1^4}{16(1-m)} + \ell_{49}((\frac{i_2^2 \ln i_2}{2} - \frac{i_2^2}{4}) \\
&\quad - (\frac{i_1^2 \ln i_1}{2} - \frac{i_1^2}{4})) + \ell_{50}(\frac{i_2^2 - i_1^2}{2}), \\
\ell_{87} &= \frac{\ell_{51}(i_2^5 - i_1^5)}{5} + \frac{\ell_{52}(i_2^4 - i_1^4)}{4} + \frac{\ell_{53}(i_2^3 - i_1^3)}{3} + \ell_{54}(i_2 - i_1) + \ell_{59}((\frac{i_2^2 \ln i_2}{2} - \frac{i_1^2 \ln i_1}{2}) \\
&\quad - (\frac{i_2^2 - i_1^2}{4}) + \frac{\ell_{60}(i_2^2 - i_1^2)}{2}), \\
\ell_{88} &= \frac{\ell_{68}(i_2^6 - i_1^6)}{6} + \frac{\ell_{69}(i_2^5 - i_1^5)}{5} + \frac{\ell_{70}(i_2^4 - i_1^4)}{4} + \frac{\ell_{71}(i_2^3 - i_1^3)}{3} + \frac{\ell_{77}(i_2^2 - i_1^2)}{2} + \ell_{78}((\frac{i_2^2 \ln i_2}{2} \\
&\quad - \frac{i_1^2 \ln i_1}{2}) - (\frac{i_2^2 - i_1^2}{4})) + \ell_{73}((\frac{i_2^4 \ln i_2}{4} - \frac{i_1^4 \ln i_1}{4}) - (\frac{i_2^4 - i_1^4}{16})) - \ell_{74}(i_2 - i_1) - \ell_{75}(\ln i_2 \\
&\quad - \ln i_1), \\
\ell_{89} &= \frac{\ell_{85} - \ell_{87} - \ell_{88}}{\ell_{86}}, \\
b_1 &= (\frac{-T_m}{B_m(i_1 - i_2)})^2, b_2 = \frac{-2C_3 T_m}{B_m(i_1 - i_2)}, b_3 = \frac{-T_m}{B_m(i_1 - i_2)}, b_4 = \frac{-i_2^2}{2} b_3^2 - i_2(C_1 b_3 + C_3 b_3) \\
&\quad - C_1 C_3 \ln(i_2),
\end{aligned}$$

$$\begin{aligned}
b_5 &= \frac{-i_2^2 b_3^2}{4} - i_2(C_1 b_3 + C_3 b_3) - \frac{C_1 C_3 (\ln i_2)^2}{2} - b_4 \ln i_2, \\
b_6 &= \frac{-b_1 i_2^2}{2} - C_3^2 (\ln i_2) - b_2 i_2, \quad b_7 = \frac{-b_1 i_2^2}{4} - \frac{C_3^2 (\ln i_2)^2}{2} - b_2 i_2 - b_6 \ln i_2, \\
b_8 &= \frac{-B_m b_3^2}{4} - \frac{b_1}{4} T_m, \quad b_9 = -B_m (C_1 b_3 + C_3 b_3) - b_2 T_m, \quad b_{10} = -B_m b_4 - b_6 T_m, \\
b_{11} &= \frac{-B_m C_1 C_3}{2} - \frac{T_m C_3^2}{2}, \quad b_{12} = -B_m b_5 - b_7 T_m, \quad b_{13} = \frac{-(g_r + b_r) T_m}{B_m (i_1 - i_2)}, \\
b_{14} &= C_3 g_r + C_1 b_r, \quad b_{15} = C_4 g_r + C_2 b_r, \quad b_{16} = \frac{m H_y a_1^2}{1 - m}, \quad b_{17} = \frac{b_{16}}{i_2} + \frac{b_{16}}{i_2} \ln(i_2), \\
b_{18} &= \frac{-i_2^2}{2} + i_2^2 \ln(i_2), \quad b_{19} = \frac{-i_2^3 b_{13}}{3} - b_{14} \left( \frac{i_2^2 \ln(i_2)}{2} - \frac{i_2^2}{4} \right) - \frac{b_{15} i_2^2}{2}, \\
b_{20} &= \frac{-i_2^3 b_{13}}{9(1 - m)} - \frac{b_{14}}{(1 - m)} \left( \frac{i_2^2 \ln(i_2)}{2} - \frac{i_2^2}{4} \right) - \frac{b_{15} i_2^2}{4(1 - m)} - \frac{b_{19} \ln(i_2)}{(1 - m)}, \quad b_{21} = \frac{b_{13}}{9(1 - m)}, \\
b_{22} &= \frac{b_{15}}{4(1 - m)} - \frac{2b_{14}}{8(1 - m)}, \quad b_{23} = \frac{b_{14}}{4(1 - m)}, \quad b_{24} = \frac{b_{16}}{i_2} - \frac{b_{19}}{(1 - m)}, \quad b_{25} = -b_{17} - b_{20}.
\end{aligned}$$



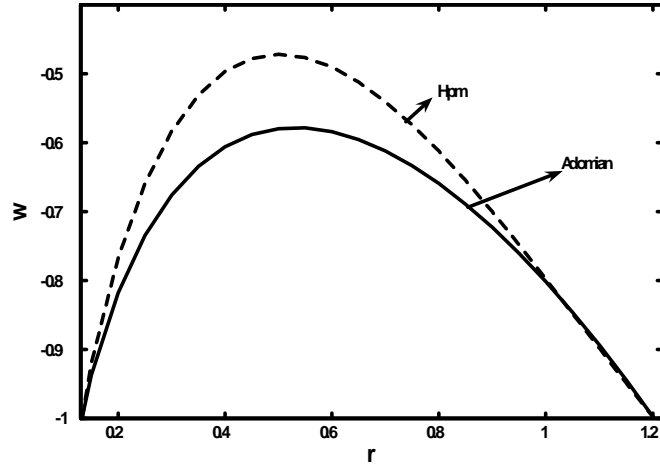


**Fig. 2.1**, Velocity field for  $m = 0.27$ ,  $m_t = 1.22$ ,  $g_r = 2.46$ ,  $b_r = 2.43$ ,  $B_m = 4.86$ ,  $H_y = 0.12$ ,  $Q = 0.01$ ,  $\epsilon = 0.13$ ,  $\Phi = 0.25$ ,  $z = 0.15$ ,  $\frac{d\Phi}{dz} = 0.53$ .

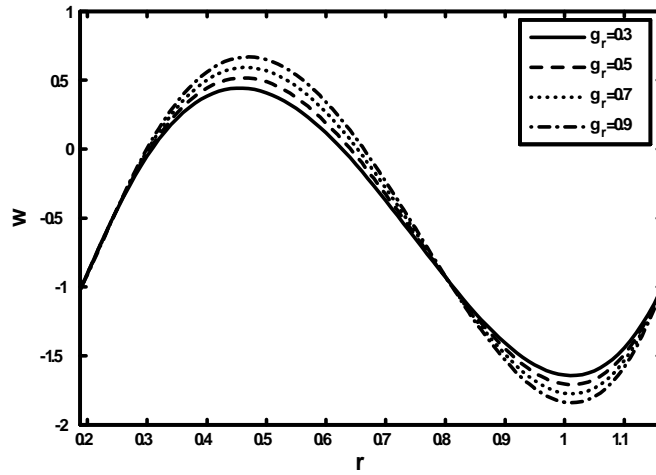


**Fig. 2.2**, Velocity field for  $m = 0.96$ ,  $H_y = 0.02$ ,  $z = 0.05$ ,  $\epsilon = 0.19$ ,  $\Phi = 0.53$ ,  $T_m = 6.12$ ,  $Q = 0.02$ ,  $b_r = 4.61$ ,  $B_m = 5.21$ .

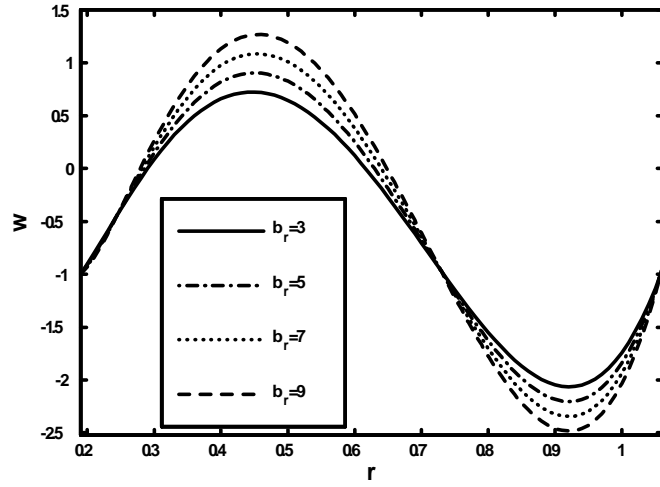


**Fig. 2.3**, Velocity field for  $m = 0.94$ ,  $g_r = 4.8$ ,  $B_m = 4.21$ ,  $T_m = 3.12$ ,  $H_y = 0.05$ ,  $Q = 0.03$ ,  
 $z = 0.03$ ,  $\epsilon = 0.19$ ,  $\Phi = 0.31$ .

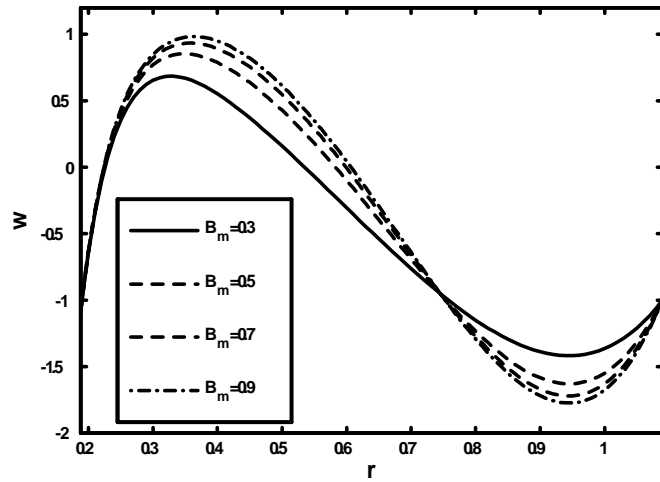


**Fig. 2.4**, Velocity field for  $m = 0.86$ ,  $\Phi = 0.36$ ,  $b_r = 3.51$ ,  $Q = 0.09$ ,  $g_r = 4.85$ ,  $z = 0.46$ ,  
 $T_m = 5.95$ ,  $H_y = 0.18$ ,  $\epsilon = 0.19$ .

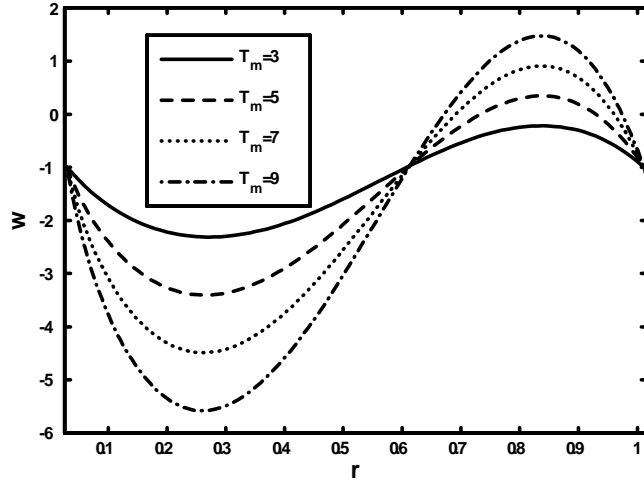


**Fig. 2.5**, Velocity field for  $m = 0.61$ ,  $b_r = 4.55$ ,  $g_r = 3.95$ ,  $B_m = 0.1$ ,  $H_y = 0.16$ ,  $Q = 0.02$ ,  $\epsilon = 0.03$ ,  $\Phi = 0.18$ ,  $z = 0.01$ .

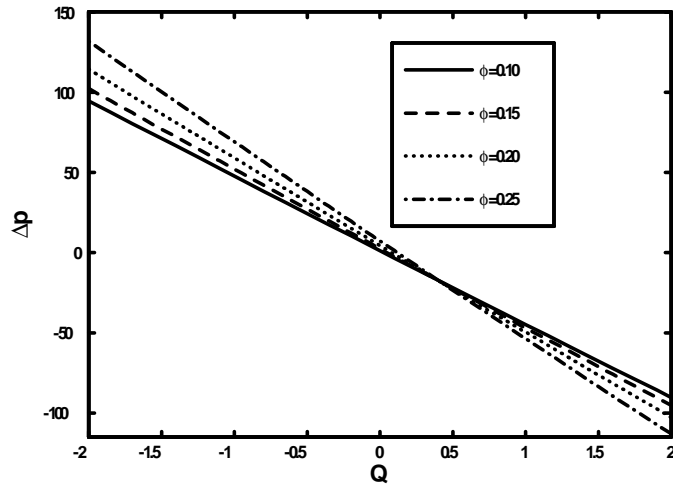


**Fig. 2.6**, Pressure rise distribution for  $m = 0.02$ ,  $T_m = 0.51$ ,  $g_r = 0.52$ ,  $b_r = 0.22$ ,  $B_m = 0.81$ ,  $H_y = 0.11$ ,  $\epsilon = 0.03$ .

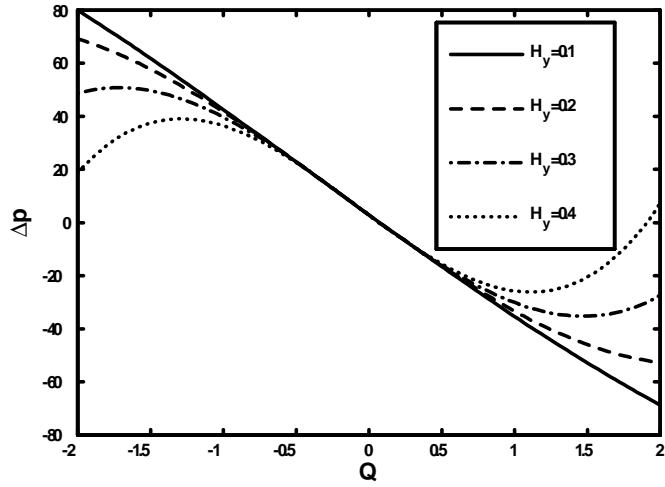


**Fig. 2.7**, Pressure rise distribution for  $\Phi = 0.05$ ,  $T_m = 5.14$ ,  $m = 0.1$ ,  $g_r = 3.32$ ,  $b_r = 2.22$ ,  
 $B_m = 2.41$ ,  $\epsilon = 0.02$ .

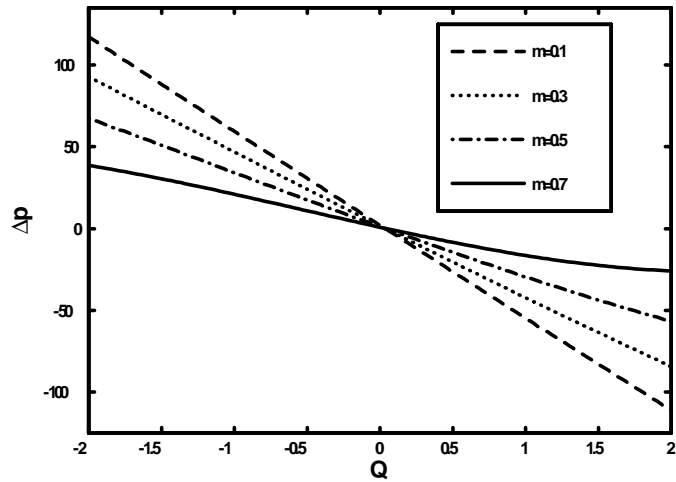


**Fig. 2.8**, Pressure rise distribution for  $B_m = 0.18$ ,  $\epsilon = 0.11$ ,  $T_m = 0.22$ ,  $g_r = 0.52$ ,  $H_y = 0.01$ ,  
 $\Phi = 0.13$ ,  $b_r = 0.23$ .

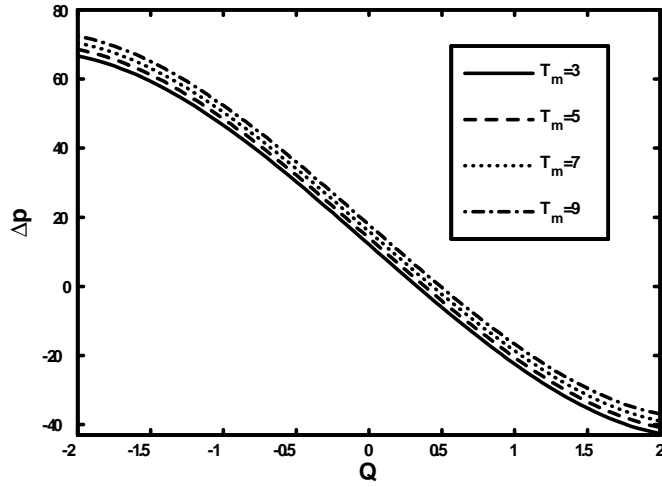


**Fig. 2.9**, Pressure rise distribution for  $m = 0.11$ ,  $\epsilon = 0.01$ ,  $B_m = 6.49$ ,  $H_y = 0.14$ ,  $g_r = 8.92$ ,  
 $b_r = 3.62$ ,  $\Phi = 0.03$ .

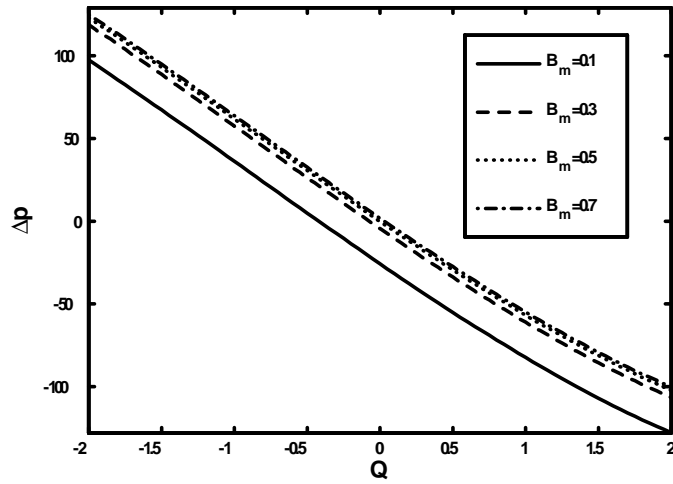


**Fig. 2.10**, Pressure rise distribution for  $\Phi = 0.15$ ,  $m = 0.1$ ,  $\epsilon = 0.11$ ,  $g_r = 3.4$ ,  $H_y = 0.12$ ,  
 $b_r = 4.92$ ,  $T_m = 3.44$ .

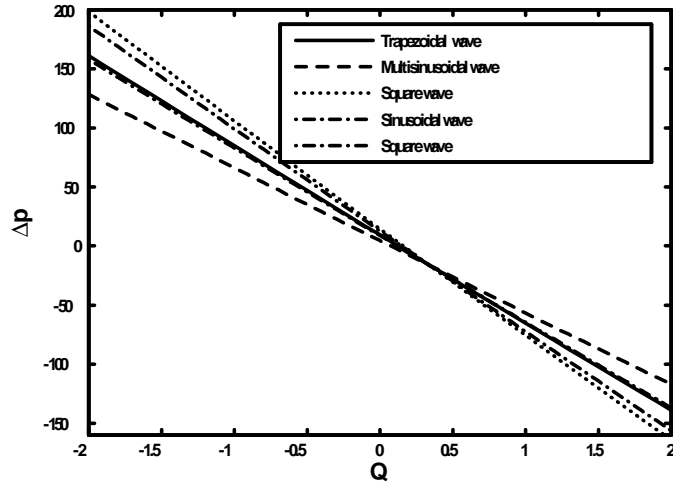


**Fig. 2.11**, Pressure rise distribution for  $m = 0.01$ ,  $\epsilon = 0.13$ ,  $g_r = 2.43$ ,  $\Phi = 0.19$ ,  $T_m = 4.77$ ,  
 $b_r = 5.71$ ,  $B_m = 4.82$ ,  $H_y = 0.14$ ,  $d = 2.1$ .

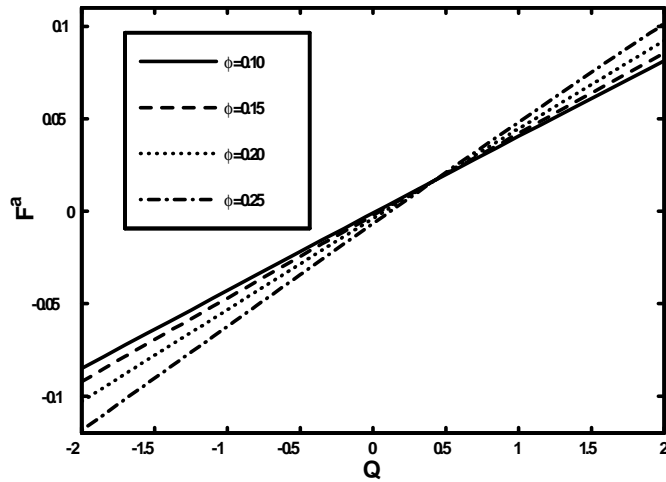


**Fig. 2.12**, Frictional force (on inward cylinder) for  $\epsilon = 0.03$ ,  $T_m = 0.51$ ,  $m = 0.02$ ,  $b_r = 0.22$ ,  
 $B_m = 0.81$ ,  $H_y = 0.11$ ,  $g_r = 0.52$ .

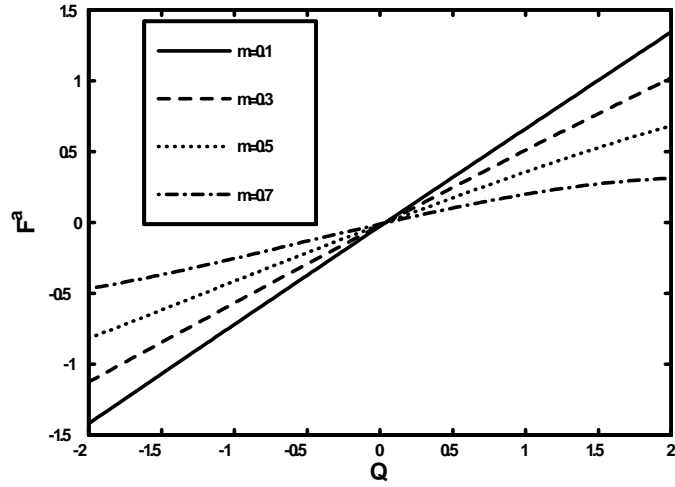


**Fig. 2.13**, Friction force (inward cylinder) for  $H_y = 0.01$ ,  $\Phi = 0.13$ ,  $\epsilon = 0.11$ ,  $T_m = 0.22$ ,  
 $g_r = 0.52$ ,  $b_r = 0.23$ ,  $B_m = 0.18$ .

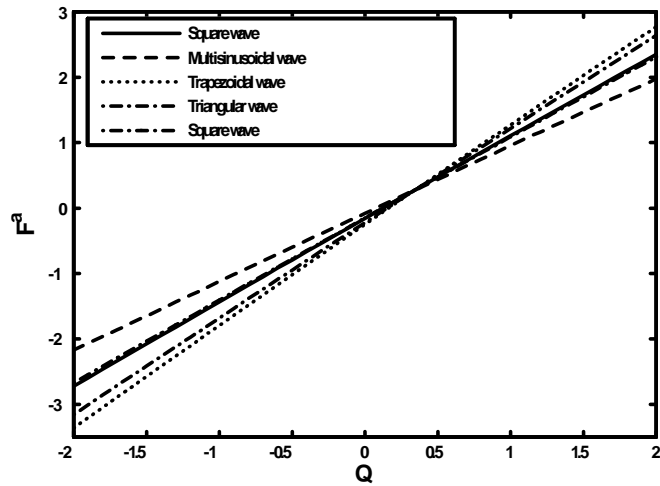


**Fig. 2.14**, Friction force (inward cylinder) for  $m = 2.1$ ,  $\epsilon = 0.13$ ,  $b_r = 5.71$ ,  $T_m = 4.77$ ,  
 $B_m = 4.82$ ,  $m = 0.01$ ,  $g_r = 2.43$ ,  $H_y = 0.14$ ,  $\Phi = 0.19$ .

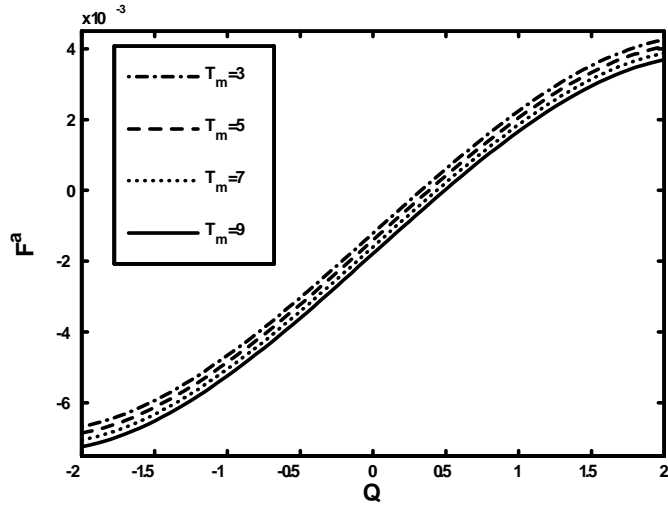


**Fig. 2.15**, Frictional force (on inward cylinder ) for  $\epsilon = 0.01$ ,  $b_r = 3.62$ ,  $\Phi = 0.03$ ,  $H_y = 0.14$ ,  
 $g_r = 8.92$ ,  $m = 0.11$ .

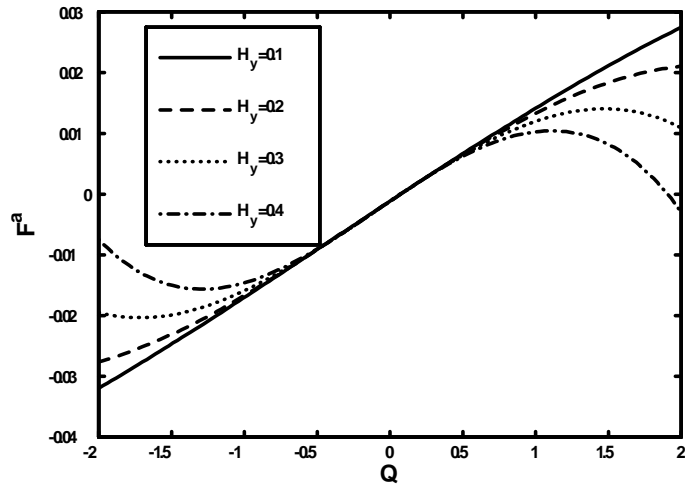


**Fig. 2.16**, Frictional force (on inward cylinder ) for  $B_m = 2.41$ ,  $T_m = 5.14$ ,  $g_r = 3.32$ ,  
 $\Phi = 0.05$ ,  $b_r = 2.22$ ,  $\epsilon = 0.02$ ,  $m = 0.1$ .



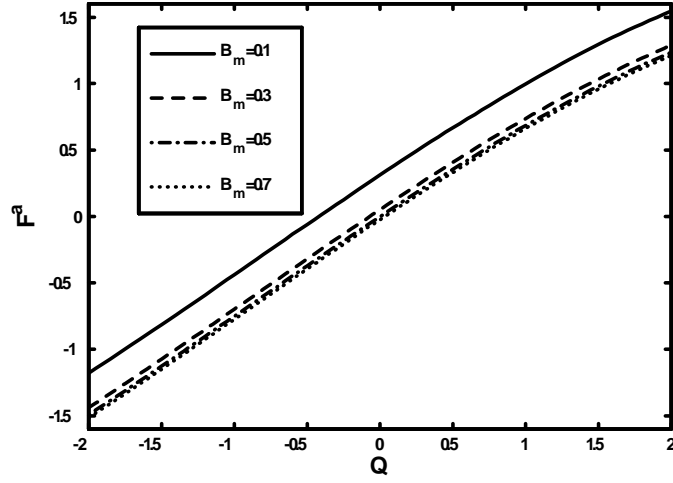


**Fig. 2.17**, Frictional force (on inward cylinder ) for  $T_m = 3.44$ ,  $\Phi = 0.15$ ,  $\epsilon = 0.11$ ,  $H_y = 0.12$ ,  
 $g_r = 3.4$ ,  $b_r = 4.92$ ,  $m = 0.1$ .

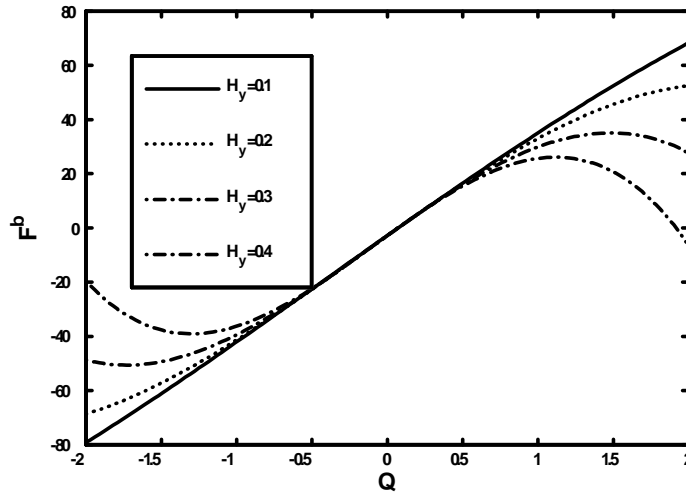


**Fig. 2.18**, Frictional force (on outward cylinder ) for  $m = 0.1$ ,  $\Phi = 0.05$ ,  $B_m = 2.41$ ,  
 $T_m = 5.14$ ,  $g_r = 3.32$ ,  $b_r = 2.22$ ,  $\epsilon = 0.02$ .

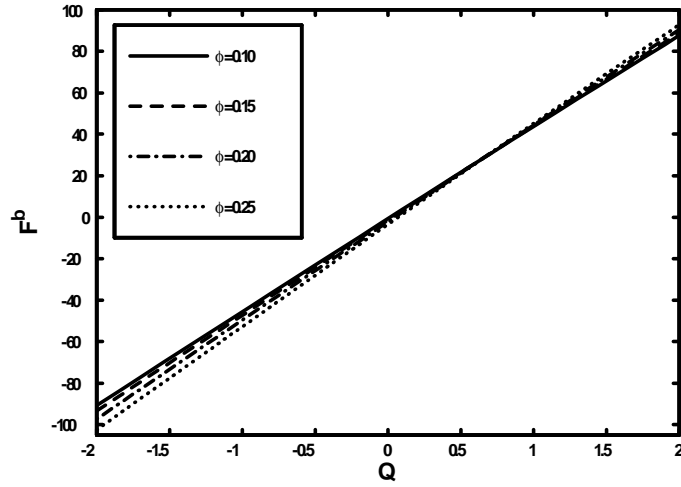


**Fig. 2.19**, Frictional force (on outward cylinder ) for  $m = 0.02$ ,  $g_r = 0.52$ ,  $b_r = 0.22$ ,  
 $T_m = 0.51$ ,  $\epsilon = 0.03$ ,  $B_m = 0.81$ ,  $H_y = 0.11$ .

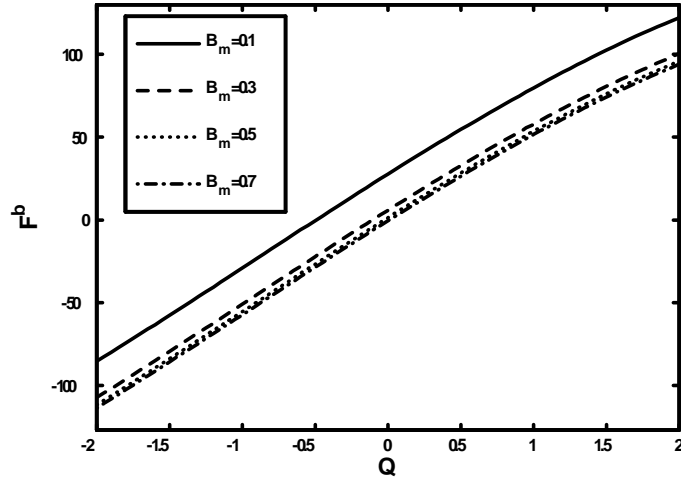


**Fig. 2.20**, Frictional force (on outward cylinder )for  $\Phi = 0.15$ ,  $m = 0.1$ ,  $g_r = 3.4$ ,  $T_m = 3.44$ ,  
 $H_y = 0.12$ ,  $b_r = 4.92$ ,  $\epsilon = 0.11$ .

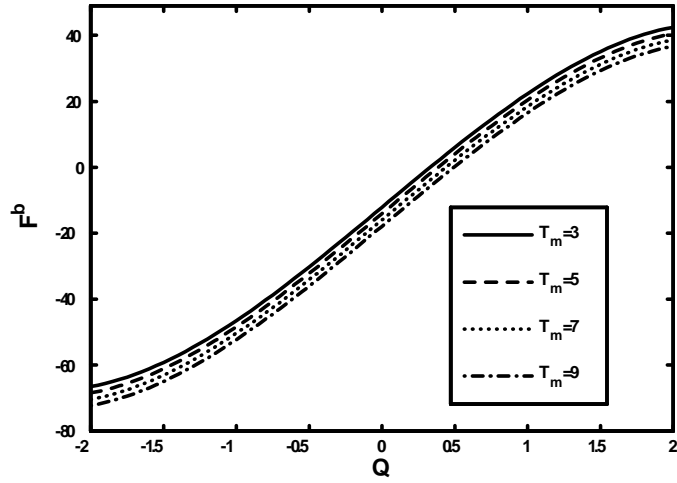


**Fig. 2.21**, Frictional force (on outward cylinder ) for  $\Phi = 0.03$ ,  $\epsilon = 0.01$ ,  $H_y = 0.14$ ,  
 $B_m = 6.49$ ,  $g_r = 8.92$ ,  $b_r = 3.62$ ,  $m = 0.11$ .

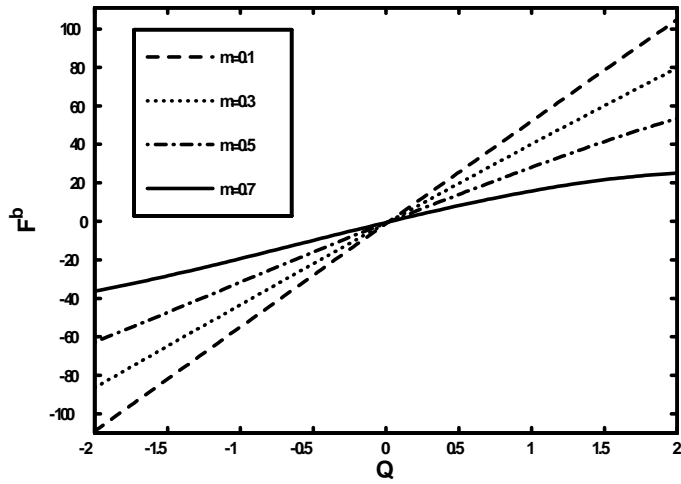


**Fig. 2.22**, Friction force (on outward cylinder ) for  $H_y = 0.01$ ,  $\epsilon = 0.11$ ,  $\Phi = 0.13$ ,  $g_r = 0.52$ ,  
 $B_m = 0.18$ ,  $T_m = 0.22$ ,  $b_r = 0.23$ .

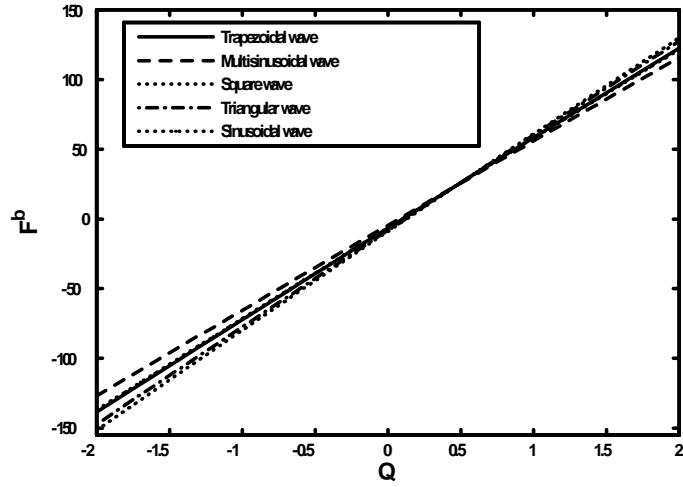


**Fig. 2.23**, Friction force (outward cylinder ) for  $\epsilon = 0.13$ ,  $b_r = 5.71$ ,  $g_r = 2.43$ ,  $B_m = 4.82$ ,  $\Phi = 0.19$ ,  $T_m = 4.77$ ,  $m = 0.01$ ,  $H_y = 0.14$ ,  $d = 2.1$ .

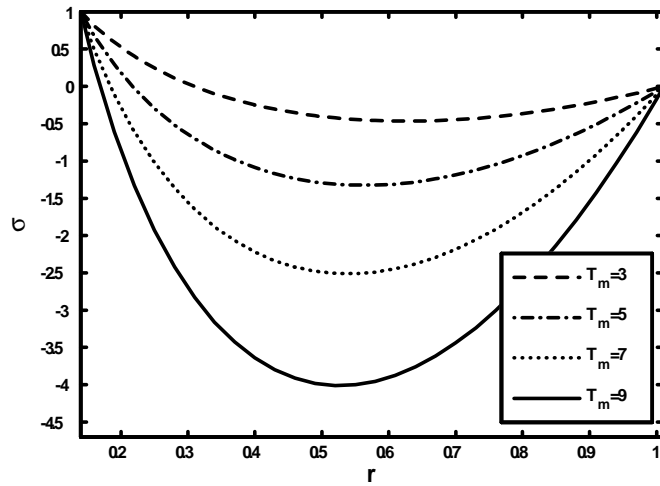


**Fig. 2.24**, Concentration field for  $z=0.06$ ,  $B_m = 3.55$ ,  $\Phi = 0.03$ ,  $\epsilon = 0.14$ .

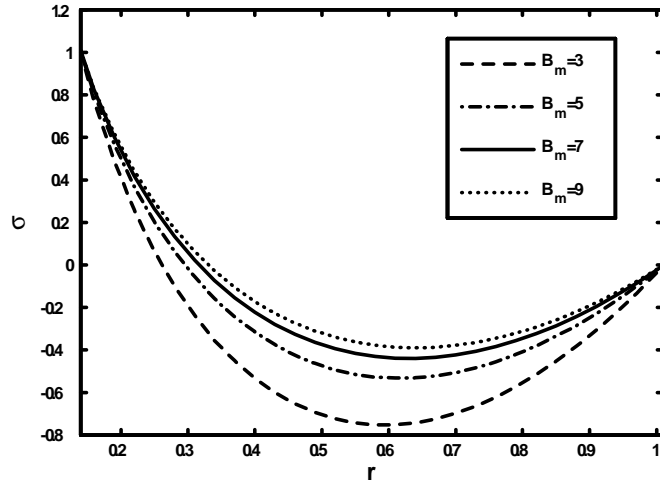


**Fig. 2.25**, Concentration field for  $z = 0.06$ ,  $\Phi = 0.03$ ,  $\epsilon = 0.14$ ,  $T_m = 3.55$ .

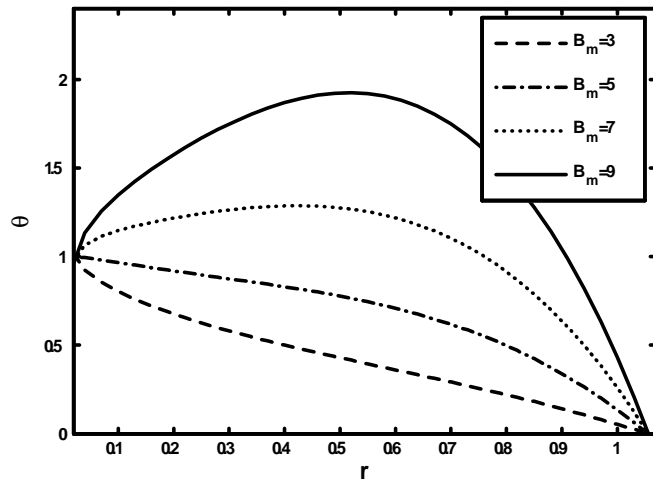


**Fig. 2.26**, Temperature profile for  $z = 0.31$ ,  $T_m = 0.03$ ,  $\Phi = 0.06$ ,  $\epsilon = 0.02$ .

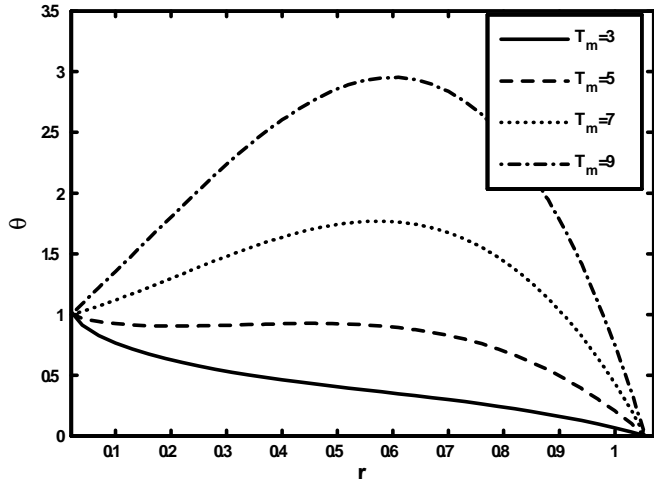


Fig. 2.27, Temperature profile for  $z=0.31$ ,  $\epsilon = 0.02$ ,  $B_m = 0.03$ ,  $\Phi = 0.06$ .

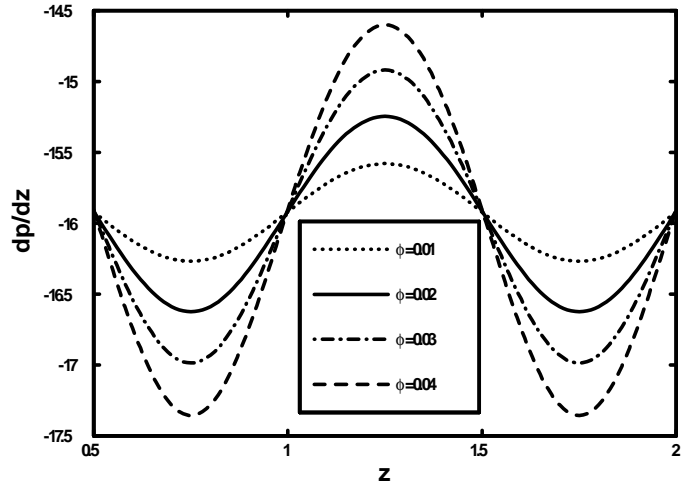
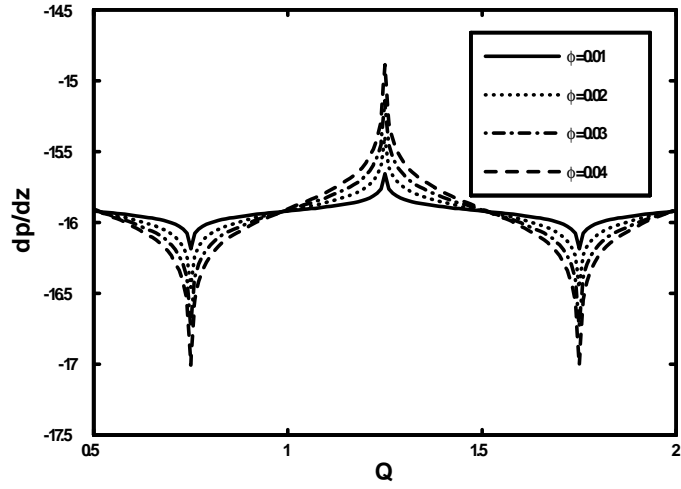
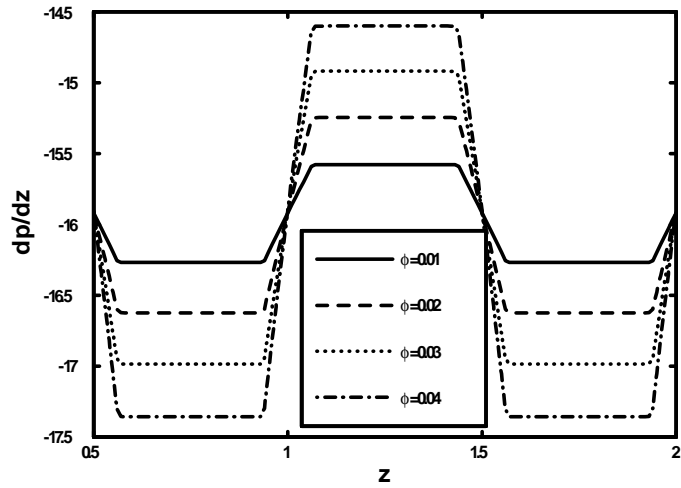


Fig. 2.28, Pressure gradient distribution for sinusoidal wave for  $H_y = 0.13$ ,  $B_m = 2.72$ ,  $\epsilon = 0.11$ ,  $g_r = 2.44$ ,  $Q = 0.42$ ,  $m = 0.23$ ,  $T_m = 2.88$ ,  $b_r = 2.77$ .



**Fig. 2.29**, Pressure gradient distribution (triangular wave) for  $m = 0.23$ ,  $\epsilon = 0.11$ ,  
 $B_m = 2.72$ ,  $g_r = 2.44$ ,  $b_r = 2.77$ ,  $Q = 0.42$ ,  $T_m = 2.88$ ,  $H_y = 0.13$ .



**Fig. 2.30**, Pressure gradient distribution (square wave) for  $H_y = 0.13$ ,  $\epsilon = 0.11$ ,  $B_m = 2.72$ ,  
 $g_r = 2.44$ ,  $b_r = 2.77$ ,  $Q = 0.42$ ,  $T_m = 2.88$ ,  $m = 0.23$ .

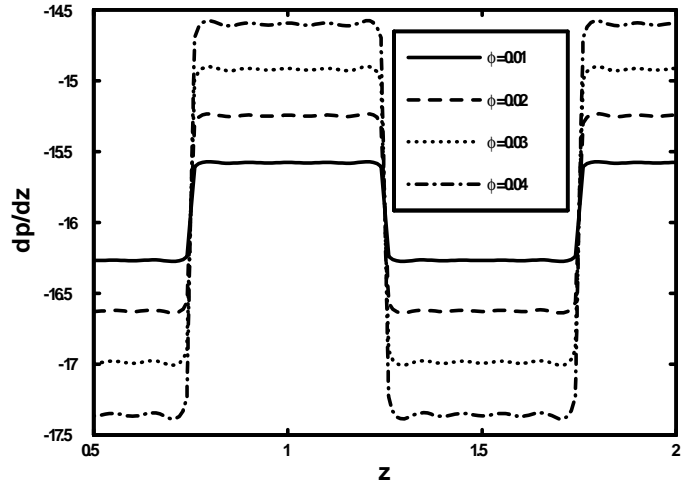


**Fig. 2.31**, Pressure gradient distribution (trapezoidal wave) for  $m = 0.23$ ,  $\epsilon = 0.11$ ,  
 $T_m = 2.88$ ,  $g_r = 2.44$ ,  $b_r = 2.77$ ,  $Q = 0.42$ ,  $H_y = 0.13$ ,  $B_m = 2.72$ .

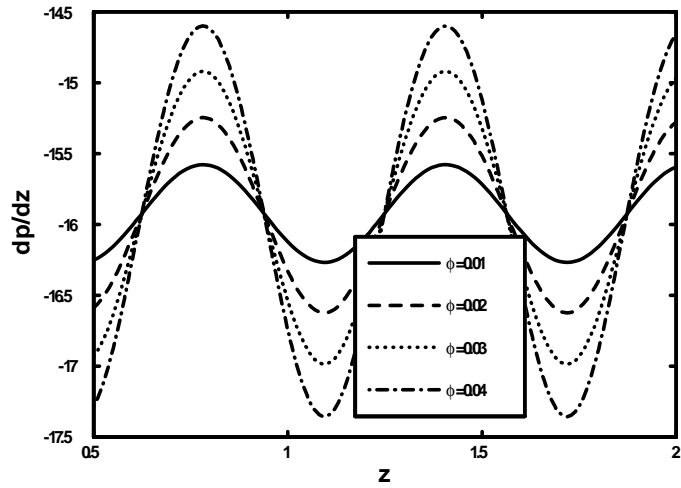


**Fig. 2.32**, Pressure gradient distribution (multisinusoidal wave) for  $d = 1.77$ ,  $m = 0.23$ ,  
 $H_y = 0.13$ ,  $b_r = 2.77$ ,  $\epsilon = 0.11$ ,  $Q = 0.42$ ,  $T_m = 2.88$ ,  $g_r = 2.44$ ,  $B_m = 2.72$ .



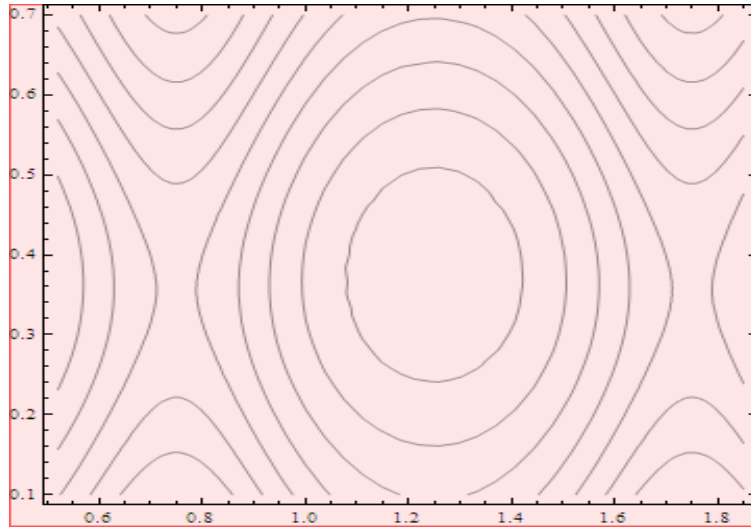


**Fig. 2.33**, Streamlines for sinusoidal wave for  $b_r = 5.22$ ,  $\Phi = 0.10$ ,  $\epsilon = 0.25$ ,  $H_y = 0.11$ ,  
 $T_m = 3.92$ ,  $Q = 0.53$ ,  $m = 0.19$ ,  $g_r = 4.44$ ,  $B_m = 5.83$ , .

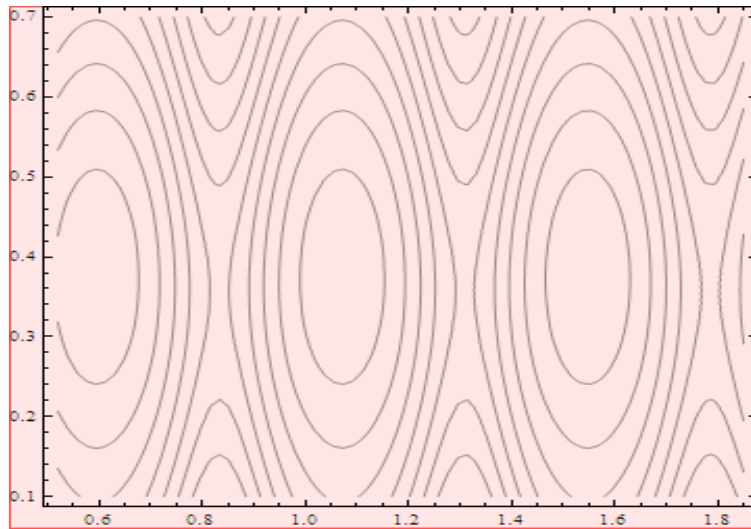


**Fig. 2.34**, Streamlines for Multisinusoidal wave for  $Q = 0.53$ ,  $\Phi = 0.10$ ,  $m = 0.19$ ,  $T_m = 3.92$ ,  
 $\epsilon = 0.25$ ,  $m = 2.1$ ,  $H_y = 0.11$ ,  $B_m = 5.83$ ,  $g_r = 4.44$ ,  $b_r = 5.22$ .

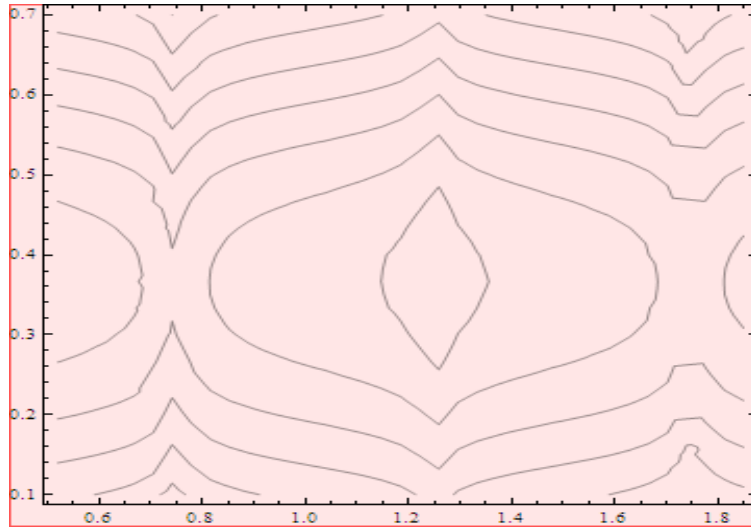


**Fig. 2.35**, Streamlines for Triangular wave for  $T_m = 3.92$ ,  $\Phi = 0.10$ ,  $m = 0.19$ ,  $\epsilon = 0.25$ ,  
 $H_y = 0.11$ ,  $B_m = 5.83$ ,  $b_r = 5.22$ ,  $Q = 0.53$ ,  $g_r = 4.44$ .

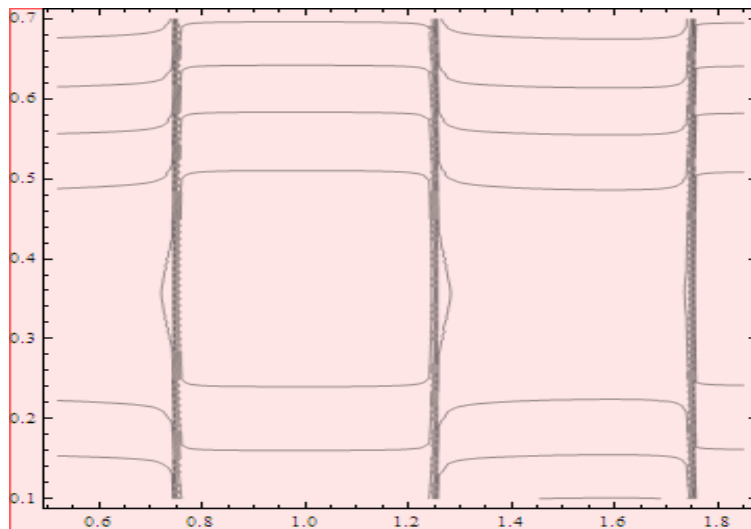


**Fig. 2.36**, Streamlines for Square wave for  $B_m = 5.83$ ,  $\Phi = 0.10$ ,  $m = 0.19$ ,  $H_y = 0.11$ ,  
 $Q = 0.53$ ,  $g_r = 4.44$ ,  $\epsilon = 0.25$ ,  $b_r = 5.22$ ,  $T_m = 3.92$ .

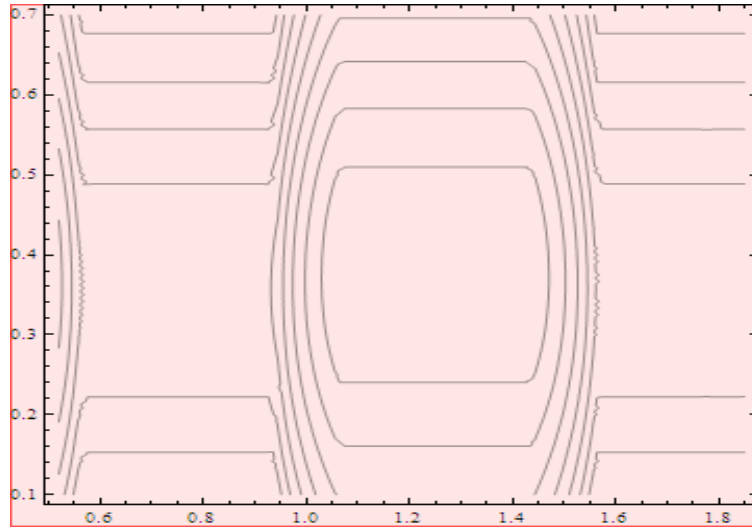


**Fig. 2.37**, Streamlines for Trapezoidal wave for  $g_r = 4.44$ ,  $m = 0.19$ ,  $\epsilon = 0.25$ ,  $T_m = 3.92$ ,  
 $B_m = 5.83$ ,  $H_y = 0.11$ ,  $Q = 0.53$ ,  $b_r = 5.22$ ,  $\Phi = 0.10$ .

# Bibliography

- [1] T. W. Latham, Fluid motion in a peristaltic pump, MS. Thesis, Massachusetts Institute of Technology, Cambridge, 1966.
- [2] A. H. Shapiro, M. Y. Jafferin, S. L. Weinberg, Peristaltic pumping with long wavelengths at low Reynolds number, *J. Fluid Mech.* 35(1969)669.
- [3] J. C. Burns, T. Parkes, Peristaltic motion, *J. Fluid Mech.* 29(1967)731.
- [4] C. Barton, S. Raynor, Peristaltic flow in tubes, *Bull. Math. Biophys.* 30(1968)663.
- [5] Y. C. Fung, C. S. Yih, Peristaltic transport, *J. Appl. Mech.* 35(1968)669.
- [6] M. Ealshahed and M. H. Haroun, Peristaltic transport of Johnson-Segalman fluid under effect of a magnetic field, *Math. Prob in Eng.* 6(2005)663.
- [7] Kh. S. Mekheimer, Y. Abd Elmaboud, Peristaltic flow of a couple stress fluid in an annulus; Application of an endoscope, *Physica A.* 387(2008)2403.
- [8] S. Nadeem, T. Hayat, N. S. Akbar and M. Y. Malik. On the influence of heat transfer in peristalsis with variable viscosity, *Int. J. of Heat and Mass Transfer.* 52(2009)4722.
- [9] M. H. Haroun, Effect of Deborah number and phase difference on peristaltic transport of a third order fluid in an asymmetric channel, *Commun Nonlinear Sci Numer Simulat.* 4(2007) 463.
- [10] M. Kothandapani, S. Srinivas, Peristaltic Transport of a Jeffrey fluid under the effect of magnetic field in an asymmetric channel, *Int. J. Non-linear Mechanics.* 43 (2008) 915.

- [11] S. Nadeem and N. S. Akbar, Series solutions for the peristaltic flow of a Tangent hyperbolic fluid in a uniform inclined tube, *Zeitschrift fur Naturforschung*, 65a(2010)887.
- [12] D. Tripathi, S. K. Pandey, S. Das, Peristaltic Flow of Viscoelastic Fluid with Fractional Maxwell Model through a Channel, *Appl. Math. Comp.* 215(2010)3645.
- [13] N. S. Akbar, S. Nadeem and C. Lee, Peristaltic flow of a Prandtl fluid model in an asymmetric channel, *Int. J. of Physical Sciences*. 7(2012)687.
- [14] S. U. S. Choi, Enhancing thermal conductivity of fluids with nanoparticles, in: D. A. Siginer, H.P. Wang (Eds.), *Developments and Applications of Non-Newtonian Flows*, ASME, New York. 66 (1995) 99 – 105.
- [15] J. Buongiorno, Convective Transport in Nanofluids. *Journal of Heat Transfer (American Society Of Mechanical Engineers)*. 128(3) (2010) 240.
- [16] A. V. Kuznetsov and D. A. Nield, Natural convective boundary-layer flow of a nanofluid past a vertical plate, *Int. J. Thermal Sci.* 49(2010)243.
- [17] K. Sadik and A. Pramuanjaroenkij. Review of convective heat transfer enhancement with nanofluids. *Int. J. of Heat and Mass Transfer*. 52 (2009) 3187.
- [18] W. A. Khan and I. Pop, Boundary-layer flow of a nanofluid past a stretching sheet, *Int. J. of Heat and Mass Transfer*. 53(2010)2477.
- [19] S. E. B. Marga, S. J. Palm, C. T. Nguyen, G. Roy and N. Galanis, Heat transfer enhancement by using nanofluids in forced convection flows, *Int. J. of Heat and Fluid Flow*. 26(2005)530.
- [20] P. Rana and R. Bhargava, Flow and heat transfer of a nanofluid over a nonlinearly stretching sheet: A numerical study, *Comm. Nonlinear Sci. Num. Simul.* DOI : 10.1016/j.cnsns.2011.05.009.
- [21] N. S. Akbar, S. Nadeem, T. Hayat and A. A. Hendi, Effects of heat and mass transfer on the peristaltic hyperbolic tangent fluid in an annulus, *Int. J. of Heat and Mass Transfer*. 54(2011)4360 – 4369.

- [22] N. S. Akbar and S. Nadeem, Endoscopic effects on the peristaltic flow of a nanofluid, *Commun. Theor. Phys.* 56(2011)761.
- [23] N. S. Akbar, S. Nadeem, T. Hayat and A. A. Hendi, Peristaltic flow of a nanofluid in a non-uniform tube, *Heat and Mass Transfer.* 48(2012)451.
- [24] J. H. He, Application of homotopy perturbation method to nonlinear wave equations, *Chaos, Solitons & Fractals.* 26(2005)695.
- [25] A. M. Wazwaz, A reliable modification of Adomian Decomposition method, *Applied Mathematics and Computation.* 102(1999)77 – 86.
- [26] A. M. Wazwaz, The modified Adomian Decomposition method for analytic treatment of differential equation, *Applied Mathematics and Computation.* 173(2006)165 – 176.
- [27] N. T. Eldabe, E. M. Elghazy. A. Ebaid, Closed form solution to a second order boundary value problem and its application in fluid mechanics, *Physics Letters A.* 363(2007)257–259.